ULTRA-WIDEBAND IMPULSE RADIO WITH DIVERSITY RECEPTION

TAN SHEU SHEU

NATIONAL UNIVERSITY OF SINGAPORE

2004

ULTRA-WIDEBAND IMPULSE RADIO WITH DIVERSITY RECEPTION

TAN SHEU SHEU

(B. Eng)

A THESIS SUBMITTED

FOR THE DEGREE OF MASTER OF ENGINEERING

DEPARTMENT OF ELECTRICAL AND COMPUITER ENGINEERING

NATIONAL UNIVERSITY OF SINGAPORE

2004

ACKNOWLEDGEMENTS

I would like to express my heartfelt gratitude and utmost appreciation to both of my supervisors, Dr. B. Kannan and Dr. A. Nallanathan, for their invaluable guidance, continuing support and constructive suggestions throughout the entire course of my graduate study in National University of Singapore. Their deep insight and wide knowledge has helped me out at the various phase of my research. It has been an enjoyable and a cultivating experience working with them.

Next, I would like to thank my great colleagues in EE-I2R lab for all their helps and for making my study life in NUS so wonderful.

Last but not least, I would also like to thank my family members who always been the best supports in my life.

SUMMARY

Impulse radio (IR) is based on the ultra-wideband (UWB) time-hopping spread spectrum technology which employs extremely short duration pulses to convey information by shifting the position of the pulses in the time domain with great accuracy.

In this thesis, the influence of temporal and spatial diversities on the performance of Ultra-wideband impulse radio systems is analyzed. We investigate how antenna diversity (uniform linear array and rectangular array) can be used to improve the bit error rate performance and can cope with the effects of multiuser interference (MUI) of an IR system in multiuser environments with multipath fading channel. We highlight the effects of the number of employed antenna elements and the number of the selected multipaths on the bit error rate (BER) performance in single-user and multiuser environments. We compare the diversity performance of the IR systems with uniform linear arrays and rectangular arrays at the receiver. The application of beamforming technique and the utilization of Rake receiver are considered. The channel model is based on the Saleh-Valenzuela (S-V) model with slight modifications. Analytical and simulation results show that the BER performance of the IR system can be improved when the number of array elements is increased. The performance can be further improved by coherently adding more multipaths at the receiver.

Due to high bandwidth, a UWB impulse radio multiple access system can accommodate many users. In this thesis, the multiple access capacity of M-ary pulse position modulation (PPM) impulse radio systems with diversity reception in dense

multipath environments is analyzed. We investigate the use of antenna arrays at the receiver to improve the multiple access performance of the system in terms of the number of simultaneous active users supported by the system for a given bit error rate and bit transmission rate. The bit error rate (BER) of M-ary IR UWB systems with diversity reception is derived. Numerical results show that the multiple access capacity of the M-ary IR system can be improved significantly by increasing the number of elements of the antenna array and coherently adding more paths at the receiver.

In summary, antenna arrays can be used in conjunction with the Rake receiver to exploit spatial and path diversity provided by the antenna array and the Rake receiver, respectively, to combine the different multipath components in a way that improves the BER and multiple access performance of the UWB IR systems.

CONTENTS

LIST OF FIGURES

LIST OF TABLES

CHAPTER 1

INTRODUCTION

1.1 Background

During the last decade, communication technology has undergone rapid development for wireless applications, facing challenges in the allocation of frequency resources. The growing demand for capacity in wireless communication requires a new type of wireless communication method which does not affect the current existing systems. An emerging technology that fulfills this requirement is Ultra-wideband (UWB) impulse radio (IR) system which does not require extra frequency band allocation unlike the conventional communication systems using information-bearing sinusoidal RF carriers. The Ultra-wideband radio technology is currently receiving a great deal of global attention and holds promises for revolutionizing wireless communications.

Ultra-wideband (UWB) is a wireless technology that is known as ‘baseband carrierless impulse’ technology. The technique for generating UWB signals has been known for three decades [1] and was mostly used for radar applications where they yield high resolution positioning and ground penetrating capabilities [2]. A description of early UWB work can be found in [3]. During the past few years, there has been a renewed interest in utilizing this technology for UWB spread-spectrum communications due to the impulsive nature of the transmitted UWB signal that has advantages over the

narrowband communications waveform with attractive features for asynchronous multiple access communications in dense multipath environments.

The novel UWB radio technology has recently received legal adoption by the authorities in the United State. In 1998, the Federal Communications Commission (FCC) first proposed UWB transmission under part 15 rules and asked for comments from industry [4, 5]. In 2002, it issues a first report and order that permits the marketing and operation of certain types of products incorporating ultra-wideband and approved the use of UWB as an overlay system for frequencies from 3.1 to 10.1 GHz [6]. The spectrum below 3GHz is avoided for fear of interference with GPS, aeronautical and maritime navigation. This ruling opens the way for coexistence with traditional and protected radio services and allows the potential use of UWB transmission without the allocated spectrum. Following the FCC ruling, a standards committee has been established by the IEEE, i.e. IEEE 802.15 Working Group for Wireless Personal Area Networks [7] that should develop standards for wireless personal area networks including UWB systems.

UWB radio is the generic term describing radio systems having very large bandwidths. Specifically, a definition used within the FCC's First Report and Order [6] and defines a radio system to be an UWB system if the fractional bandwidth B_f of the signal is greater than 20% or the -10dB bandwidth of the signal is at least 500MHz at all time of transmission. The fractional bandwidth is defined by the expression

$$B_f = 2\frac{f_H - f_L}{f_H + f_L} \tag{1.1}$$

where f_H is the upper frequency of the -10dB emission point and f_L is the lower frequency of the -10dB emission point. The center frequency of the signal spectrum, f_C emitted by such a system is defined as the average of the upper and lower -10dB emissions points, that is

$$f_C = \frac{f_H + f_L}{2} \tag{1.2}$$

Traditional communications systems normally use signals having a fractional bandwidth less than 1%. Wideband CDMA has a fractional bandwidth of approximately 2%. Figure 1-1 compares the fractional bandwidth of the ultra-wideband and narrowband system.

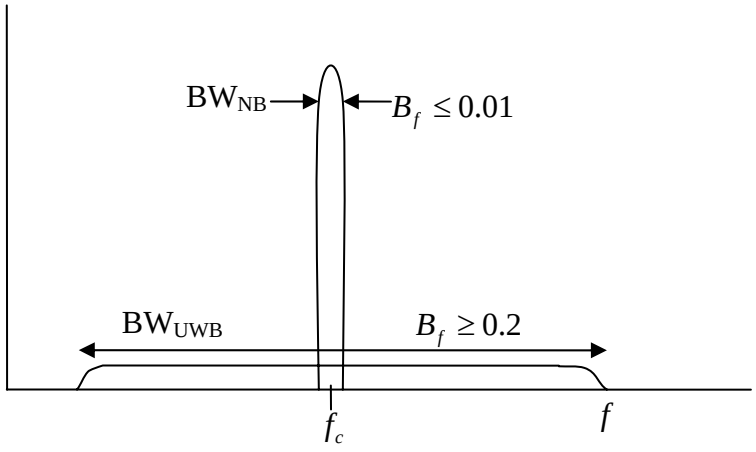

Figure 1-1: Fractional bandwidth comparison between UWB systems and narrowband system

Typically, UWB radio systems employ pulse modulation where extremely narrow bursts of RF energy are modulated and emitted to convey information. The basic concept of UWB is to generate, transmit and receive trains of extremely short duration burst of impulses (referred to as monocycles) – typically in the duration of tens of

picoseconds to a few nanoseconds, by precisely controlling their relative position in the time axis with very low duty cycles (less than 1%). The short pulses are generally modeled with Gaussian monocycle. According to the scheme proposed by Win and Sholtz [8], data is transmitted by using pulse-position-modulation (PPM) at a rate of many pulses per data symbol. Several pulses are used to represent a symbol that attempt to use the time diversity to improve the system performance. Multiple access (MA) is achieved by means of time-hopping spread spectrum (THSS) technique with a different hopping code for each user [8]. This wideband communication system is referred as an impulse radio because it utilizes the available impulse signal technology [9].

Conventional “narrowband” systems use radio frequency to move the signal from baseband to the actual carrier frequency in the frequency domain where the system is allowed to operate. Conversely, in UWB implementations, one directly modulates a short burst of pulses that has a very sharp rise and fall time, thus spreading the transmitted energy very thinly across a wide spectrum of frequency from near D.C. to a few gigahertz [8]. Hence, the power spectrum of the time-hopped IR signal has an ultra-wideband bandwidth on the order of gigahertz and a very low power spectral density well below the thermal noise floor. This assures that the UWB signals do not interfere with narrowband radio systems operating in dedicated bands and is able to co-exist with other existing radio systems without producing additional significant interference by means of overlay principle [10]. It further contributes to the anti-jamming capability and low probability of detection or intercept (LPD/LPI) by unintended listener for secure communications [11].

UWB signals are transmitted in baseband and no carrier signal is involved. This means that the signal energy is concentrated in the lowest possible frequency band that supports its wide transmission bandwidth. UWB signal radiated at lower frequencies tends to have better material penetration properties than signals radiated at higher frequency. Besides, carrier free modulations makes receiver design of UWB systems less complex as no carrier synchronization is needed, eliminating the need for oscillators, mixers and other costly RF hardware. Thus, it significantly reduces the complexity of the system and manufacturing cost [12].

The use of UWB signals with gigahertz bandwidths is robust against multipath fading due to its fine delay resolution capability [13]. Pulse repetition time is much larger than the width of the pulse that leads to elimination of significant multipath fading. As multipath components have differential delays of the order of nanoseconds which is approximately equal to the inverse of the spreading bandwidth, they can be easily resolved. Hence, it can reduce the fading effects even in indoor environments. The fine multipath resolution inherent in the short time-duration pulses can reduce fluctuations in signal level and hence lower the required transmitted power. In indoor communications scenario, delay between multipaths is much less and therefore for traditional wideband systems such as wideband CDMA, the use of Rake receiver to extract multipath components is ineffective as most of the multipaths are not resolvable. However, for UWB communications systems, the UWB pulse duration is less than the typical delay between multipath components, the time diversity can be exploited using a Rake receiver even in an indoor environment.

The use of sub nanosecond pulses enables the UWB systems achieve a high processing gain which allow large number of users to be accommodated in the systems. With bandwidth restrictions effectively removed, UWB system offers high data transfer rate. By transmitting extremely narrow pulses instead of continuous waves, the power consumption is very low. Since UWB signal bandwidth is much larger than the information bandwidth, the system can operate at low signal to noise ratio. For these low SNR values, the capacity of the system increases almost linearly with power [12]. The unique features provided by UWB have made the UWB IR technology attractive for short range, high speed, fully mobile multiple access communications over the indoor wireless channels.

There must be a payoff in the use of impulse radio with attractive features. Ultra-fine time resolution will need accurate time synchronization. Besides, it requires additional correlators to capture adequate signal energy. The adopted monocycle waveform should be designed optimally to minimize the power leakage in sensitive frequency bands.

There are numerous application areas in which UWB technology can provide superior performance. The potential applications of UWB technology encompass wireless communications systems, measurement systems, imaging systems, ground-penetrating radar, medical systems, wall imaging systems, surveillance systems and vehicular radar systems [14].

1.2 Previous Works on UWB

Performance of digital IR under ideal propagation conditions, where there is only a single path between each user's transmitter and the other intended users receiver, under perfect power control has been investigated in [8]. Due to the large UWB bandwidth, an impulse radio multiple access system may accommodate many users. In view of this, previous published works have addressed the issue of multiple access performance of UWB system based on single antenna [15-18]. In [15], multiple access capability of binary PPM IR system assuming free space propagation conditions and additive white Gaussian noise is studied.

The use of non-binary PPM modulation is attractive as it increases the data transmission rate without increasing the transmission bandwidth. The work in [16] investigates the use of M-ary equally correlated (EC) block waveform encoded PPM signals to increase the number of users supported by the system in free space propagation condition. The multiple access performance for different set of M-ary PPM signal designs, i.e. orthogonal, equally correlated, N-orthogonal is discussed in [19].

Reflections and diffractions caused by many obstacles in indoor environments create a multipath channel comprising many propagation paths with different time delay. The existence of multipath in indoor transmission channels places fundamental limitations on the performance of wireless communications systems. Unlike conventional radio system, UWB systems is more robust to multipath effect as large number of fading signal components can be distinguished due to the high temporal resolution, resulting

in significant multipath diversity. As a consequence, Rake receiver can be used advantageously to reap the benefits of multipath diversity in IR systems as the multipath signals can be combined constructively at the receiver. Analysis on Rake-type receivers for UWB system in dense multipath environments can be found in [20-25]. Rake receiver consists of multiple fingers where each finger can extract the signal from one of the multipath components created by the channel. The multipath characteristics of the IR system based on single antenna reception under perfect power control is studied in [26-29]. The issue of multiple access performance of the UWB IR systems in dense multipath environments is discussed in [30].

There has been lots of research being carried out to model the characteristic of the channel for UWB system [31-34]. The work in [31] presented a statistical path loss model for indoor UWB signals of nominal center frequency of 5GHz in indoor environments. An UWB channel measurement and modeling effort, targeted towards wireless personal area network (WPAN) applications has been described in [32] where a serial time-domain deconvolution technique called CLEAN algorithm has been proposed to extract the channel impulse response functions from all the channel sounding. In [33], a stochastic tapped delay line model based on a measurement campaign in an office building has been suggested. The work in [34] contributed to an understanding of the indoor UWB propagation channel including the time-of arrival, angle-of arrival and level distributions of a collection of received signal.

Based on clustering phenomenon observed in several channel measurements, the working group of IEEE P802.15 has proposed an UWB channel model derived from the Saleh-Valenzuela model with a couple of modifications [35]. The proposed

channel model recommended using a lognormal distribution rather than a Rayleigh distribution for the multipath gain magnitude.

There has been research carried out to study the interference and its effects incurred by UWB signals [36-39]. In [36], the level of interference caused by different UWB signals to various other radio systems such as GSM900, UMTS/Wideband code-division multiple-access (WCDMA), and global position system (GPS) was evaluated. It suggests that proper selection of UWB pulse waveform and pulse width can minimize the interference. In [37], a new pulse design algorithm utilizing ideas of prolate spheroidal wave functions was proposed to meet the power spectral constraint of FCC UWB mask. In [39], an M-ary scheme using Walsh codes that is effective to reduce interference of UWB systems to existing radio systems was presented.

On the other hand, there are studies which deal with the effect of interference form RF band occupied by other communications system to UWB and methods to mitigate these effects. UWB system design needs to take into account all sources of interference and all tools to mitigate interference (DSP, FEC, waveform design, analog filtering, etc) [40] analyzed the performance of UWB communications in the presence of interference. The authors in [41] presented a novel algorithm using frequency domain processing and a time domain suppression technique to mitigate external interference in UWB system. [42] studied the effect of radio frequency interference to a victim UWB receiver and interference cancellation is introduced. In [43], narrowband interference suppression algorithms so called MMSE-Rake was suggested whereas in [44], doublet pulse has been proposed to mitigate the interference from narrowband signals.

The use of extremely narrow pulses in UWB requires an accurate channel estimation method. In [45], a blind adaptive channel estimation algorithm for system identification on impulse radio channels has been investigated. The authors in [46] discussed the use of channel parameter estimation to assess the percentage of capture energy with Rake receiver. An isolated monopulse is transmitted through the channel to estimate the channel. The authors in [47] derived channel estimates from information bearing signal rather than from monopulse. The estimation method is based on the maximum-likelihood criterion and is applied to two different scenarios: either with known symbol (data aided) or with unknown symbol (non-data aided).

Attractive features of UWB IR technology provide communication design challenges, yielding a rich source of research problem. Besides the above mention research, there are other research areas such as channel acquisition time [48, 49], signal selection [50], capacity [51, 52], receiver implementation issue [53-56], UWB ad-hoc networks issue [57-60], etc.

1.3 Motivation

The key motivation for using THSS impulse radio is the ability to highly resolve multipath. Unlike narrow radio systems, UWB systems suffer much less from signal fading effects because the extremely narrow pulses propagating over different paths causes a large number of independently fading signal components that can be distinguished due to the high resolution, resulting in significant multipath diversity. In order to fully take advantages of this high delay resolution, the Rake receiver must be able to capture most of the energy carried by a large number of different multipath

signals. Indeed, diversity reception with antenna array will improve the total amount of captured energy.

Much attention has been paid to design and implementation of antenna arrays in wireless communications. The motivation is that antenna array is a promising approach for capacity expansion and performance improvement in wireless systems [61]. The purpose of antenna diversity is to take advantage of the different paths of a wave propagating in a reflective environment in order to improve overall system gain.

Since a complete theory that characterizes the interaction of UWB signal with antenna array has not been adequately addressed, it is important to understand the multiple access IR performance improvement by using diversity reception with antenna array. In fading channel scenarios, antenna array can also be used in conjunction with Rake receiver to exploit spatial and temporal diversity in order to reduce the probability of deep fades while combining desired signal energy from different propagations paths [62-65].

Due to UWB significant bandwidth and the use of time hopping spread spectrum technique, an impulse radio system can support multiple access capability. With diversity reception, it is possible to increase the multiple access capacity of impulse radio system in multiuser environments. The diversity gain achieved allows the system to support a larger number of simultaneous active users [66, 67].

1.4 Contribution of Thesis

In this thesis, we give a comprehensive investigation on the diversity reception of UWB IR system.

In this thesis, the BER performance and characteristic of the IR systems with antenna array using Selective Rake (SRake) receiver in the presence of multipaths and multiuser interference (MUI) is presented. Particular attention is given to the effects of the number of employed antenna elements and the number of the selected multipaths on the BER performance in single user and multiuser environments. The application of beamforming technique and the utilization of Rake receiver are considered. The channel model is based on Saleh-Valenzuela (S-V) model with slight modifications. The performances of the systems with uniform linear arrays and rectangular arrays receiver are also compared. Analytical and simulation results show that the BER performance of the IR system can be improved when the number of array elements is increased. The performance can be further improved by coherently adding more multipaths at the receiver.

With ideal propagation conditions, ultra wideband radio promises a great multiple access capacity. In this thesis, we present the multiple access performance analysis of the M-ary equally correlated (EC) block waveform PPM IR system with antenna array using Rake receiver in the presence of multipath and multiple-user interference (MUI). We investigate how antenna diversity obtained by antenna array in conjunction with path diversity provided by rake receiver can be used to improve the multiple access performance of M-ary IR system. We highlight the effects of the number of employed

antenna elements and selected multipath on the multiple access performance in dense multipath environments. The bit error rate (BER) of M-ary IR UWB systems with diversity reception is derived. Numerical results show that the multiple access capacity of the M-ary IR system can be improved significantly by increasing the number of elements of the antenna array and coherently adding more paths at the receiver.

1.5 Organization of Thesis

This thesis covers the range of topics related to the diversity reception of UWB IR systems in dense multipath environments. The organization of the thesis is as follows

In Chapter 2, the principle of THSS PPM IR system model is explained in details. UWB IR signal model based on PPM will be described. The principle of Rake receiver will be explained as well.

In Chapter 3, performance of binary modulated UWB Multiple Access IR Systems with antenna array in dense multipath environments is investigated. An application of antenna array in UWB systems is introduced and the space-time channel model is described. The IR receiver architectures, processing and BER analysis with diversity reception are presented.

In Chapter 4, the influence of spatial and temporal diversities on the multiple access performance of M-ary equally correlated pulse position modulation (PPM) impulse radio systems is presented and analyzed. We investigate the use of antenna array at the receiver to improve the multiple access performance of the system in terms of the

number of simultaneous active users supported by the system for a given bit error rate and bit transmission rate.

Finally, in chapter 5, we draw conclusions on the thesis and make some suggestions for future works.

CHAPTER 2

UWB IR SYSTEMS MODEL

2.1 Introduction

The last decade has witnessed a paradigm flow from low bit rate narrowband wireless systems to broadband wireless systems. This trend is being continued with the recent emergence of the ultra-wideband systems.

The idea of transmitting digital information using ultra-short impulses was first presented in [9] and called impulse radio. It relies on pulse position modulation and time diversity that is gained by repeating the same symbol many times, according to a certain code, which embodies IR with a very high processing gain. Impulse radio system has been recently considered as a good candidate for short range, high data rate indoor wireless communications in dense multipath environments [68].

In this chapter, UWB IR system model is discussed. The principle of time hopping spread spectrum PPM impulse radio signal model is explained. Brief descriptions about simple receive signal processing and receiver structure for IR system is given. The basic concept about diversity reception and array property are presented as well.

2.2 Impulse Radio Signal Model

In this section, binary PPM Impulse radio signal model with TH will be described.

In an IR system, the transmitted signal of each user consists of impulses of sub-nanosecond duration. Each user transmits one pulse per transmit frame. Each frame of T_f seconds contains N_h hopping chips with duration T_c seconds per chip. In each T_f, one pulse will be placed in one of the N_h slots according to the corresponding user time-hopping (TH) sequence. Each data symbol is transmitted repeatedly in N_s consecutive frames in order to attain diversity and make soft decisions at the receiver. The location of the transmitting pulse within the allocated hopping slot is determined by the information bit.

A typical transmitted time-hopping PPM signal conveying information exclusively in the time shift for the u^{th} user can be modeled as [8]

$$S_{tr}^{(u)}(t) = \sum_{j=0}^{j=\infty} w_{tr}(t - jT_f - c_j^{(u)}T_c - \delta d_{\lfloor j/N_s \rfloor}^{(u)}) \tag{2.1}$$

where t represent the transmitters' clock time, T_f is the frame duration and T_c is the chip period. $w_{tr}(t)$ represents the transmitted monocycle pulse waveform that nominally begin at time zero on the transmitter clock. The superscript (u) indicates the user-dependent quantities with $1 \le u \le N_u$ where N_u is the total number of simultaneous active users. The index j is the number of pulses that have been transmitted, and also the number of time hops that the signal $S_{tr}^{(u)}(t)$ has experienced. T_f corresponds to the frame interval and is typically hundred or thousand times wider

than the monocycle width, resulting in a signal with very low duty cycle. $c_j^{(u)}$ is the unique time hopping sequence assigned to the u^{th} user whereas T_c is the duration of an addressable time bin. N_s is the number of the pulses used to transmit one data symbol called the length of the repetition code. $d^{(u)}_{\lfloor j/N_s \rfloor}$ is the function of the data sequence and the notation of $\lfloor\ \rfloor$ represent the integer portion of the argument. The notation of δ is the PPM time delay parameter.

The detailed structure of each time shift component is described as follow:

A. Uniform Pulse Train Spacing

In this scheme, low duty cycle pulse train is used as the base waveform and the form $\sum_{j=0}^{j=\infty} w\left(t - jT_f\right)$ consist of monocycle pulses spaced T_f seconds apart in time as shown in figure 2-1. T_f is usually hundreds or thousand times wider than the period of the monopulse.

In PPM impulse radio system, N_s pulses are used to represent one symbol. Hence, every transmitted symbol is repeated N_s frames (one per frame) with each frame having duration of T_f. As such, there are N_s frames in one symbol period of T_s, where

$$T_s = N_s T_f \tag{2.2}$$

with $N_s \gg 1$. The symbol transmission rate, R_s is given by

$$R_s = \frac{1}{T_s} = \frac{1}{N_s T_f} \tag{2.3}$$

For a fixed T_f, the symbol rate determines the number N_s of monocycles that are modulated by a given binary symbol. Figure 2-1 shows the u^{th} user frame without any time-hopping code or data modulation.

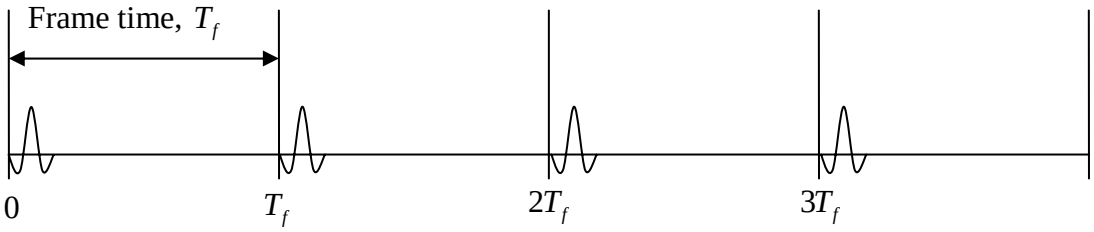

Figure 2-1: Uniform pulse train (no modulation, no dithering)

B. Pseudorandom Time-hopping

Multiple access signals composed of uniformly spaced pulses shown in figure 2-1 are vulnerable to occasional catastrophic collisions where a large number of pulses from two signals are received simultaneously, as what might happen in ALOHA systems.

For UWB IR system, in order to support multiple accessing capabilities, each user (indexed by u) is assigned a distinct pulse time shift pattern $\left\{c_j^{(u)}\right\}$ called a time-hopping sequence to "pseudo randomly" shift the position of a periodic pulse train from its nominal position to eliminate catastrophic collisions. The TH sequence will therefore provide an additional time shift of $c_j^{(u)} T_c$ seconds to the j^{th} monocycle in

the pulse train. These hopping sequences $\left\{c_j^{(u)}\right\}$ are pseudorandom in which each sequence element is an integer in the range of

$$0 \le c_j^{(u)} \le N_h \tag{2.4}$$

Thus, the time shifts are discrete values between 0 and $N_h T_c$ seconds.

The hopping codes could be based on pseudo-noise (PN) sequences or sequences designed to minimize interference between users. The addressable time-hopping duration is assumed as

$$N_h T_c \le T_f \tag{2.5}$$

where a short time interval may be required to read the output of a monocycle correlator and reset the correlator.

A small guard time of T_g can be introduced between two successive frames to account for processing delay between two successively received frames at the receiver. Hence, the ratio of $\frac{N_h T_c}{T_f}$ which indicates the fraction of the frame time over which TH is allowed may be less than one. If the ratio of $\frac{N_h T_c}{T_f}$ is too small, there may be a large catastrophic collision probability of multiple users' signal. Conversely, if $\frac{N_h T_c}{T_f}$ is large enough and with the well designed PN sequences, the multiple access interference can be modeled as a Gaussian random process. One effect of time hopping is to 'smooth' the signal spectrum in the frequency domain which result in reduced power spectral density. An example of a very simple time hopping scheme with three possible hop

positions is shown in figure 2-2. In this figure, within each frame, a pulse is pseudo-randomly positioned according to the value of the hopping code at that time.

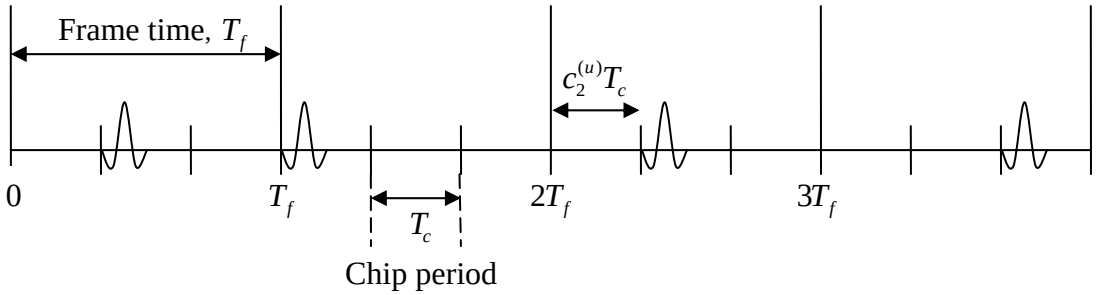

Figure 2-2: Time hopped Gaussian pulse train example where pulses has been shifted according to the time hopping sequence of 1,0,1,2 with 3 possible hop positions in a frame

C. Data Modulation

Pulse position modulation (PPM) is used for symbol encoding whereby each symbol is encoded by delaying the N_s pulses with an additional time shift. The information bit to be transmitted determines the location of pulse within the allocated hopping slot.

The data sequence $\left\{d_j^{(u)}\right\} \in \{0,1\}$ of the u^{th} user is binary (0 or 1) symbols stream that conveys some form of information. For performance prediction purpose, the data sequence $\left\{d_j^{(u)}\right\}$ is modeled as a wide-sense stationary random process composed of equally likely symbols.

The system under study uses fast time hopping, which means that there are $N_s > 1$ pulses transmitted for one symbol. Since this is an 'oversample' modulation, the modulating data symbol changes only after every N_s hops as N_s monocycles are transmitted per symbol. Therefore,

$$d^u_{iN_s} = d^u_{iN_s+1} = ... = d^u_{(i+1)N_s-1} = D^u_i \quad (2.6.a)$$

for all i. D^u_i is the i^{th} transmitted symbol and d^u_j is the i^{th} repeated transmitted symbol in the j^{th} frame for $j = iNs, iNs+1, iNs+2, ..., (i+1)Ns-1$. d^u_j will repeat for N_s times for each transmitted symbol. Different symbols are assumed to be equiprobable.

δ is a fixed time delay and referred to modulation index. Assume that a new data symbol begins with pulse index $j = 0$, the index of the data symbol modulating pulse j is $\lfloor j/N_s \rfloor$. In this modulation method, when the data symbol $\left(d^{(u)}_j\right)$ is '0', no additional time shift is added on the monopulse whereas when the data symbol is '1', a time shift of δ is added to a monocycle. The data modulation further 'smooths' the power spectral density of the pseudo random time-hopping signal.

The parameter δ can be chosen to optimize the performance. δ should be designed such that the cross-correlation between the $w(t)$ and $w(t-\delta)$ is minimum. In other words,

$$\delta = \arg\min_{\delta'} \left(\int_0^{\tau_m+\delta'} w(t) w(t-\delta') dt \right) \quad (2.6.b)$$

where τ_m is the received pulse width. The optimal value of δ for single user channel

environment was discussed in [15]. If duration of δ is longer than the duration of the monopulse, then the transmitted signals representing 0 and 1 are orthogonal.

In Figure 2-3, we demonstrate the binary pulse position modulated data for the i^{th} transmitting symbol when the transmitted data is zero or one. As can be seen from the figure, there is an additional shift of δ when the transmitted data is one compared to sending a zero.

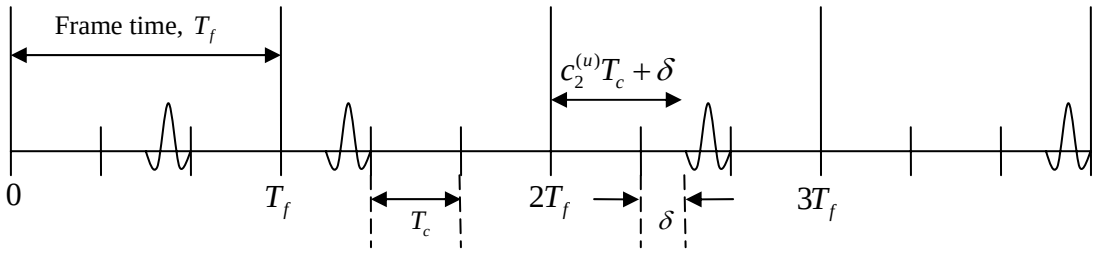

(a)

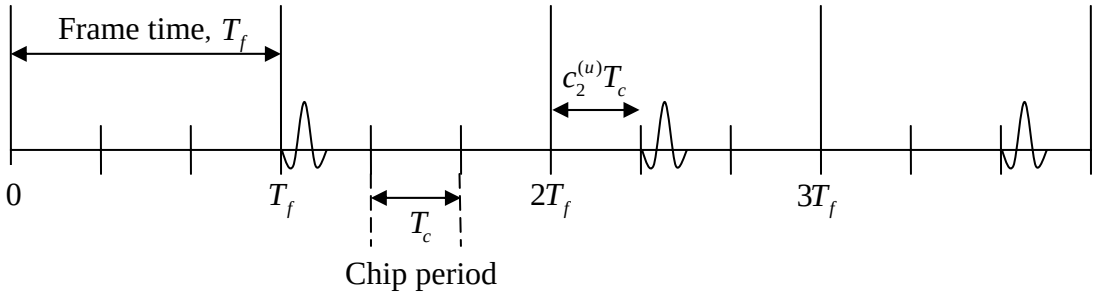

(b)

Figure 2-3: Time hopped Gaussian pulse train with the time hopping sequence of 1,0,1,2
(a) Representing bit '1'with $D_i^{(u)} = 1$
(b) Representing bit '0'with $D_i^{(u)} = 0$

2.3 Data Modulation Techniques

Besides pulse position modulation that has been described in session 2.2, other forms of data modulation can be employed to enhance the performance of the synchronization loops, implementation complexity, interference rejection, etc.

Several modulation techniques have been proposed for UWB signals to modulate the transmitted data; some techniques are more effective than others. Most techniques vary the signals in time or amplitude as a modulation scheme. Some of these popular approaches are pulse position modulation (PPM) and a variety of pulse amplitude modulations (PAM) including binary phase shift keying (BPSK) and on-off keying (OOK) [69] as described below:

A. Pulse Position Modulation (PPM)

Generated pulses are identical, but distinguish the symbol representation of the signal by its position in time. PPM is an orthogonal signaling technique in time. For PPM signaling, the normalized square Euclidean distance between signal $s_1(t)$ and $s_2(t)$ is defined as

$$d^2\left(s_1(t), s_2(t)\right) = \frac{1}{2E_{bit}} \int_o^{T_{bit}} \left|s_1(t) - s_2(t)\right|^2 dt \qquad (2.7.a)$$

$$= \left(1 - \gamma_w(t)\right)$$

where

$$\gamma_w(\tau) = \frac{\int_{-\infty}^{\infty} w(t)w(t-\tau)\,dt}{\int_{-\infty}^{\infty} w^2(t)dt} \qquad (2.7.b)$$

E_{bit} is the bit energy and T_{bit} is the bit duration. The Euclidean distance between any two signals for PPM signaling is less then BPSK signaling. Therefore, the processing gain required for PPM should be larger than BPSK in order to keep the same performance. However, PPM is difficult to realize and has a more stringent constraint on timing since the information is carried by the timing offset. Time-hopping combined with pulse position modulation proposed by Scholtz was originally proposed for UWB systems and is adopted in our study.

B. Pulse Amplitude Modulations (PAM)

PAM modulated the information on the amplitude of a transmitted pulse. Pulses vary in amplitude as according to the represented symbol. The 2-PAM, known as antipodal signaling or BPSK, sends a positive pulse when bit'1' is sent, and negative one for bit '0'. Antipodal signaling can be attractive due to its energy efficiency. As the antipodal signaling provides simplicity compared to M-PAM, antipodal signaling is the chosen modulation in order to avoid pulse amplitude control and automatic gain control circuitry.

C. On-Off Keying (OOK)

On-off keying modulation uses mostly in binary symbol representation with a present of pulse representing a '1' while absence of the pulse representing a '0'. On-off keying is not very energy efficient, but its simplicity may be desirable for low cost systems.

2.4 Representation of UWB Waveform

In an UWB IR system, the choice of pulse shape will strongly affect the choice of receiver bandwidth and the performance of the system. A variety of pulse shapes have been proposed for UWB impulse radio systems including Gaussian pulse, Gaussian monocycles and the Manchester monocycles [70].

It is desirable for UWB signals to spread the energy as widely as possible in frequency to minimize the power spectral density. Thus, these pulses have to be designed for ideal transmission power spectrum and to avoid having a DC component. The spectrum of the signal and the bandwidth is largely determined by the pulse shape.

The ideally modeled pulse shape propagating in free space is the first derivative of the Gaussian pulse generated by the transmitter. In the receiver of the IR system, the receiving antenna system modifies the shape of the transmitted monocycle waveform $w_{tr}(t)$ to $w(t)$ at the output of the antenna system which is modeled as second derivative Gaussian waveform where

$$w(t) = \left[1 - 4\pi\left(\frac{t - t_d}{\tau_m}\right)^2\right] \exp\left[-2\pi\left(\frac{t - t_d}{\tau_m}\right)^2\right] \tag{2.8}$$

in which t_d corresponds to the location of the pulse center in time and τ_m is a parameter which determines the temporal width of the pulse. Figure 2-4 shows the waveform of monopulse $w(t)$ with $t_d = 0$ and $\tau_m = 0.7531ns$. The monocycle waveform $w(t)$ has duration denoted by τ_w . The bandwidth of a pulse is defined as

$$B_c = \frac{1}{\tau_w} \tag{2.9}$$

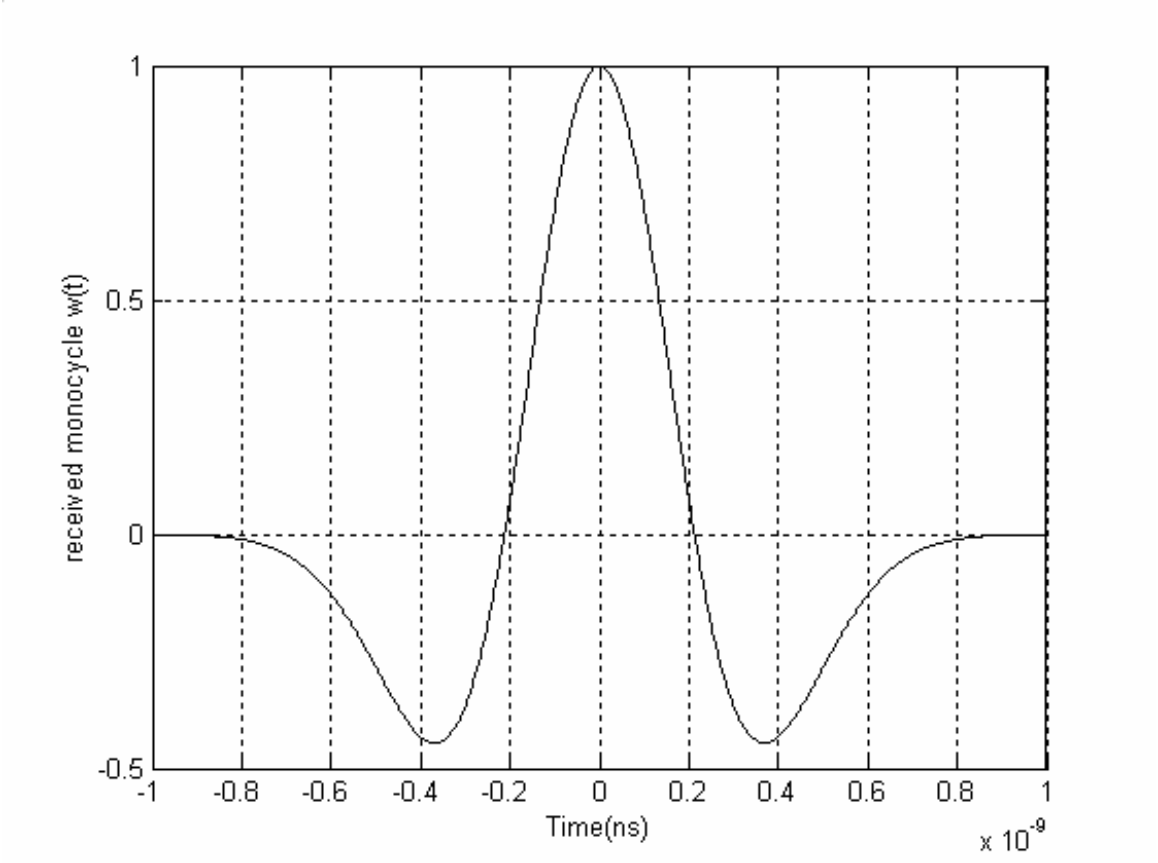

Figure 2-4: Ideal received monocycle pulse shape at the output of the antenna subsystem for $t_d = 0$ and $\tau_m = 0.7531ns$

The autocorrelation $R(x)$ of the Gaussian monopulse $w(t)$ in figure 2-4 is defined as

$$R(x) = \left[1 - 4\pi\left[\frac{t-t_d}{\tau_m}\right]^2 + \frac{4\pi^2}{3}\left[\frac{t-t_d}{\tau_m}\right]^4\right]\exp\left(-\pi\left[\frac{t-t_d}{\tau_m}\right]^2\right) \tag{2.10}$$

In our study, we normalized the Gaussian monocycle waveform which is modeled as

$$w(t) = \sqrt{\frac{8}{3\times\tau_m\times N_s}}\left(\left[1-4\pi\left(\frac{t-t_d}{\tau_m}\right)^2\right]\exp\left[-2\pi\left(\frac{t-t_d}{\tau_m}\right)^2\right]\right) \tag{2.11}$$

where the factor $\sqrt{\frac{8}{3\times\tau_m\times N_s}}$ ensures that the total energy of N_s pulses represents one bit is normalized to one. Therefore,

$$N_s \int_{-\infty}^{\infty} w^2(t)dt = 1 \tag{2.12}$$

The pulse shape is selected such that it has an average value of zero, i.e.,

$$\int_{-\infty}^{\infty} w(t)dt = 0 \tag{2.13}$$

2.5 Impulse Radio Receiver Signal Processing

In ideal multiple access system, when N_u users are active, the composite received signal at the output the receiver's antenna can be modeled as

$$r(t) = \sum_{u=1}^{N_u} \alpha_u s_{rec}^{(u)}(t - \tau_u) + n(t) \tag{2.14}$$

where α_u models the attenuation over the propagation path of the signal $s_{rec}^{(u)}(t - \tau_u)$, received from the u^{th} user. τ_u represents the time asynchronism between the clock of the u^{th} user and the receiver. The waveform $n(t)$ represents the Additive White Gaussian Noise present at the correlator input with double-sided power spectral density of $\frac{N_0}{2}$.

Without lost of generality, we assume that the receiver is determining the data sent by the user 1 and the received signal can be written as

$$r(t) = \alpha_1 s_{rec}^{(1)}(t - \tau_1) + n_{tot}(t) \tag{2.15}$$

$$n_{tot} = \sum_{u=2}^{N_u} \alpha_u s_{rec}^{(u)}(t - \tau_u) + n(t)$$

where n_{tot} is the noise from multiple access and AWGN.

As UWB IR signals are modulated in time, detection methods must be based on the resolving of the time sampling of the transmitted signals. With the knowledge of the position of monopulses in time, the optimum receiver for a binary modulated impulse radio signal in additive white Gaussian noise is a correlator receiver [8]. The IR receiver is based on the theory of hypothesis testing for fully coherent data detection. The performance analysis of the UWB IR system with multiple access interference must be based on the decision statistic used at the receiver. Correlation techniques are used for this application, where a decoding sequence known as the template signals present at the receiver. The architecture of the receiver is shown in figure 2-5.

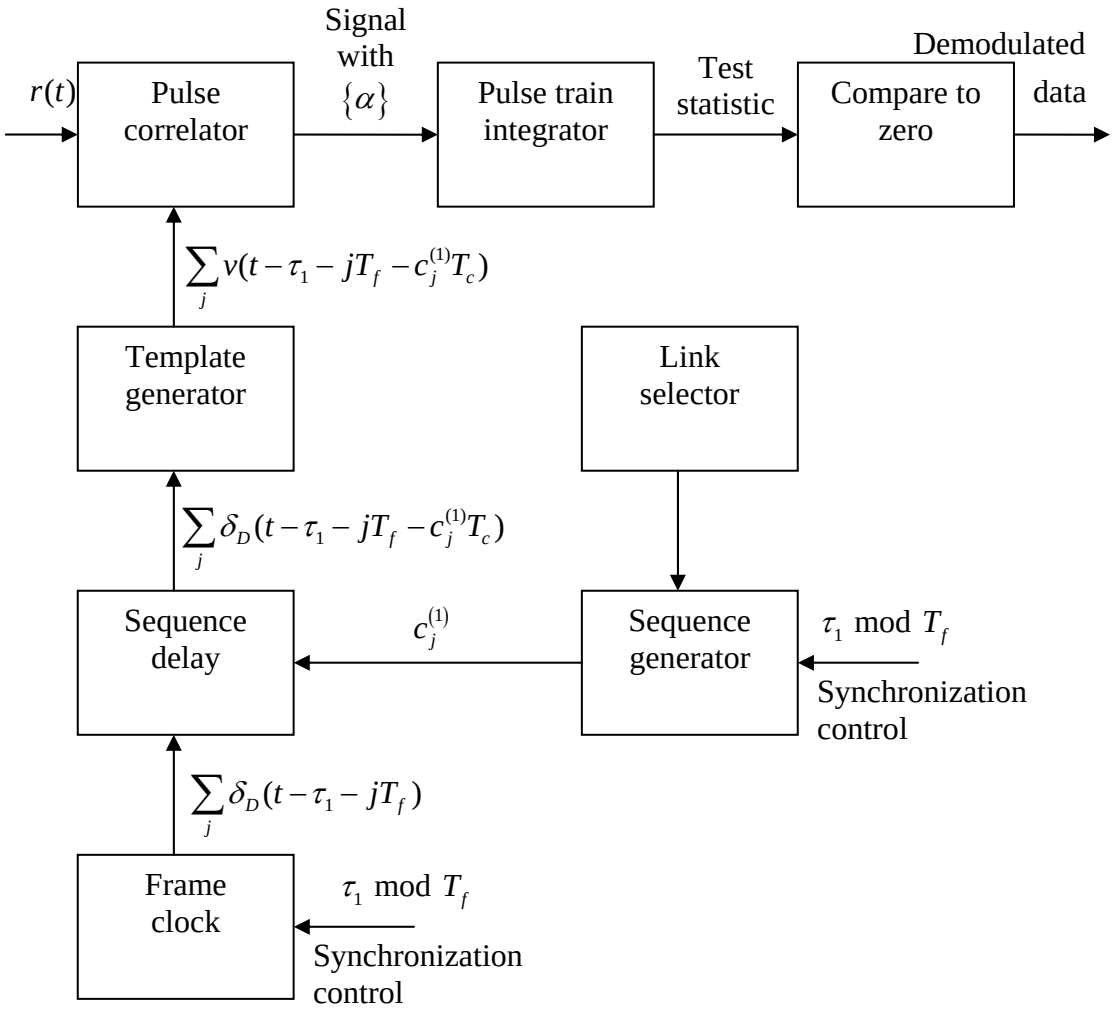

Figure 2-5: Processing structure of the IR receiver

Specifically, from (2.6), $\left\{D_i^u\right\}_{i=-\infty}^{\infty}$ is a binary symbol stream of the u^{th} user for the i^{th} symbol that conveys information in some form. The receiver must decide whether the transmitted symbol D_i^u of the desired user (user 1) is '0' or '1' based on an observation of the received signal $r(t)$ in a time interval of one symbol duration, $T_s = N_s T_f$ at the antenna terminals.

If no other user is present and $\left\{D_i^1\right\}_{i=-\infty}^{\infty}$ is composed of independent random variables, the optimum receiver is a correlation receiver where the received signal $r(t)$ is correlated with the template signal $v(t)$ with the test statistic shown below

$$\text{"decide } D_i^{(1)}=0\text{"} \text{ if } \underbrace{\sum_{j=0}^{N_s-1} \overbrace{\int_{\tau_1+jT_f}^{\tau_1+(j+1)T_f} r(t)v(t-jT_f-c_j^{(1)}T_c)dt}^{\text{pulse correlator output}}}_{\text{test statistic, } \Im} \geq 0 \tag{2.16}$$

$$\text{"decide } D_i^{(1)}=1\text{"} \text{ if } \sum_{j=0}^{N_s-1} \int_{\tau_1+jT_f}^{\tau_1+(j+1)T_f} r(t)v(t-jT_f-c_j^{(1)}T_c)dt < 0$$

$v(t)$ is the template waveform shown in figure 2-6 and is defined as

$$v(t) = w(t) - w(t-\delta) \tag{2.17}$$

The test statistic consists of summing the N_s correlations of the correlator's template signal $v(t)$ at various time shifts with the received signal $r(t)$. If the correlation output is equal or more than zero, the corresponding transmitted symbol is decided as bit '0'. If the correlation output is less than zero, the transmitted symbol is decided as bit '1'. Since the monopulse $w(t)$ is nonzero only in the time interval of $[0, \tau_w]$ where τ_w is the duration of monopulse, the support of template waveform $v(t)$ is $[0, \tau_w + \delta]$.

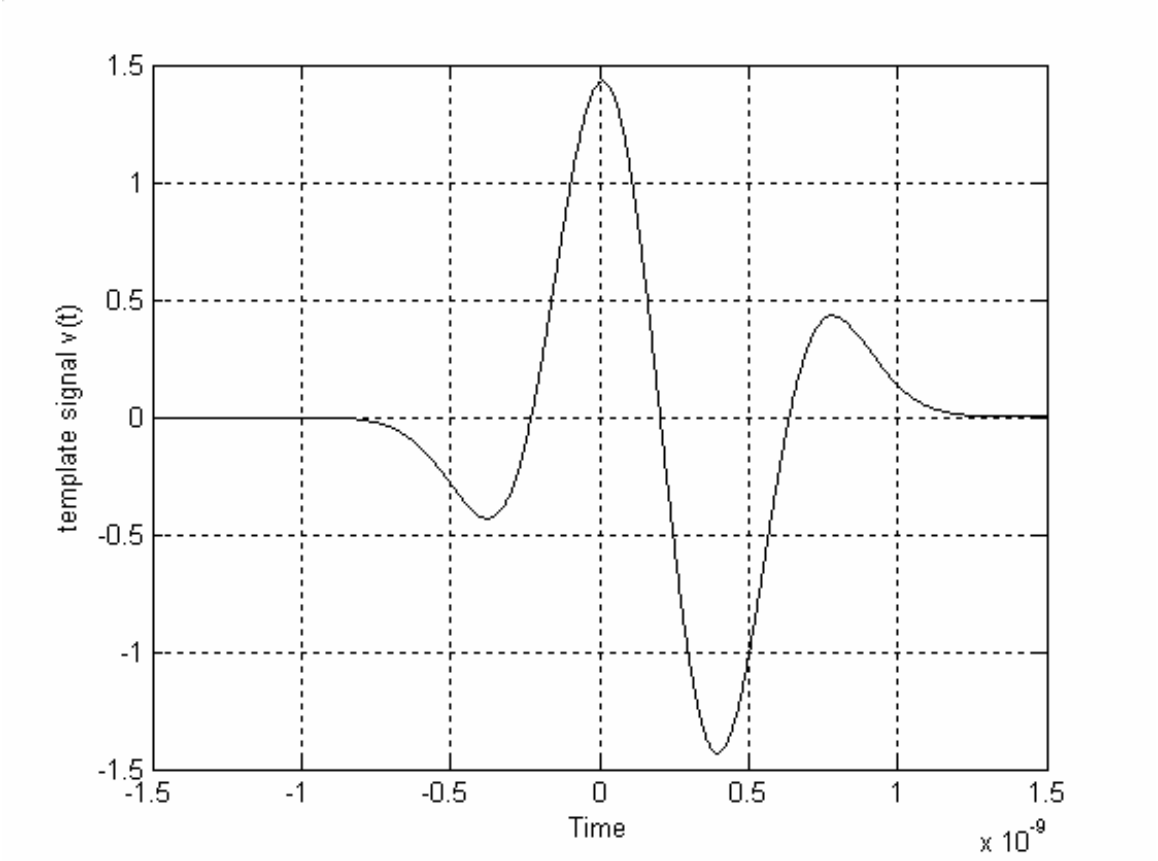

Figure 2-6: Template signal, $v(t)$ used at the receiver of time-hopping impulse radio system

Strictly speaking, the decision rule in (2.16) is no longer optimum when other users are present. The noise from multiple access is not really Gaussian. The optimum receiver needs to make use of the information that the receiver knows about the structure of the multiple access noise. This optimum detection leads to a complicated processing structure at the receiver.

However, if the number of users is large, it is reasonable to approximate the combined effect of the multiuser as a Gaussian random process [8]. With this assumption, the total noise from the multiple access and AWGN, n_{tot} can be modeled as white Gaussian random process. The test statistic in the multi-user environment (bit '1' transmitted) can be written as

$$\Im = m + n_d \tag{2.18}$$

where

$$m = \sum_{j=0}^{N_s-1} \int_{\tau_1+jT_f}^{\tau_1+(j+1)T_f} \left[\alpha_1 \sum_{j=0}^{N_s-1} w(t - jT_f - c_j^{(1)}T_c - \delta - \tau_1) \right] \times v(t - jT_f - c_j^{(1)}T_c - \tau_1)dt \tag{2.19}$$

and

$$n_d = \sum_{j=0}^{N_s-1} \int_{\tau_1+jT_f}^{\tau_1+(j+1)T_f} n_{tot} \times v(t - jT_f - c_j^{(1)}T_c - \tau_1)dt \tag{2.20}$$

2.6 Rake Receiver Structure

As signal propagates over a wideband channel, where the signal bandwidth is much greater then the coherence bandwidth of the radio channel, it will experience frequency selective fading. Propagation delay spread in the radio channel merely provides multiple versions of the transmitted signal at the receiver. Spread spectrum system of IR has the ability to resolve closely spaced multipath components encountered in the channel. The detection of SS signal in a multipath environment leads to a Rake receiver. It is designed to exploit the path diversity to resolve the components of a received signal which arrived in different times and combine them to improve the signal-to-noise ratio. In fact, Rake receiver attempts to collect the energy by collecting the time-shifted versions of the original signal by providing a separate correlation receiver for each of the multipath signals. Discussions on classical Rake receivers can be found in [71, 72].

The basic idea of a Rake receiver was first proposed by Price and Green [72]. Rake receiver consists of a bank of L fingers (correlators) to separately detect the L

multipath components. Each finger can detect/extract the signal from one of the multipath components created by the channel. The outputs of each correlator are then weighted to provide a better estimate of the transmitted signal than is provided by a single component. Demodulation and bit decisions are then based on the weighted outputs of the L correlators. By demodulating several replicas of the transmitted signal, where each replica experiences a particular multipath delay, the Rake receiver is able to align the replicas in time and thus provide a better estimate of the original signal. Rake receiver that processes the received signal in an optimum manner will achieve the performance of an equivalent L^{th} order diversity communication system.

The structure of a Rake receiver is shown in figure 2-7. Rake receiver employs a single delay line model through which the received signal is passed. The time-varying tap weight $\{\alpha_l(t)\}$ corresponding to the L different delays are uncorrelated. At the output of the Rake receiver, a combining scheme can be employed to make use of the resolvable paths. The available diversity combining schemes are maximum ratio combing (MRC), equal gain combining (EGC) and selection combining (SC).

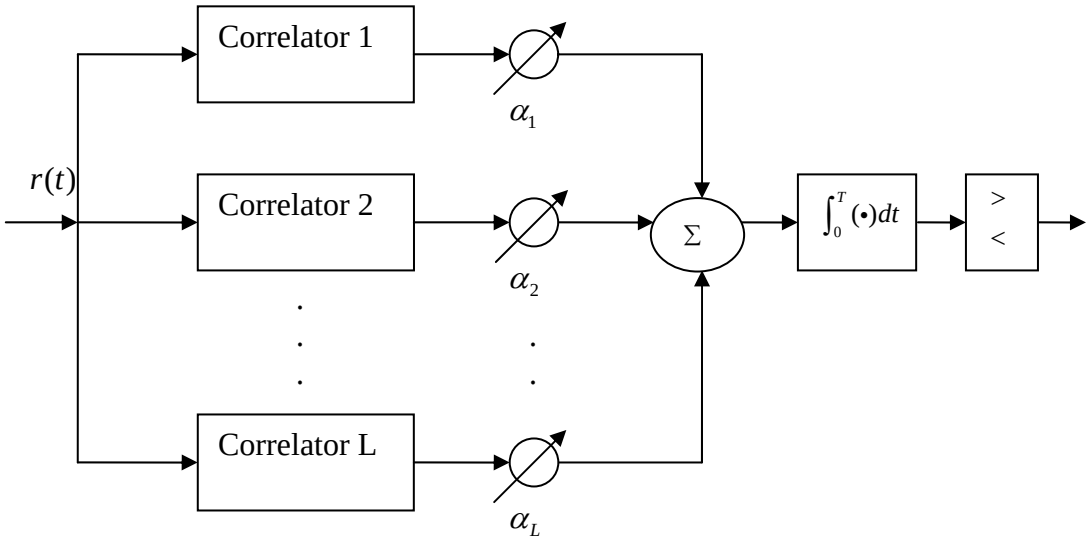

Figure 2-7: Structure of the Rake receiver with L branches

2.7 Diversity Reception

Diversity is a powerful communication receiver technique that provides wireless link improvement. Specially, diversity reception is a promising technique designed to overcome channel fading by providing several replicas of the same information signal transmitted over different fading branches to the receiver.

Diversity exploits the random nature of radio propagation by finding independent signals paths for communications. The diversity concept is based on the fact that the probability for all diversity branches having deep fades simultaneously is very low. if one radio path undergoes a deep face, another independent path may have a strong signal. By having more than one path to select from, the performance of the system can be improved.

A commonly used method to implement diversity reception in wireless system is to use multiple antennas to attain space diversity, also known as antenna diversity. As these reception antennas are spaced sufficiently far apart, independently fading components of transmitted signals can be obtained. For spatial diversity to work effectively, the signal received by various antenna branches must be sufficiently decorrelated so that if one of the elements is in deep fades, there is still hope of recovering the signal by receiving it at another elements. Combining techniques are then employed to form decision metric. In UWB IR system, antenna diversity can be used to collect the energy from different multipaths that arrived at the receiver [64].

Antenna diversity can be exploited by arranging multiple antennas in an array. In this thesis, two simple types of array will be considered, namely uniform linear array and rectangular planar array.

2.8 Property of Antenna Array

For UWB array, delay and sum processing technique is applied to process the received signal [73]. The delay equations which describe the propagation of the signal across the array are needed. Then, as in figure 2-8, with a plane wave incident at an azimuth angle of θ degrees with respect to broadside, the relative propagation distance between two antennas is $d\sin\theta$. In order to resolve both the azimuth angle of incidence and the elevation angle, in one hemisphere, another dimension must be added to the array. This leads to the planar structure shown in figure 2-9. In this case, the incremental delay in the x direction is given by $\left(\frac{d_x}{c}\right)\cos\theta\sin\phi$ and in the y direction by $\left(\frac{d_y}{c}\right)\sin\theta\sin\phi$.

d_x is the antenna spacing in the x direction and d_y is the antenna spacing in y direction.

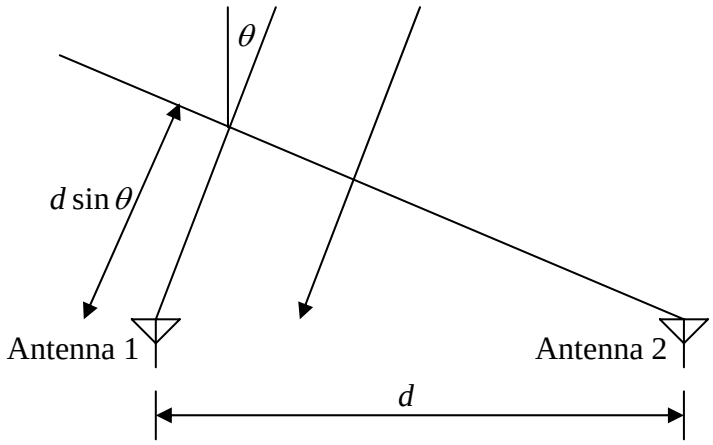

Figure 2-8: Differential propagation distance between antenna elements for plane wave incidence

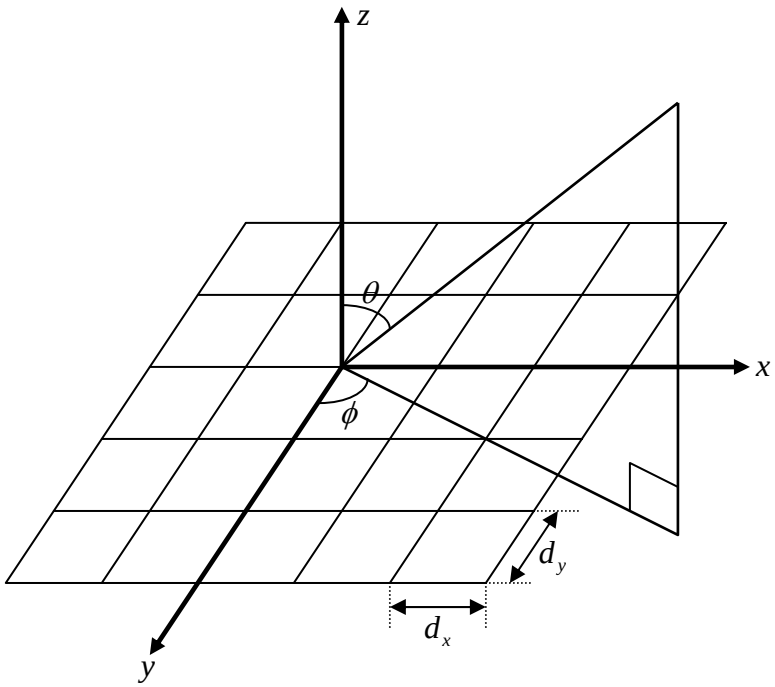

Figure 2-9: Planar array geometry and definitions

CHAPTER 3

PERFORMANCE OF UWB IR SYSTEMS WITH ANTENNA ARRAY

3.1 Introduction

In this chapter, the influence of temporal and spatial diversities on the performance of Ultra-wideband impulse radio systems is analyzed. We investigate how antenna diversity (uniform linear array and rectangular array) can be used to improve the bit error rate performance and can cope with the effects of multiuser interference (MUI) of IR system in multipath fading channel with multiuser environments.

This chapter presents the bit error rate (BER) performance and characteristic of the binary modualated IR systems with antenna array using Selective Rake (SRake) receiver in the presence of multipaths and multiuser interference (MUI). Particular attention is given to the effects of the number of employed antenna elements and the number of the selected multipaths on the BER performance in single user and multiuser environments. The performances of the systems with uniform linear arrays and rectangular arrays receiver are also compared.

Analytical and simulation results show that the BER performance of the IR system can be improved when the number of array elements is increased. The performance can be further improved by coherently adding more multipaths at the receiver.

3.2 Application of Antenna Array in UWB IR Systems

The ill effects of the multipath fading and multiple access in wireless systems can be reduced by employing spatial diversity. In this thesis, multi-element antenna array at the receiver is employed to attain the diversity. Two types of equally-spaced array configurations are considered, namely rectangular planar arrays $(A \times B)$ and uniform linear arrays $(A \times 1)$.

For the rectangular planar array, the elements are placed along a rectangular grid [67] as shown in figure 3-1.

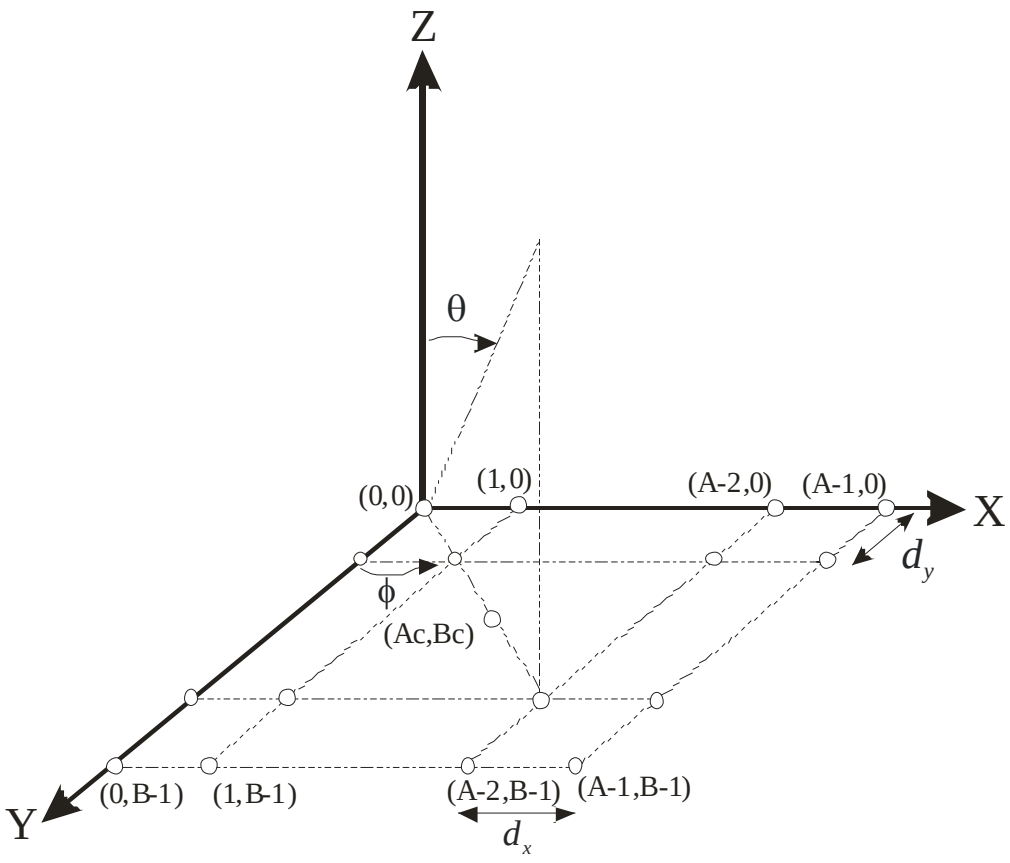

Figure 3-1: Planar array of elements on a rectangular lattice

In this figure, θ is the elevation look angle whereas ϕ is the azimuth angle. (A_c, B_c) in the figure is the coordinate of the center element which is also the reference element. For the rectangular array, there are B rows of elements parallel to the x axis and each row contains A elements. For uniform linear array, the antenna elements are placed linearly along the x axis with the element at the origin acting as the reference element.

The delay and sum beamformer is used to process the received signals at the array elements. By coherently combining the signals from different antenna elements, the performance of UWB IR system could be improved significantly [64]. The beamformer output for a rectangular planar array steered to an azimuth angle of ϕ and an elevation angle of θ, on incidence of a plane wave from an azimuth angle of ϕ_0 and an elevation angle of θ_0 can be written as [74]

$$\mathrm{B}(\phi,\theta,t) = \sum_{a=0}^{A-1}\sum_{b=0}^{B-1} a_{a,b}(\phi,\theta) \times w\left(t-\tau_{a,b}\right) \tag{3.1}$$

$$\tau_{a,b} = (a_r - a)\frac{d_x}{c}(u-u_0) + (b-b_r)\frac{d_y}{c}(v-v_0) \tag{3.2}$$

where $u = \sin\phi\sin\theta$, $u_0 = \sin\phi_0\sin\theta_0$, $v = \cos\phi\sin\theta$ and $v_0 = \cos\phi_0\sin\theta_0$. c is speed of light and the notation of d_x and d_y represent the spacing between the antenna elements in x and y direction respectively. (a_r, b_r) is the coordinate of the reference element. $a_{a,b}(\phi,\theta)$ is the element pattern of the element position at (a,b) coordinate in the array. We assume that each element has an isotropic pattern. Therefore, $a_{a,b}(\phi,\theta)$ is equal to one. $\tau_{a,b}$ is the time delay of the signal received by the $(a,b)^{th}$ element with respect to the reference element and is a function of direction of arrival and geometry of the array.

The beamformer expression depends on the received signal pulse shape and the time delay of the received signal. We assume that the signals are on the xy plane and hence the elevation angle, $\theta = 90^0$. Figure 3-2 shows the 3-dimensional plot of the antenna array response, $B(\phi, \theta, t)$ to the received waveform $w(t)$ for a 25 elements of rectangular planar array with signal incident at azimuth angle of 45^0 ($\phi_0 = 45^0$), and elevation angle of 90^0 ($\theta_0 = 90^0$).

For the uniform linear array, the summation of the n element is omitted and the beamformer output can be written as

$$\mathrm{B}(\phi, \theta, t) = \sum_{a=0}^{A-1} a_a(\phi, \theta) \times w(t - \tau_a) \tag{3.3}$$

$$\tau_a = (A_c - m)\frac{d_x}{c}(u - u_0) \tag{3.4}$$

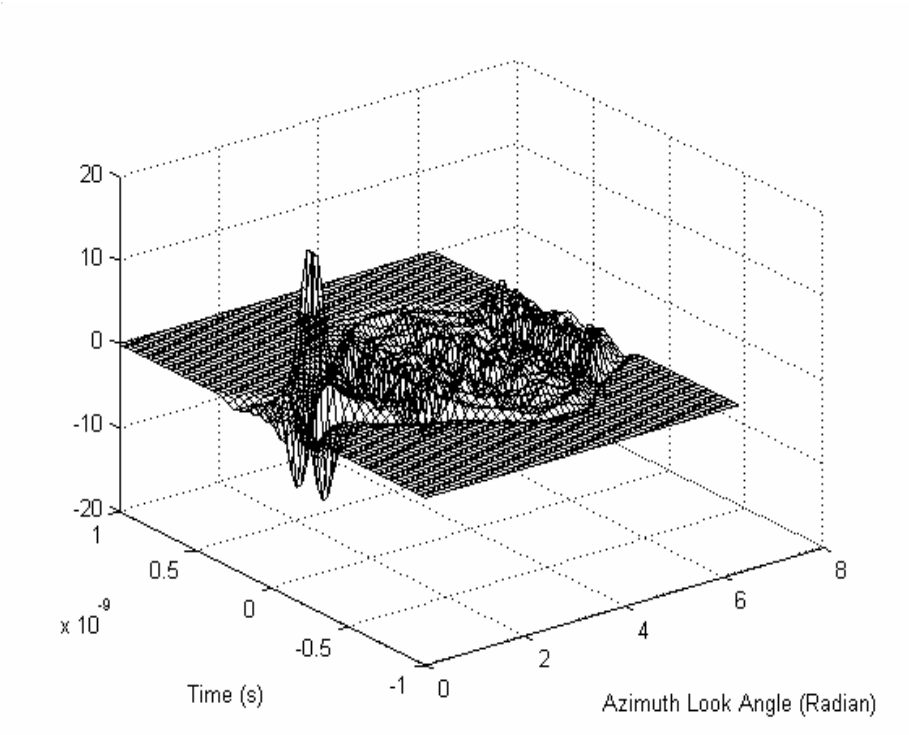

Figure 3-2: The beamforming output of a (5×5) rectangular planar array as a function of time and azimuth look angle with $\theta = 90^0$ $\phi_0 = 45^0$, $\theta_0 = 90^0$.

3.3 Channel Model

For the channel model, we consider a wireless indoor IR multipath channel with AWGN. The channel model is based on Saleh-Valenzuela (S-V) model with slight modifications that can be referred in the report of IEEE P802.15 WPAN [35, 64, 75]. For the S-V channel model, the magnitude of the channel gain followed a Rayleigh distribution. However, the proposed channel model for UWB from IEEE P802.15 used a log normal distribution for the multipath gain magnitude instead of Rayleigh distribution as many observations show that lognormal distribution seems to better fit the measurement data from channel modeling.

S-V channel model is characterized by clustering phenomenon of rays. The clustering phenomenon is that rays arrive in several groups within an observation window. Each cluster consists of many rays. The magnitudes of the clusters are attenuated exponentially with time controlled by cluster decay factor (Γ) and the magnitudes of rays within each cluster decay exponentially with time controlled by the ray decay factor (γ). Typically, the cluster decay factor is larger than the ray decay factor $(\Gamma > \gamma)$ and therefore we assumed the rays within different clusters do not overlap. We consider constant cluster arrival rate (Λ) and ray arrival rate (λ) where $\lambda > \Lambda$ with deterministic cluster and ray arrival time. Each ray within each cluster has an associated time delay, an azimuth angle, ϕ and an elevation angle, θ. Independent fading is assumed for each cluster, for each ray within the clusters and for each antenna element.

Let the arrival time of the q^{th} cluster denoted by τ_q in which $q = 0,1,2,...Q-1$and the arrival time of the k^{th} ray measured from the beginning of the q^{th} cluster be denoted by $\tau_{k,q}$, where $k = 0,1,2...K-1$. Q is the total number of clusters and K is the total number of rays within each cluster. The total number of multipath, L_{total} is defined as

$$L_{total} = Q \times K \tag{3.5}$$

The discrete time channel impulse response is represented as

$$h(t) = \sum_{a=0}^{A-1}\sum_{b=0}^{B-1}\sum_{q=0}^{Q-1}\sum_{k=0}^{K-1}\alpha_{k,q,a,b}\delta\left(t-\tau_{a,b}-\tau_q-\tau_{q,k}\right) \tag{3.6}$$

$$= \sum_{a=0}^{A-1}\sum_{b=0}^{B-1}\sum_{q=0}^{Q-1}\sum_{k=0}^{K-1}\alpha_{k,q,a,b}\delta\left(t-\tau_{k,q,a,b}\right)$$

$$= \sum_{a=0}^{A-1}\sum_{b=0}^{B-1}\sum_{l=0}^{L_{total}-1}\alpha_{l,a,b}\delta\left(t-\tau_{l,a,b}\right)$$

where $\alpha_{k,q,a,b} \in \Re$, $\tau_{k,q,a,b} = \tau_{a,b} + \tau_q + \tau_{k,q}$ and $\delta(t)$ is the Dirac delta function. $\left\{\alpha_{k,q,a,b}\right\}$ are the gain coefficients of each k^{th} ray within each q^{th} cluster for each antenna element with coordinate (a,b). $\tau_{a,b}$ is the time delay of the $(a,b)^{th}$ element which is a function of the array's geometry, the azimuth angle and the elevation angle The equation of $\tau_{a,b}$ is defined in (3.2). $\tau_{k,q,a,b}$ is the time delay of the k^{th} ray of the q^{th} cluster associated with a certain antenna element position at the grid (a,b) of the array with respect to the first ray of the first cluster at the reference antenna element.

The magnitudes of the channel gain follow a lognormal distribution [35]. The channel coefficients are defined as:

$$\alpha_{k,q,a,b} = a_{k,q,a,b}\xi_{q,a,b}\beta_{k,q,a,b} \tag{3.7}$$

where

$$20\log_{10}\left(\xi_{q,a,b}\beta_{k,q,a,b}\right) \propto Normal\left(\mu_{k,q,a,b}, \sigma_1^2 + \sigma_2^2\right) \tag{3.8}$$

$\xi_{q,a,b}$ corresponds to the fading associated with the q^{th} cluster of the $(a,b)^{th}$ antenna element whereas $\beta_{k,q,a,b}$ reflects the fading associated with the k^{th} ray in the q^{th} cluster of the $(a,b)^{th}$ antenna element. $a_{k,q,a,b}$ is the sign +/- with equal probability for the channel gain to consider the signal inversion due to the reflection. The log value of each channel gain follows a normal distribution with mean $\mu_{k,q,a,b}$ and variance $\sigma_1^2 + \sigma_2^2$ where σ_1^2 is the variance of the cluster lognormal fading term in dB and σ_2^2 is the variance of the ray lognormal fading term in dB. The normalized mean square value of $\alpha_{k,p,a,b}$ is defined as

$$\mathrm{E}\left[\alpha_{k,p,a,b}^2\right] = \Omega_0 e^{-\tau_{q,a,b}/\Gamma} e^{-\tau_{k,q,a,b}/\gamma} \tag{3.9}$$

where

$$\Omega_0 = \frac{\alpha_{0,0,a_r,b_r}^2}{\sum_{q=0}^{Q-1}\sum_{k=0}^{K-1}\alpha_{k,q,a_r,b_r}^2} \tag{3.10}$$

Ω_0 is the average power of the first ray of the first cluster of the reference antenna element $\left(a_r, b_r\right)$ which has been normalized by the total power of the reference antenna element. The $\mu_{k,q,a,b}$ is then defined as

$$\mu_{k,q,a,b} = \frac{10\ln\left(\Omega_0\right) - 10\tau_{q,a,b} - 10\tau_{k,q,a,b}}{\ln(10)} - \frac{\left(\sigma_1^2 + \sigma_2^2\right)\ln(10)}{20} \tag{3.11}$$

A complex tap channel model is not being used to model the UWB channel since real valued simulation of RF is more suitable for UWB as there is no carrier frequency for

UWB signal to cause complex low pass equivalent model. Complex base band model is more suitable to model the narrow band channel model.

We assume perfect channel estimation in this study. The channel is also assumed to change slowly with time and to have a multipath spread of τ_s where $\tau_s > 1/BW$ with BW being the bandwidth of the signal. Hence, the channel is modeled as frequency-selective channel.

3.4 Impulse Radio Receiver Array Processing for Binary Modulated Signal

In an impulse radio channel under multipath environments, a Rake receiver can be used to resolve the multipath components having differential delays of the order of nanosecond [20] which is approximately equal to the inverse of the spreading bandwidth. Rake receiver consists of multiple fingers (correlators) where each finger can extract signal from one of the multipath components. A selective Rake receiver (SRake) with L_f fingers selects the first L_f dominant paths, each is processed in a separate finger and combines them using maximal-ratio combining (MRC) to provide diversity.

We use Selective Rake (SRake) receiver with $(A \times B)$ antenna array, each element with L_f-Rake fingers as shown in figure 3-3 where the space-time correlators can be used to process the received signals that are separated in space and time. It is assumed that the receiver is perfectly synchronized to the hopping code of the desired user and knows the time delay of each selected path.

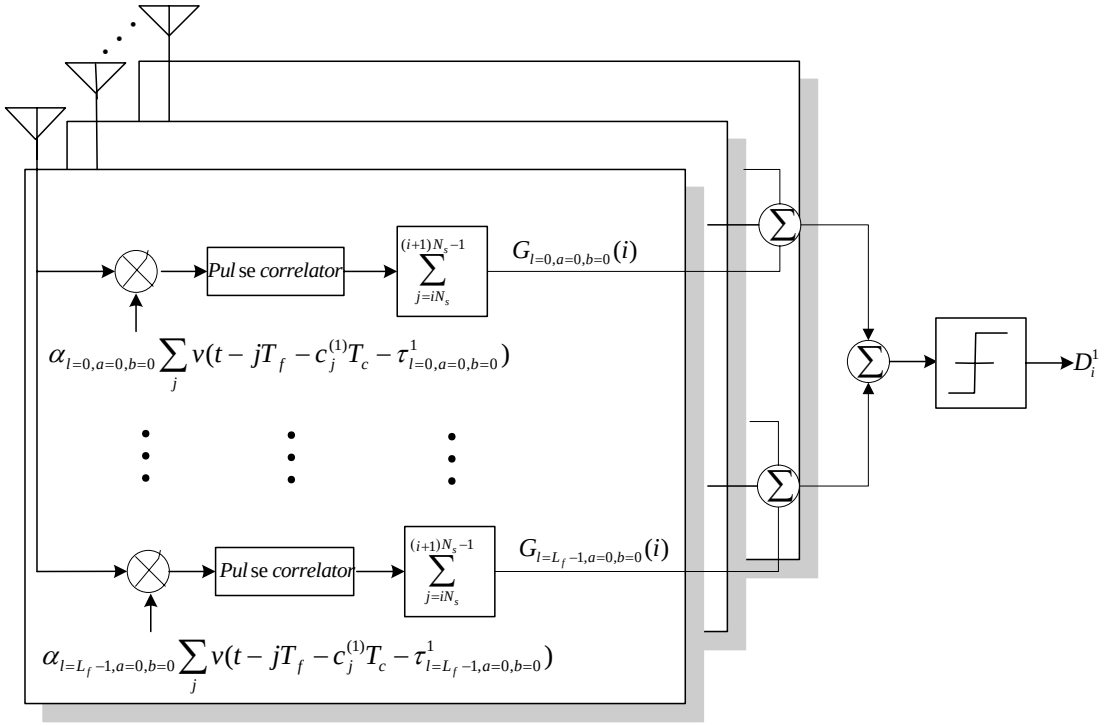

Figure 3-3: Block diagram of SRake receiver with antenna array for binary modulated PPM IR signal

Let's assume the receiver is interested in determining the data sent by the user 1, and the receiver selects the first $L_f^{u=1}$ dominant paths of the user 1. The received signal can be written as

$$r(t)=\sum_{a=0}^{A-1}\sum_{b=0}^{B-1}\sum_{l=0}^{L_f^1-1}\alpha_{l,a,b}^1 s_{rec}^1\left(t-\tau_{l,a,b}^1\right)+n_{ns}(t)+n_{ma}(t)+n_{m,n}(t) \tag{3.12}$$

where

$$n_{ns}(t)=\sum_{a=0}^{A-1}\sum_{b=0}^{B-1}\sum_{l=L_f^1}^{L_{total}^1-1}\alpha_{l,a,b}^1 s_{rec}^1\left(t-\tau_{l,a,b}^1\right) \tag{3.13}$$

and

$$n_{ma}(t)=\sum_{u=2}^{N_u}\sum_{a=0}^{A-1}\sum_{b=0}^{B-1}\sum_{l=0}^{L_{total}^u-1}\alpha_{l,a,b}^u s_{rec}^u\left(t-\tau_{l,a,b}^u\right) \tag{3.14}$$

$n_{ns}(t)$ is the interference from the non-selected paths of the user 1, $n_{ma}(t)$ is the interference from undesired users and $n_{a,b}(t)$ is the AWGN noise for the $(a,b)^{th}$ element with double-sided power spectral density of $N_0/2$ watts/Hz. $\{\alpha^u_{l,a,b}\}$ are the channel gain coefficients of l^{th} path for the $(a,b)^{th}$ antenna element of the u^{th} user. $\tau^u_{l,a,b}$ is the time delay of the l^{th} path of the $(a,b)^{th}$ element for user u relative to the 1st path of the reference element (a_r,b_r) of the user 1, τ^1_{1,a_r,b_r}. We assume $\tau^1_{1,a_r,b_r} = 0$.

For the IR system in the single user environment, multiple access noise $n_{ma}(t)$ will be omitted and the received signal become

$$r(t) = \sum_{a=0}^{A-1}\sum_{b=0}^{B-1}\sum_{l=0}^{L_f^1-1}\alpha^1_{l,a,b}s^1_{rec}\left(t-\tau_{l,a,b}\right) + n_{ns}(t) + n_{m,n}(t) \tag{3.15}$$

If the IR system operates in the only AWGN environment, the received signal can be written as

$$r(t) = \sum_{a=0}^{A-1}\sum_{b=0}^{B-1}s^1_{rec}\left(t-\tau_{a,b}\right) + n_{a,b}(t) \tag{3.16}$$

The received signals at the Rake receiver will be correlated with the template waveform at each finger of the receiver of each antenna element. The correlator output at the selected l^{th} path of the $(a,b)^{th}$ element for the i^{th} symbol is as follow

$$G_{l,a,b}(i) = \int_{t=iN_sT_f+\tau^1_{l,a,b}}^{(i+1)N_sT_f+\tau^1_{l,a,b}} r(t)\sum_{j=iN_s}^{(i+1)N_s-1}\alpha^1_{l,a,b}v\left(t-jT_f-c^1_jT_c-\tau^1_{l,a,b}\right)dt \tag{3.17}$$

$$= \int_{t=iN_sT_f+\tau^1_{l,a,b}}^{(i+1)N_sT_f+\tau^1_{l,a,b}} r(t)\alpha^1_{l,a,b}v_{bit}(t)dt$$

where

$$v_{bit}(t) = \sum_{j=iN_s}^{(i+1)N_s-1} v\left(t - jT_f - c_j^1 T_c - \tau_{l,a,b}^1\right) \tag{3.18}$$

$$= w_{bit}(t) - w_{bit}(t-\delta)$$

$v_{bit}(t)$ is the template signal for one bit duration. The bit waveform, $w_{bit}(t)$ is defined as

$$w_{bit}(t) = \sum_{j=iN_s}^{(i+1)N_s-1} w\left(t - jT_f - c_j^1 T_c - \tau_{l,a,b}^1\right) \tag{3.19}$$

$w_{bit}(t)$ is signal representing bit '0', whereas $w_{bit}(t-\delta)$ representing signal of bit '1'. The embedded one pulse template signal is $v(t) = w(t) - w(t-\delta)$ in which $w(t)$ is the received monocycle. $v_{bit}(t)$ consists of N_s of embedded one pulse template signal, $v(t)$. Note that there is a channel gain $\alpha_{l,a,b}^1$ in front of the template signal for the maximal ratio combining purpose.

For each finger of the receiver, the associated path selected by that particular finger is treated as desired signal (s_d) and the rest of the received paths are treated as noise (n_d). The rest of received paths from the user of interest are treated as self noise interference and the other paths received from other multiple access users is treated as multiuser interference. Hence, for finger that selects the l^{th} path of the $(a,b)^{th}$ element, the correlator output for that particular finger can be written as

$$G_{l,a,b}(i) = \underbrace{\int_{t=iN_sT_f+\tau_{l,a,b}^1}^{(i+1)N_sT_f+\tau_{l,a,b}^1} \left(\alpha_{l,a,b}^1 s_{rec}^1\left(t-\tau_{l,a,b}^1\right)\right)\alpha_{l,a,b}^1 v_{bit}(t)dt}_{s_d} + \underbrace{\int_{t=iN_sT_f+\tau_{l,a,b}^1}^{(i+1)N_sT_f+\tau_{l,a,b}^1} \left(n_{total}\right)\alpha_{l,a,b}^1 v_{bit}(t)dt}_{n_d} \tag{3.20}$$

where

$$n_{total} = \sum_{\substack{l=0 \\ l\neq l^{th}}}^{L_{total}^1-1} \alpha_{l,m,n}^1 s_{rec}^1\left(t-\tau_{l,m,n}^1\right) + \sum_{u=2}^{N_u}\sum_{l=0}^{L_{total}^u-1} \alpha_{l,m,n}^u s_{rec}^u\left(t-\tau_{l,m,n}^u\right) + n_{m,n}(t) \tag{3.21}$$

The test statistic of the i^{th} transmitted symbol depends on the sum of the pulse correlator outputs of each selected path of each antenna element, which is

$$G(i) = \sum_{a=0}^{A-1} \sum_{b=0}^{B-1} \sum_{l=0}^{L_f^1 - 1} G_{l,a,b}(i) \tag{3.22}$$

The receiver correlates the received signal with a template signal, v_{bit} and makes binary decisions depending on the sign of correlation values based on the test statistic as shown below:

$$G(i) \geq 0 \Rightarrow D_i^1 = 0 \tag{3.23}$$

$$G(i) < 0 \Rightarrow D_i^1 = 1$$

If the sum of the pulse correlator output is greater or equal to zero $\left(G(i) \geq 0\right)$, the transmitted signal for the i^{th} symbol is decided as bit '0' $\left(D_i^1 = 0\right)$. Else, if the sum of the pulse correlator output $G(i)$ is less than zero $\left(G(i) < 0\right)$, the transmitted symbol for the i^{th} symbol is decided as bit '1' $\left(D_i^1 = 0\right)$.

3.5 BER Analysis for Binary PPM IR Modulated Signal

In this chapter, binary PPM IR modulation is considered. The binary IR signal model has been described in section (2.2). The demodulation format considered here is based on correlation. The UWB received basic monopulse $w(t)$ has energy denoted by E_w and is defined as

$$E_w = \int_{-\infty}^{\infty} w^2(t) dt \tag{3.24}$$

The correlation function of the monopulse is defined as

$$\lambda_w(\tau) = \int_{-\infty}^{\infty} w(t)w(t-\tau)\,dt \tag{3.25}$$

The normalized correlation function of a monopulse is given by

$$\gamma_w(\tau) = \frac{\int_{-\infty}^{\infty} w(t)w(t-\tau)\,dt}{\int_{-\infty}^{\infty} w^2(t)dt} \tag{3.26}$$

$$= \frac{\lambda_w(\tau)}{\lambda_w(0)} = \frac{\lambda_w(\tau)}{E_w}$$

The transmitted signal that represents the i^{th} symbol is composed of N_s time shifted version of the pulses. Thus, the energy of one bit symbol is defined as

$$E_{bit} = \int_{-\infty}^{\infty} s_{rec}^2(t)dt \tag{3.27}$$

$$= \int_{-\infty}^{\infty} w_{bit}^2(t)\,dt$$

$$= N_s \int_{-\infty}^{\infty} w^2(t)\,dt = N_s E_w$$

E_{bit} is normalized to have a unity-energy, hence $E_{bit} = 1$. The equation of normalized monopulse shape is shown in (2.11).

The correlation function of a received signal is given by

$$\lambda_{bit,pq}(\tau) = \int_{-\infty}^{\infty} s_{rec,p}(t)s_{rec,q}(t)\,dt \tag{3.28}$$

$$= \int_{-\infty}^{\infty} w_{bit}(t)w_{bit}(t-\tau)\,dt$$

$$= N_s \int_{-\infty}^{\infty} w(t)w(t-\tau)\,dt$$

$$= N_s \lambda_w(\tau)$$

where $p,q=0,1$ and $p \neq q$. $w_{bit}(t)$ is defined in (3.19). The normalized correlation function of the signal can be defined as

$$\rho_{pq} = \frac{\int_{-\infty}^{\infty} s_{rec,p}(t)\, s_{rec,q}(t)\, dt}{E_{bit}} \tag{3.29}$$

$$= \frac{\int_{-\infty}^{\infty} w_{bit}(t)\, w_{bit}(t-\delta)\, dt}{\int_{-\infty}^{\infty} w_{bit}^2(t)\, dt}$$

$$= \frac{1}{N_s} \sum_{k=0}^{N_s-1} \gamma_w\left(\tau_p^k - \tau_q^k\right)$$

For binary PPM IR signal as described in section (2.2),

$$\rho_{pq} = \gamma_w(\tau) \qquad p,q=0,1;\ p \neq q \tag{3.30}$$

as the correlation value for each pulse within one bit is the same. Note that

$$\rho_{01} = \rho_{10} = \rho \tag{3.31}$$

The cross-correlation between the template waveform, $v(t)$ and received monopulse, $w(t)$ is defined by

$$R_{wv}(\tau) = \int_{-\infty}^{\infty} w(t-\tau)\, v(t) dt \tag{3.32}$$

As $v(t)$ has non-zero values only in the interval of $[0, \tau_w + \delta]$, $R_{wv}(\tau)$ will have non-zero value in the interval $[-\tau_w, \tau_w + \delta]$. The notation of τ_w is the duration of a monopulse.

From (3.20), the desired correlator output of the l^{th} finger of the $(m,n)^{th}$ element if the transmit signal is '0' is given by,

$$s_{d0} = \left(\alpha^1_{l^{th},(a,b)^{th}}\right)^2 \int_{t=iN_sT_f+\tau^1_{l,a,b}}^{(i+1)N_sT_f+\tau^1_{l,a,b}} w_{bit}(t)\left(w_{bit}(t) - w_{bit}(t-\delta)\right) dt \tag{3.33}$$

$$= \left(\alpha^1_{l^{th},(a,b)^{th}} \right)^2 N_s R_{wv}(0)$$

$$= \left(\alpha^1_{l^{th},(a,b)^{th}} \right)^2 E_{bit} \frac{\int_{t=iN_sT_f+\tau^1_{l,a,b}}^{(i+1)N_sT_f+\tau^1_{l,a,b}} {w_{bit}}^2(t)\,dt - \int_{t=iN_sT_f+\tau^1_{l,a,b}}^{(i+1)N_sT_f+\tau^1_{l,a,b}} w_{bit}(t) w_{bit}(t-\delta)\,dt}{\int_{t=iN_sT_f+\tau^1_{l,a,b}}^{(i+1)N_sT_f+\tau^1_{l,a,b}} {w_{bit}}^2(t)\,dt}$$

$$= \left(\alpha^1_{l^{th},(a,b)^{th}} \right)^2 E_{bit}(1-\rho)$$

where ρ is normalized correlation function of the signal and is defined in (3.30). If the transmit signal is '1', the desired correlator output of the l^{th} finger of the $(a,b)^{th}$ element is given by

$$s_{d1} = \left(\alpha^1_{l^{th},(a,b)^{th}} \right)^2 \int_{t=iN_sT_f+\tau^1_{l,a,b}}^{(i+1)N_sT_f+\tau^1_{l,a,b}} w_{bit}(t-\delta)\left(w_{bit}(t) - w_{bit}(t-\delta) \right) dt \tag{3.34}$$

$$= \left(\alpha^1_{l^{th},(a,b)^{th}} \right)^2 E_{bit}(\rho-1)$$

For the transmitted signal of '0', the total desired correlator signal output which is the sum of all selected fingers of all the antenna elements' outputs is

$$s_{D0} = \left(\sum_{a=0}^{A-1} \sum_{b=0}^{B-1} \sum_{l=0}^{L^1_f-1} {\alpha^1_{l,a,b}}^2 \right) E_{bit}(1-\rho) \tag{3.35}$$

If the transmitted bit is '1', the total desired correlator signal output is

$$s_{D1} = \left(\sum_{a=0}^{A-1} \sum_{b=0}^{B-1} \sum_{l=0}^{L^1_f-1} {\alpha^1_{l,a,b}}^2 \right) E_{bit}(\rho-1) \tag{3.36}$$

The total signal energy contained in all the selected paths from all the antenna elements can be written as

$$E_s = {s_{D0}}^2 = {s_{D1}}^2 \tag{3.37}$$

$$= {N_s}^2 \left(\sum_{a=0}^{A-1} \sum_{b=0}^{B-1} \sum_{l=0}^{L^1_f-1} {\alpha^1_{l,a,b}}^2 \right)^2 {R_{wv}}^2(0)$$

$$= \left(\sum_{a=0}^{A-1} \sum_{b=0}^{B-1} \sum_{l=0}^{L_f^1-1} {\alpha_{l,a,b}^1}^2 \right) {E_{bit}}^2 (1-\rho)^2$$

We assume the channel coefficients remain unchanged for one bit duration. The correlator output for the AWGN noise term of the l^{th} path at the $(a,b)^{th}$ antenna element is

$$\int_{t=iN_sT_f+\tau_{l,a,b}^1}^{(i+1)N_sT_f+\tau_{l,a,b}^1} n_{(a,b)}(t)\,\alpha_{l^{th},(a,b)^{th}}^1 v_{bit}(t)dt \tag{3.38}$$

The overall correlation outputs due to AWGN noise of the received signal is the sum of all the correlations of all the antenna elements. The mean of this noise term is zero and its variance is

$$\sigma_n^2 = \frac{N_0}{2} \left(\sum_{a=0}^{A-1} \sum_{b=0}^{B-1} \sum_{l=0}^{L_f^1-1} {\alpha_{l,a,b}^1}^2 \right) \int_{-\infty}^{\infty} v_{bit}^2(t)\,dt \tag{3.39}$$

$$= \frac{N_0}{2} \left(\sum_{a=0}^{A-1} \sum_{b=0}^{B-1} \sum_{l=0}^{L_f^1-1} {\alpha_{l,a,b}^1}^2 \right) \int_{-\infty}^{\infty} \left(w_{bit}(t) - w_{bit}\left(t-\delta\right) \right)^2 dt$$

$$= \frac{N_0}{2} \left(\sum_{a=0}^{A-1} \sum_{b=0}^{B-1} \sum_{l=0}^{L_f^1-1} {\alpha_{l,a,b}^1}^2 \right) E_{bit} 2 \frac{\left(\int_{-\infty}^{\infty} {w_{bit}(t)}^2 dt - \int_{-\infty}^{\infty} w_{bit} w_{bit}(t-\delta)\,dt \right)}{\int_{-\infty}^{\infty} {w_{bit}(t)}^2 dt}$$

$$= N_0 E_{bit} \left(\sum_{a=0}^{A-1} \sum_{b=0}^{B-1} \sum_{l=0}^{L_f^1-1} {\alpha_{l,a,b}^1}^2 \right) (1-\rho)$$

For the system that performs in a multiuser environment, we will consider the interference from the multiple users and from the non-selected paths. The transmission time difference between the l^{th} path of the user 1 for the $(a,b)^{th}$ element and the other paths from the same user or the other users is

$$\tau_{k,(a,b)}^u - \tau_{l,(a,b)}^1 = j_{k,l,(a,b)}^u T_f + Z_{k,l,(a,b)}^u \tag{3.40}$$

where $j^{u}_{k,l,(a,b)}$ is the value of time uncertainty rounded to the nearest integer, and $Z^{u}_{k,l,(a,b)}$ is the error in this rounding process. Since $Z^{u}_{k,l,(a,b)}$ is a round-off error of a large random variable, it can be modeled as uniformly distributed random variable over $\left[-T_f/2, T_f/2\right]$. The probability density function of $Z^{u}_{k,l,(a,b)}$ is

$$p_Z = \frac{1}{T_f} \tag{3.41}$$

The model of $j^{u}_{k,l,(a,b)}$ won't be needed as the final calculations are independent of it. The monopulse shape is selected such that it has an average value of zero, i.e., $\int_{-\infty}^{\infty} w(t)dt = 0$, thus ensuring that the average of the total interference at the output of the receiver is zero. These assumptions allow the use of Central Limit theorem [8]. The variance of total zero mean interference from the MUI and non-selected path with the use of central limit theorem can be written as

$$\sigma_I^2 = \frac{N_s}{T_f} \sum_{u=1}^{N_u} \sum_{a=0}^{A-1} \sum_{b=0}^{B-1} \sum_{l=0}^{L_f-1} \sum_{\substack{k=0 \\ (u=1,k\neq l)}}^{L^{u}_{total}-1} \left(\alpha^{1}_{l,(a,b)} \alpha^{u}_{k,(a,b)}\right)^2 \int_{-\infty}^{\infty} R^2_{wv}(x)dx \tag{3.42}$$

where $\int_{-\infty}^{\infty} R^2_{wv}(x)dx$ is the integration of the square value of the cross correlation value of the template waveform $v(t)$ and received monopulse, $w(t)$ at different time shift.

For the system that performs in a single user environment, only self interference will be present. Similarly, by invoking the central limit theorem as in (3.42), the variance of total zero mean interference from non-selected path can be defined as

$$\sigma_{SI}^2 = \frac{N_s}{T_f} \sum_{a=0}^{A-1} \sum_{b=0}^{B-1} \sum_{l=0}^{L_f-1} \sum_{\substack{k=0 \\ (k\neq l)}}^{L^{1}_{total}-1} \left(\alpha^{1}_{l,(a,b)} \alpha^{1}_{k,(a,b)}\right)^2 \int_{-\infty}^{\infty} R^2_{wv}(x)dx \tag{3.43}$$

The probability of error given the signal representing bit ‘0’ was transmitted can be written as

$$P[e/0] = \int_{-\infty}^{0} \frac{1}{\sqrt{2\pi\sigma^2}} \exp\left\{-\frac{(G - s_{D0})^2}{2\sigma^2}\right\} dG \tag{3.44}$$

$$= Q\left(\frac{s_{D0}}{\sigma}\right)$$

where

$$\sigma^2 = \sigma_n{}^2 + \sigma_I{}^2 \text{ in multiuser case} \tag{3.45}$$

and

$$\sigma^2 = \sigma_n{}^2 + \sigma_{SI}{}^2 \text{ in singer user case.} \tag{3.46}$$

$Q(x)$ is the Gaussian Q-function and is defined as

$$Q(z) = \int_{z}^{\infty} \frac{1}{\sqrt{2\pi}} \exp\left(-\frac{u^2}{2}\right) du \tag{3.47}$$

The probability of error given the signal representing bit ‘1’ was transmitted is

$$P[e/1] = \int_{0}^{\infty} \frac{1}{\sqrt{2\pi\sigma^2}} \exp\left\{-\frac{(G - s_{D1})^2}{2\sigma^2}\right\} dG \tag{3.48}$$

$$= Q\left(-\frac{s_{D1}}{\sigma}\right)$$

$s_{D0} = -s_{D1}$ and the binary symbols are assumed to have equal transmission probabilities. The average probability of bit error condition on particular instantaneous SINR per bit for single user environment is defined as

$$P_{E/\gamma_b} = Q\left(\sqrt{\frac{E_s}{\sigma_n^2 + \sigma_{SI}{}^2}}\right) \tag{3.49}$$

$$= Q\left(\sqrt{\left[\left(\frac{E_s}{\sigma_n^2}\right)^{-1} + \left(\frac{E_s}{\sigma_{SI}^2}\right)^{-1}\right]^{-1}}\right)$$

where $\frac{E_s}{\sigma_n^2 + \sigma_{SI}^{\ 2}}$ is instantaneous output SINR in single user environment.

In multiuser environment, the probability of error with MUI and interference from non-selected paths conditioned on particular instantaneous SINR per bit is defined as

$$P_{E/\gamma_b} = Q\left(\sqrt{\frac{E_s}{\sigma_n^2 + \sigma_I^2}}\right) \tag{3.50}$$

$$= Q\left(\sqrt{\left[\left(\frac{E_s}{\sigma_n^2}\right)^{-1} + \left(\frac{E_s}{\sigma_I^2}\right)^{-1}\right]^{-1}}\right)$$

where $\frac{E_s}{\sigma_n^2 + \sigma_I^2}$ is the instantaneous output SINR for multiuser environment.

For the UWB system that performs in only AWGN channel with only one antenna element, the average probability became

$$P_E = Q\left(\sqrt{\frac{E_s}{\sigma_n^2}}\right) \tag{3.51}$$

By inserting the E_s from (3.37) and σ_n^2 from (3.39), the average probability in AWGN channel can be written as

$$P_E = Q\left(\frac{\left(\sum_{a=0}^{A-1}\sum_{b=0}^{B-1}\sum_{l=0}^{L_f^1-1}\alpha_{l,a,b}^{1\ 2}\right)^2 E_{bit}^{\ 2}(1-\rho)^2}{N_0 E_{bit}\left(\sum_{a=0}^{A-1}\sum_{b=0}^{B-1}\sum_{l=0}^{L_f^1-1}\alpha_{l,a,b}^{1\ 2}\right)(1-\rho)}\right) \tag{3.52}$$

$$= Q\left(\sqrt{\frac{E_{bit}(1-\rho)}{N_0}}\right)$$

The average bit error probability in the presence of fading is defined as [76]

$$P_E = \int_0^\infty P_{E/\gamma_b}(x) pdf_{\gamma_b}(x)\, dx \tag{3.53}$$

where pdf_{γ_b} is the probability density function of the instantaneous SNR or SINR at the output of the correlator. The instantaneous SNR/SINR is depending on the channel condition. We compute the expectation of the BER over the fading by using Monte Carlo methods. Perfect power control is assumed in this study.

3.6 Numerical Results

In this section, we evaluate the performance of a UWB system with antenna array under multipath environments. It is shown via simulations that the performance of a UWB system can be improved by increasing the number of antenna elements and by selecting more multipaths.

We select the normalized Gaussian monocycle pulse shape defined in (2.11). The parameters of generating the monopulse, $w(t)$ are set as $\tau_m = 0.7531\ ns$, $t_d = 0$ and $T_w = 2\ ns$. The system parameters are as follows: every symbol transmitted repeatedly over $N_s = 16$ frames and each frame composed of $N_h = 24$ chips. The frame duration is chosen to be $T_f = 100\ ns$ and modulation index, $\delta = 0.4073\ ns$. The signals received at each of the antenna element are assumed to be in phase, and at the azimuth angle of 15^0. The inter-element spacing of the array in x and y directions is equal and

is fix to $6\,inch$. The parameters used for the channel model are taken as: cluster decay factor $\Gamma = 24$, ray decay factor $\gamma = 12$, $\sigma_1 = \sigma_2 = 3.3941dB$. The constant ray arrival rate is 0.5/ns and the constant cluster arrival rate is 0.1/ns. We have assumed $L^u_{total} = L_{total} = 20$. Note that the time delay of each antenna element with reference to the reference antenna is small and is less than the time interval of two consecutive paths. Table (3-1) shows the value of parameter.

In this study, analysis being done led to a closed form mathematical equation where multiuser interference and self interference is modeled as a zero-mean Gaussian random variables. This assumption called a 'Gaussian approximation' is not accurate enough to predict the BER especially for high SNR. For the analysis, the arrival times of multipath components for each user are assumed uniformly distributed over a frame duration. It is reasonable to assume uniformly distributed asynchronous delay between different users over a frame duration. However, assuming uniform distribution of path arrival delays over a frame period might not be valid in some practical case in which solving the problem analytically may not be feasible. Simulations that we conduct are in more practical way where the deterministic arrival rate of the multipath is adopted and asynchronous delays between different users are uniformly distributed over a frame duration.

Parameter	Value
Location of monopulse, t_d	0
Width of monopulse, τ_m	0.7531ns
Duration of monopulse, τ_w	2ns
Frame duration, T_f	100ns
Modulation index, τ_δ	0.4073ns
Number of pulses for one bit duration, N_s	16
Number of chips within a frame, N_h	24
Cluster decay factor, Γ	24
Ray decay factor, γ	12
Standard derivation of the cluster lognormal fading term, σ_1	3.3941dB
Standard derivation of the ray lognormal fading term, σ_2	3.3941dB

Table 3-1: Value of system parameters

Figure 3-4 illustrates the theoretical and simulation BER for one receive antenna (Rx=1) with various number of paths ($L_f = 5,10$) being selected over the multipath fading channel in single user environments ($N_u = 1$) and multi-user environments ($N_u = 50$) with interference from non-selected paths and MUI from 49 other active users. The performance over the AWGN channel alone also shown is this figure. Random time-hopping codes are used for each user. As observed in this figure, performance of the system degrades in the multi-user environment. However, the performance improved when more paths being selected and are added coherently at the receiver. In multipath fading environments, when L_f fingers are used in a Rake receiver, the receiver can achieve multipath diversity of order of L_f. The total energy capture by the receiver increases when more paths being selected at the receiver.

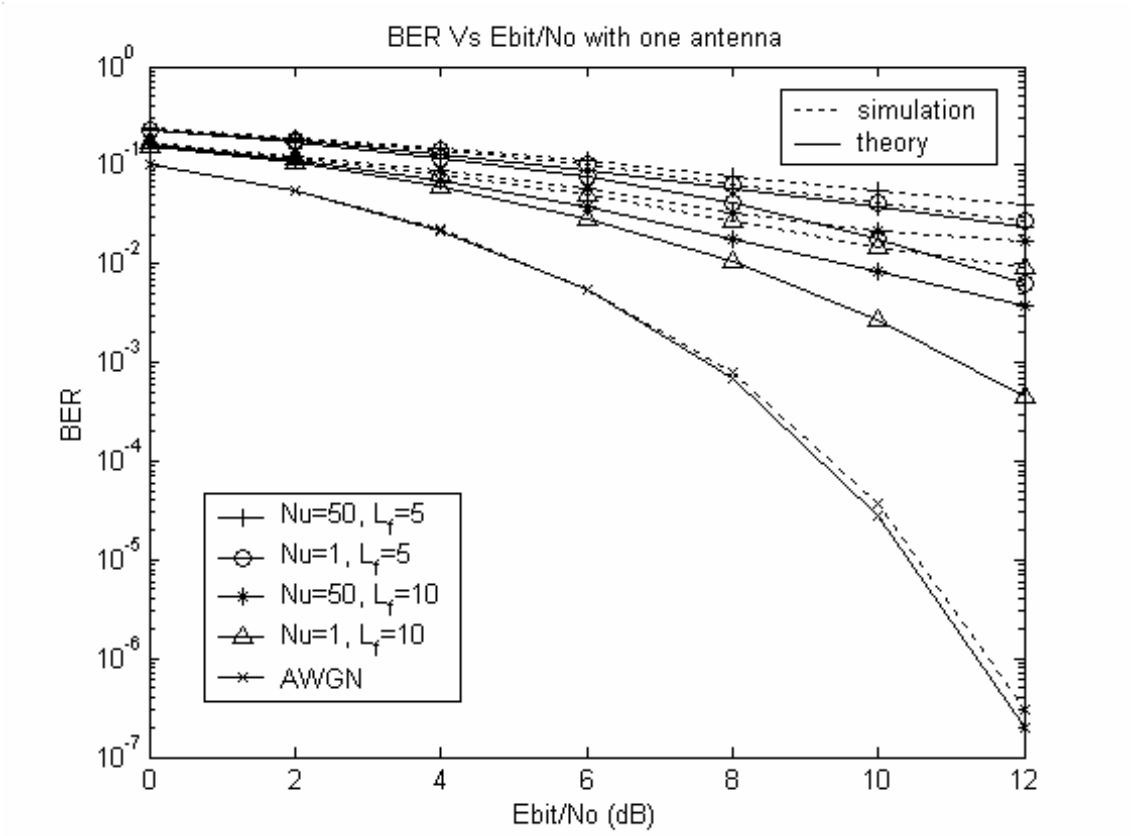

Figure 3-4: BER versus E_{bit}/N_0 with one receive antenna (Rx=1) and $L_f = 5,10$ paths being selected

Figure 3-5 shows the BER curves for uniform linear array receiver with 3 antenna elements (Rx=3) for various number of selected paths at each element ($L_f = 2,5$) in single user environments and 50 active users environments. Compare to the single antenna receiver in figure 3-4, the multi-antenna reception provides a large performance gain and is more robust against MUI. In multipath fading channel scenarios, antenna array may also be used to exploit diversity-combining techniques combine the signals from multiple antennas in a way that improve the performance of the IR systems.

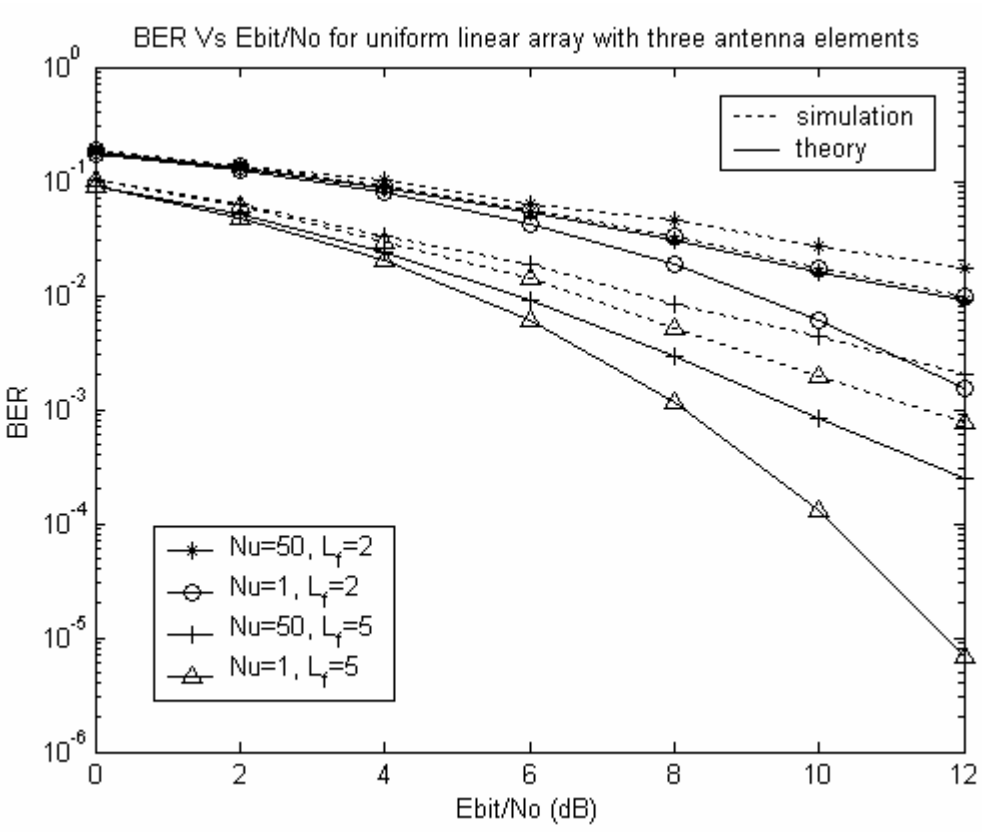

Figure 3-5 : BER versus E_{bit}/N_0 for uniform linear array with Rx=3 antenna elements with each of the antenna element select $L_f = 2,5$ paths

We will evaluate the performance of the rectangular array in figure 3-6. Figure 3-6 depicts the BER performance of the IR systems when rectangular array which consists of 9 (3×3) or 25 (5×5) elements being deployed at the receiver. For each antenna element, the first dominant path ($L_f = 1$) will be selected. This figure suggests that the performance of the IR systems can be improved by increasing the number of the array's element. Higher spatial diversity gain can be obtained to combat the distortion caused by multipath and MUI when more antenna elements are being deployed at the receiver.

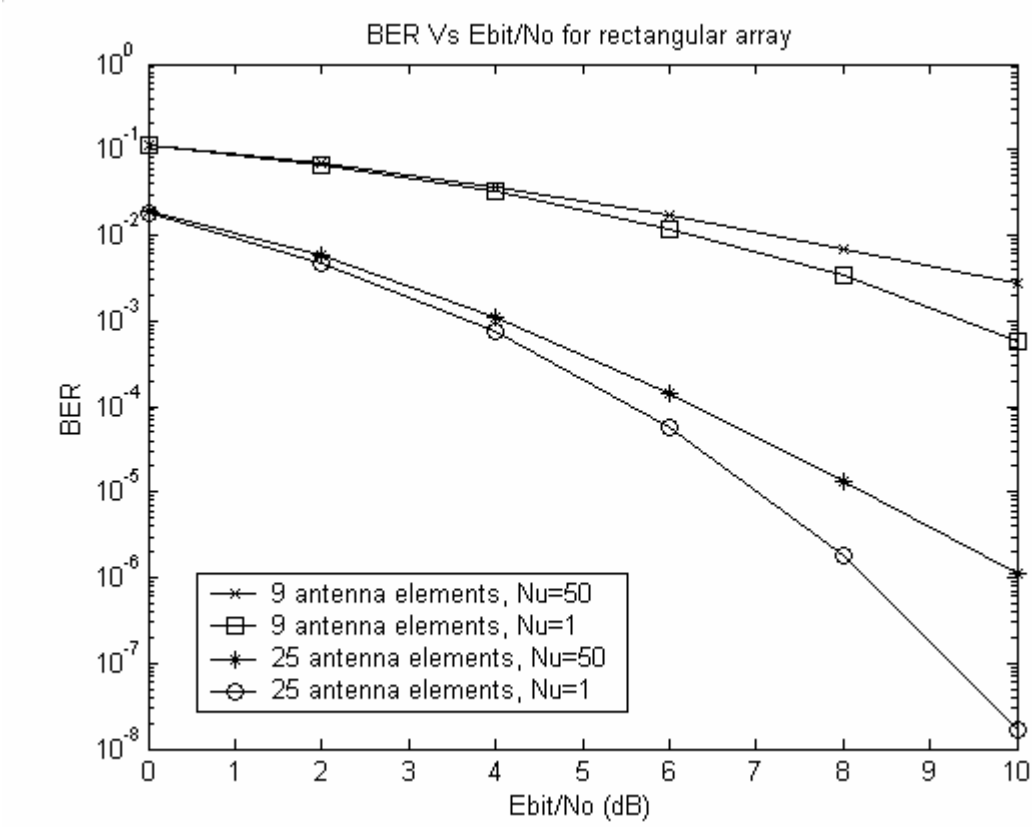

Figure 3-6: BER versus E_{bit}/N_0 for Rx=9, 25 elements of rectangular array with $L_f = 1$ path being selected at each of the antenna element

Figure 3-7 presents the BER performance as a function of the number of selected paths at each element, L_f for various numbers of employed array's element with a fix E_{bit}/N_0 of 10dB in single user environments. This figure shows that the BER performance can be improved by increasing the number of the array's element and the number of the selected multipaths at each antenna element. Obviously, the results suggest that the improvement in performance comes from two factors, the spatial diversity of multiple antennas and path diversity of the Rake receiver. The Rake receiver can be used in conjunction with an antenna array system to combine the different multipaths.

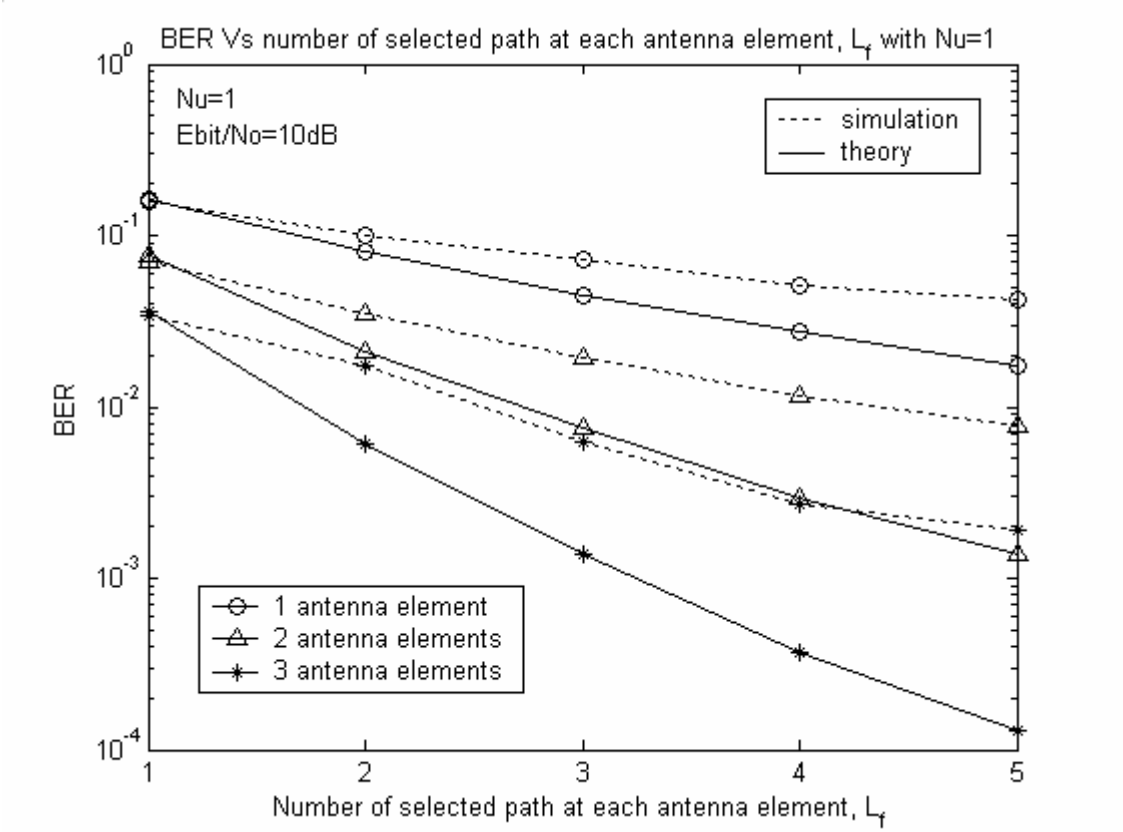

Figure 3-7: BER versus number of selected path at each antenna element, L_f for various number of array's element in single user environments

Figure 3-8 shows the theoretical and simulation BER performance in 50 active users environments for various number of employed antenna elements (Rx=1,2,3) with a fix E_{bit}/N_0 of 10dB as a function of the number of selected paths at each element (L_f). BER performance degrades when interference from other active users exist compare to figure 3-7. However, performance improves when the number of the employed array's element and the number of the selected multipath increased.

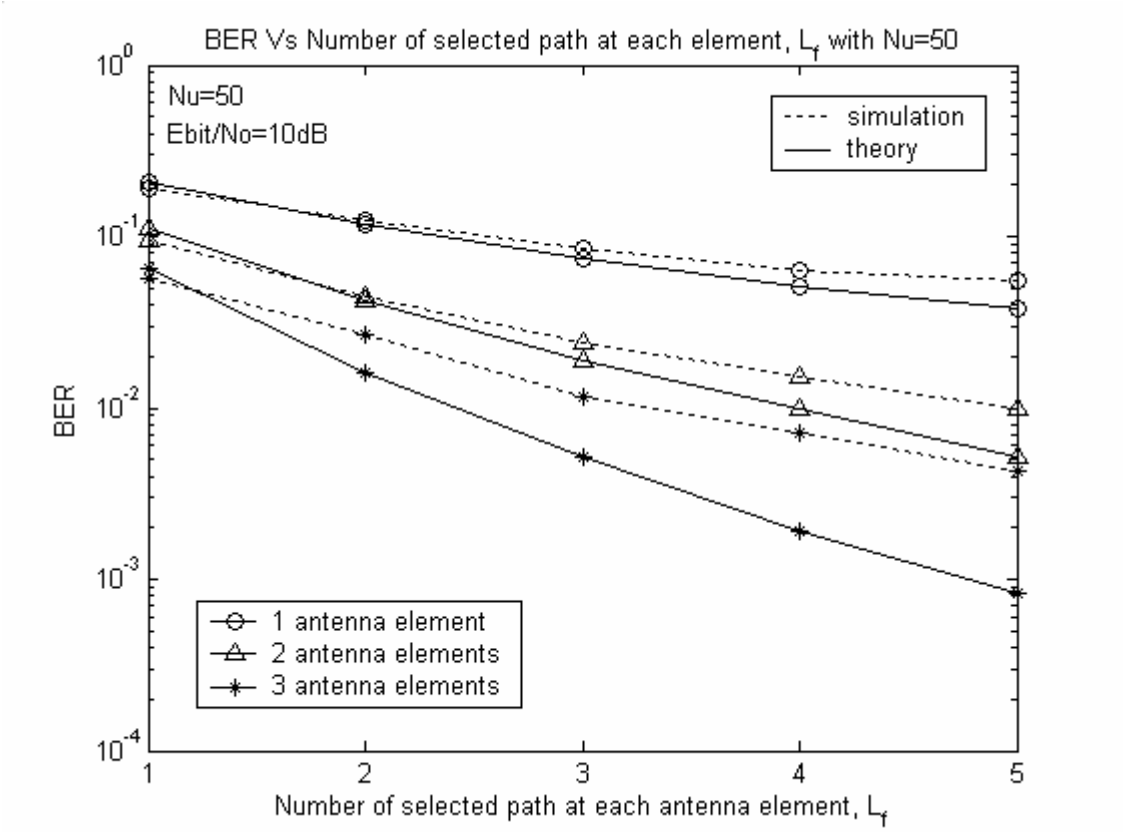

Figure 3-8: BER versus number of selected path at each antenna element, L_f for various number of array's element in 50 active users environments

Figure 3-9 presents the BER performance as a function of the number of simultaneous users, N_u when $L_f = 5,10$ paths being selected for one antenna system (Rx=1) and uniform linear array system with 3 receive antennas (Rx=3). With a fixed E_{bit}/N_0 (13 dB), the performance degrades when the number of users increases as additional power is required to achieve invariant BER performance. Clearly, this figure shows that 3 elements' array outperforms the single antenna scheme. By using antenna array, we are effectively alleviating the impact of multiple access interference experience from other users. This reduction in interference leads to an increase in multiple access capacity that can be supported by the system.

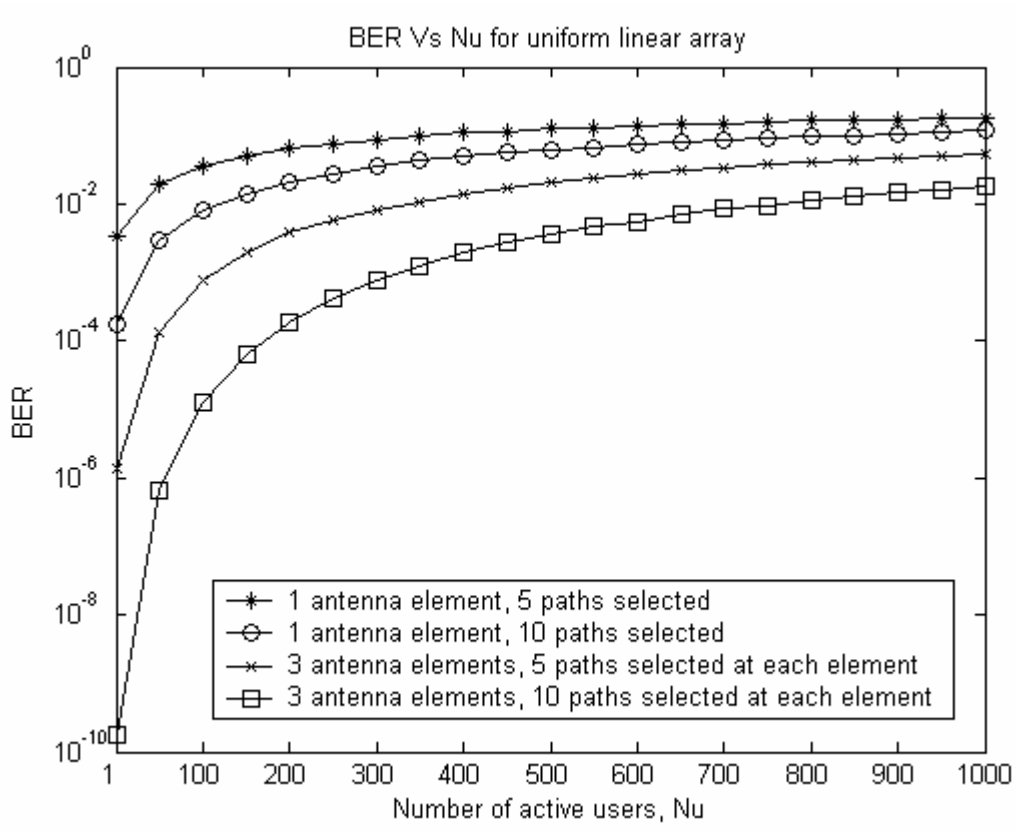

Figure 3-9: BER versus N_u for 1 antenna (Rx=1) and 3 antenna elements (Rx=3) systems with $L_f = 5,10$ paths being selected

The multiple access performance for rectangular array is evaluated in figure 3-10. Fig. 3-10 shows the BER when rectangular array with (3×3) and (5×5) elements being employed in the receiver in which each element select one path, $L_f = 1$ with fix E_{bit}/N_0 of 13dB as a function of the number of simultaneous users. The system with (5×5) array elements performs better than (3×3) elements in multipath fading environments. From this plot, if we assume that the required BER is less than 10^{-3}, the maximum number of simultaneous users is about 50 for (3×3) elements array. With (5×5) elements, this number goes up to 500 users. The result demonstrates that the system with higher number of array's element has greater tolerance to MUI and can support higher number of simultaneous users. This is due to the diversity gain across the antenna array since more elements are coherently added at the receiver to cope with the effect of MUI.

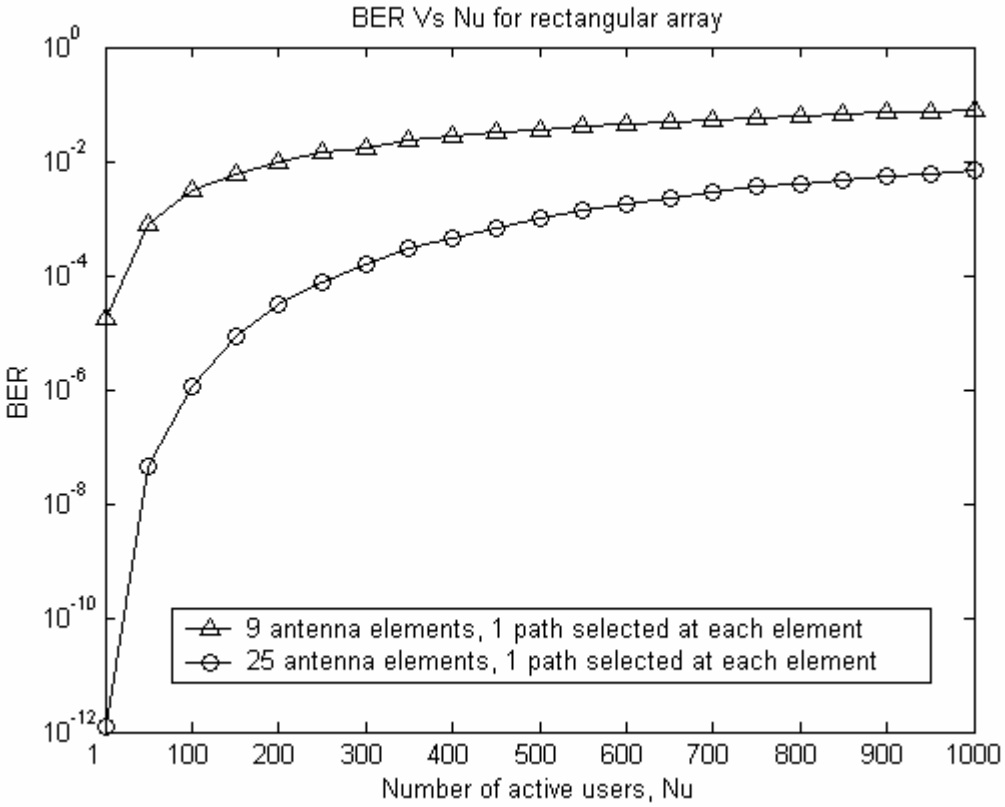

Figure 3-10: BER versus N_u for Rx=9, 25 elements of rectangular array with $L_f = 1$ path being selected in each of the antenna element

We can compare the performance of the rectangular array and uniform linear array in single user environments in figure 3-11 where the BER performance of the 9 and 25 (Rx=9,25) antenna elements with uniform linear array or rectangular array with each element select one path ($L_f = 1$) is being shown. Rectangular array performs better than uniform linear array. This is due to the geometry of the rectangular array is more concentrate. The configuration of rectangular array enables it to capture the multipath component with shorter propagation delay in average and hence the summated power of the received multipath signal is higher.

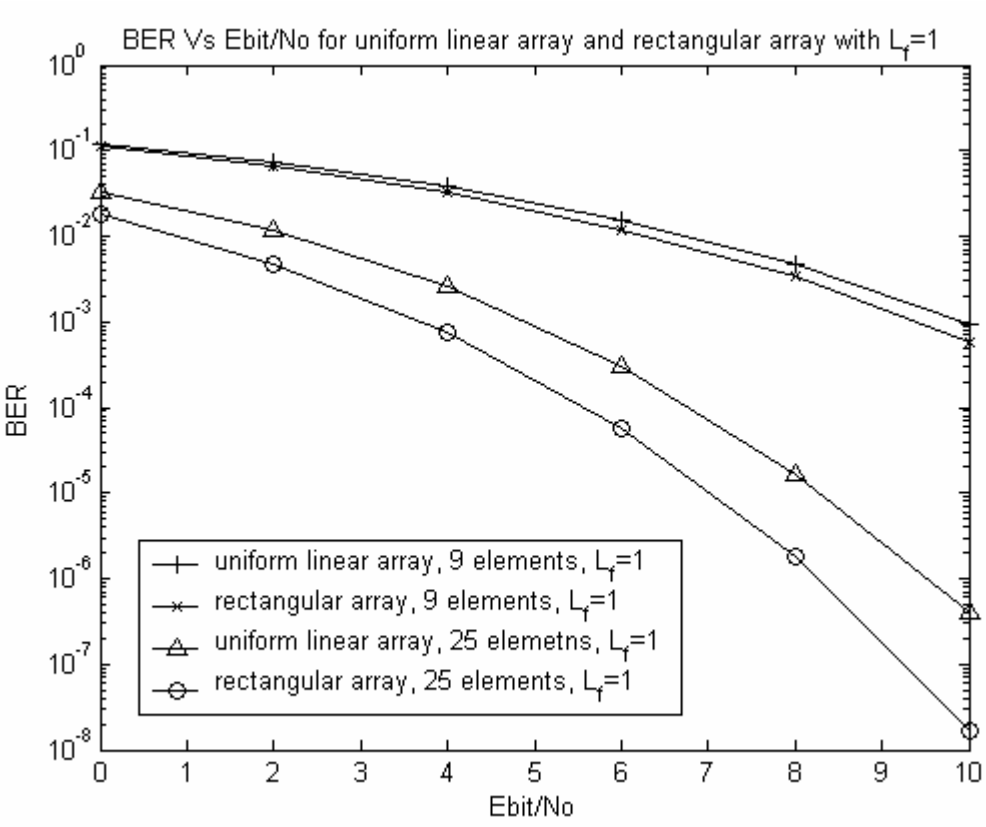

Figure 3-11: BER versus E_{bit}/N_0 for Rx=9, 25 elements of rectangular and uniform linear array with $L_f = 1$ path being selected at each of the antenna element in single user environments

3.7 Conclusions

In this chapter, the diversity performance of a UWB IR multiple access system by employing uniform linear and rectangular antenna array with SRake receiver in indoor multipath fading channel is presented.

In independent fading channel scenarios, antenna array can be used to exploit spatial diversity in conjunction with the path diversity provided by Rake receiver to combine the different multipath components in a way that mitigate the impact of multipath and suppress the effect of interference from multiple users. The diversity gain achieved enables the system to support a larger number of active users for a given BER quality threshold.

The numerical results indicate the BER performance and multiple access capacity of the UWB system improves when the number of the employed antenna elements increases. The performance of the system will further improve when more multipaths are selected and added coherently at the receiver. These results suggest that the antenna diversity can be used to improve reliability and to enhance the performance of IR systems.

CHAPTER 4

MULTIPLE ACCESS PERFORMANCE OF UWB M-ARY EQUALLY CORRELATED IR SYSTEMS WITH ANTENNA ARRAY

4.1 Introduction

In this chapter, the influence of spatial and temporal diversities on the multiple access performance of M-ary equally correlated (EC) block waveform pulse position modulation (PPM) impulse radio systems in dense multipath environments are analyzed. We investigate the use of antenna array at the receiver to improve the multiple access performance of the IR system in terms of the number of simultaneous active users supported by the system for a given bit error rate, bit transmission rate, and number of signals in the M-ary set. The application of beamforming technique and the utilization of Rake receiver are considered. The bit error rate (BER) of M-ary IR UWB systems with diversity reception is derived.

We consider M-ary equally correlated signal in this chapter as the use of M-ary block waveform signal is attractive. In single user environment, it allows to increase the data transmission rate and making efficient use of available signal to noise ratio. In a multiuser environment, the use of M-ary signals allows to increase the number of users

supported by the system for a given multiple access performance and bit transmission rate.

Numerical results show that the BER performance and multiple access capacity of the M-ary IR system can be improved significantly by increasing the number of elements of the antenna array and coherently adding more paths at the receiver. The results also show that diversity reception can be used to increase the data transmission rate supported by the system without degrading the multiple access performance for a given number of users.

4.2 M-ary Equally Correlated Block Waveform Signal Model

A typical time-hopping PPM signal for the u^{th} user can be modeled as

$$Y^{(u)}(t) = \sum_{i=0}^{\infty} \sum_{j=iN_s}^{j=(i+1)N_s-1} w(t - jT_f - c_j^{(u)}T_c - \delta_{d_i^{(u)}}^{j}) = \sum_{i=0}^{\infty} y_{i,d_i^{(u)}}^{u}(t) \tag{4.1}$$

where t represent the transmitters' clock time, $w(t)$ represents the monocycle waveform and the superscript (u) indicates the user-dependent quantities. In order to support multiple access capabilities, each user is assigned a distinctive pulse time shift pattern $\left\{c_j^{(u)}\right\}$ called a time-hopping (TH) sequence to eliminate collisions. The TH sequence will provide an additional time shift of $c_j^{(u)}T_c$ seconds to the j^{th} monocycle in the pulse train with $0 \le c_j \le N_h - 1$. The PPM is used for symbol encoding where $\delta_{d_i^{(u)}}^{j}$ corresponds to the time shift for the data modulation. The data sequence $d_i^{(u)}$ of the u^{th} user for the i^{th} data symbol is an M-ary symbol stream that convey the information where $1 \le d_i^{(u)} \le M$. The modulating data symbol changes only every N_s

hops as N_s monocycles transmitted per symbol. Hence, there are N_s frames in one symbol period of T_s, where $T_s = N_s T_f$. The symbol rate is given by $R_s = 1/T_s$.

Let the block waveform of M-ary PPM signal set be $\{s_1(t), s_2(t), ...s_M(t)\}$. $s_m(t)$ can be written as

$$s_m(t) = \sum_{j=0}^{j=N_s-1} w(t - jT_f - c_j^{(u)} T_c - \delta_m^j), \; m = 1, 2, ...M \tag{4.2}$$

$s_m(t)$ represents the m^{th} signal in an ensemble of M signals. Each signal is completely identified by the sequence of time shifts $\{\delta_m^j\}$. For a particular u^{th} user, the complete assemble of signals $\{s_m(t)\}$ can be represented in matrix of $M \times N_s$,

$$\Delta = \begin{bmatrix} \delta_1^1 & \delta_1^2 & \cdots & \delta_1^j & \cdots & \delta_1^{N_s} \\ \delta_2^1 & \delta_2^2 & \cdots & \delta_2^j & \cdots & \delta_2^{N_s} \\ \vdots & \vdots & \ddots & \vdots & \vdots & \vdots \\ \delta_m^1 & \delta_m^2 & \cdots & \delta_m^j & \cdots & \delta_m^{N_s} \\ \vdots & \vdots & \vdots & \vdots & \ddots & \vdots \\ \delta_M^1 & \delta_M^2 & \cdots & \delta_M^j & \cdots & \delta_M^{N_s} \end{bmatrix} \tag{4.3}$$

Each row corresponds to the time shift $\{\delta_m^j\}$ defining the m^{th} signal with $m = 1, 2, ...M$. N_s monopulse are used to represent one symbol and hence each signal $s_m(t)$ has duration $T_s = N_s T_f$ where T_f is the frame period. Each column in matrix (4.3) corresponds to the data modulation time shift of particular m^{th} signal in the j^{th} frame.

In this chapter, M-ary EC IR modulation is considered. For EC M-ary signal, the sequence of time shift for data modulation can be defined as

$$\delta_m^j = a_m^j \tau_\delta \in \{0, \tau_\delta\} \tag{4.4}$$

where $a_m^j = \{0,1\}$ is the binary stream representing the m^{th} cyclic shift of an m-sequence with length N_s and $N_s \geq M$. Hence, EC M-ary signal set can be written as

$$s_m(t) = \sum_{j=0}^{j=N_s-1} w(t - jT_f - c_j^{(u)}T_c - a_m^j \tau_\delta), \; m = 1,2,...M \tag{4.5}$$

Details of construction of the EC signal is described in next session.

The UWB received basic monopulse, $w(t)$ has energy denoted by E_w and the correlation function of the monopulse is defined as $\lambda_w(\tau) = \int_{-\infty}^{\infty} w(t)w(t-\tau)dt$. As in chapter 3, the normalized correlation function of monopulse is given by

$$\gamma_w(\tau) = \frac{\int_{-\infty}^{\infty} w(t)w(t-\tau)dt}{\int_{-\infty}^{\infty} w^2(t)dt} \tag{4.6}$$

$$= \frac{\lambda_w(\tau)}{\lambda_w(0)} = \frac{\lambda_w(\tau)}{E_w}$$

Since the transmitted signal of the i^{th} symbol is composed of N_s time shift of monopulse, the energy of one symbol is therefore defined as

$$E_s = \int_{-\infty}^{\infty} \left[s_m(t)\right]^2 dt = N_s E_w \tag{4.7}$$

$$= \log_2(M) E_b$$

where E_b is the bit energy. The normalized correlation function of the signals can be written as

$$\rho_{n,m} = \frac{\int_{-\infty}^{\infty} y_{i,n}^{(u)}(t) y_{i,m}^{(u)}(t)dt}{E_s} \tag{4.8}$$

$$= \frac{\int_{-\infty}^{\infty} s_n(t)s_m(t)dt}{E_s}$$

$$= \frac{1}{N_s} \sum_{j=0}^{N_s-1} \gamma_w \left(\tau_{\delta n}^j - \tau_{\delta m}^j \right)$$

The autocorrelation value of the signal will be 1, where

$$\rho_{n,n} = \rho_{m,m} = 1 \tag{4.9}$$

$$\frac{\int_{-\infty}^{\infty} s_n(t) s_n(t) dt}{E_s} = \frac{\int_{-\infty}^{\infty} s_m(t) s_m(t) dt}{E_s} = 1$$

The complete set of normalized correlation values is given by the $M \times M$ correlation matrix

$$\Re \triangleq \begin{bmatrix} \rho_{1,1}=1 & \rho_{2,1} & \cdots & \rho_{M,1} \\ \rho_{1,2} & \rho_{2,2}=1 & \cdots & \rho_{M,2} \\ \vdots & \vdots & \ddots & \vdots \\ \rho_{1,M} & \rho_{2,M} & \cdots & \rho_{M,M}=1 \end{bmatrix} \tag{4.10}$$

In this chapter, the signals considered is equally correlated. The equally correlated signal has property that correlation value between any of two signal will be the same where

$$\rho_{n,m} = \rho_{m,n} = \rho \ , \ m,n = 1,2,...M, \forall m \neq n \tag{4.11}$$

$$\frac{\int_{-\infty}^{\infty} s_n(t) s_m(t) dt}{E_s} = \frac{\int_{-\infty}^{\infty} s_m(t) s_n(t) dt}{E_s} = \rho$$

Hence the matrix of the correlation value between signals can be written as

$$\Re_{EC} \triangleq \begin{bmatrix} 1 & \rho & \cdots & \rho \\ \rho & 1 & \cdots & \rho \\ \vdots & \vdots & \ddots & \vdots \\ \rho & \rho & \cdots & 1 \end{bmatrix} \tag{4.12}$$

4.2.1 Construction of Equally Correlated Signal

In this section, the construction method of equally correlated signal is described. The construction uses a set of time-shift-keyed signals to construct the PPM signals. Let H be the cyclic Hadamard matrix. We can generate the EC signals $\{s_m(t)\}$ for $M \le N_s$ by deleting the column and the first row of H, and then use the m^{th} row of this modified matrix $(\hat{H})$ [19,77] and mapping the signal with

$$(+1) \to \tau_\delta \tag{4.13}$$

$$(-1) \to \tau_{\delta_0} = 0$$

The mapping process will produce the time shift pattern $\{\delta_m^j; j = 1, 2, ...N_s\}$ defining the m^{th} signal.

For example, with $M = N_s = 3$, the modified Hadamard matrix will become

$$\hat{\mathrm{H}} = \begin{pmatrix} +1 & -1 & -1 \\ -1 & +1 & -1 \\ -1 & -1 & +1 \end{pmatrix} \tag{4.14}$$

By mapping the matrix with $(+1) \to \tau_\delta$, $(-1) \to \tau_{\delta_0} = 0$, the ensemble of the EC signals in (4.3) can be represented as

$$\Delta_{EC} = \begin{bmatrix} \delta_1^1 & \delta_1^2 & \delta_1^3 \\ \delta_2^1 & \delta_2^2 & \delta_2^3 \\ \delta_3^1 & \delta_3^2 & \delta_3^3 \end{bmatrix} \tag{4.15}$$

$$= \begin{bmatrix} \tau_\delta & 0 & 0 \\ 0 & \tau_\delta & 0 \\ 0 & 0 & \tau_\delta \end{bmatrix}$$

As for equally correlated signal, $\delta_m^j = a_m^j \tau_\delta \in \{0, \tau_\delta\}$, if we map the matrix in (4.14) with $(+1) \to (+1)$ and $(-1) \to (0)$, the modified hadamard matrix will become

$$\tilde{\mathrm{H}} = \begin{bmatrix} a_{m=1}^{j=1} & a_1^2 & a_1^3 \\ a_2^1 & a_2^2 & a_2^3 \\ a_3^1 & a_3^2 & a_3^3 \end{bmatrix} \tag{4.16}$$

$$= \begin{bmatrix} 1 & 0 & 0 \\ 0 & 1 & 0 \\ 0 & 0 & 1 \end{bmatrix}$$

This provides an alternative way to represent the set of signals Δ_{EC} as follows

$$\Delta_{EC} = \tau_\delta \times \tilde{\mathrm{H}} \tag{4.17}$$

$$= \tau_\delta \times \begin{bmatrix} a_1^1 & a_1^2 & a_1^3 \\ a_2^1 & a_2^2 & a_2^3 \\ a_3^1 & a_3^2 & a_3^3 \end{bmatrix}$$

In general, $\tilde{\mathrm{H}}$ is a $N_s \times N_s$ matrix where each row of the matrix $\left(a_m^j,\ j = 1, 2, \ldots N_s\right)$ is an equivalent representation to the time shift pattern $\left(\delta_m^j = a_m^j \tau_\delta,\ j = 1, 2, \ldots N_s\right)$ of the particular m^{th} signal. Therefore, for equally correlated signal, the representation of the signal can be written as

$$s_m(t) = \sum_{j=0}^{j=N_s-1} w(t - jT_f - c_j^{(u)} T_c - a_m^j \tau_\delta)\ ,\ m = 1, 2, \ldots M \tag{4.18}$$

with $a_m^j = \{0, 1\}$.

The normalized correlation function of the equally correlated signals can be written as

$$\rho_{n,m} = \frac{1}{N_s} \sum_{j=0}^{N_s-1} \gamma_w \left(\tau_{\delta n}^j - \tau_{\delta m}^j\right) \tag{4.19}$$

$$= \frac{\frac{N_s - 1}{2}\lambda_w(0) + \frac{N_s + 1}{2}\lambda_w(\tau_\delta)}{N_s E_w}$$

Notice that for $N_s >> 1$,

$$\rho_{n,m} \simeq \frac{1 + \gamma_w(\tau_\delta)}{2}\ ,\ N_s >> 1 \tag{4.20}$$

where $n \neq m$. Note that $\rho_{n,m} = \rho_{m,n} = \rho$ and $\rho_{nn} = \rho_{mm} = 1$ [19].

4.3 IR Receiver Processing with M-ary Signal

In this chapter, we use Selective Rake (SRake) receiver with ($A \times B$) antenna array, each antenna element with L_f -Rake fingers. In figure 4-1, we show the structure of the Rake receiver with antenna array to process the M-ary received signal. Due to the nature of fine range resolution capability of IR signal, the dense multipath components produced by signals arriving at the receiver with different time delays (as small as fractions of nanoseconds) can be resolved, allowing the use of a Rake receiver with an antenna array to combine the signal energies that are separated in space and time.

We assume that the receiver is perfectly synchronized to the hopping code of the user of interest and knows the time delay of each selected path. In a multiuser system, without loss of generality, it is assumed that user 1 is the user of interest and the receiver intends to detect the signal representing the i^{th} data symbol. The receiver

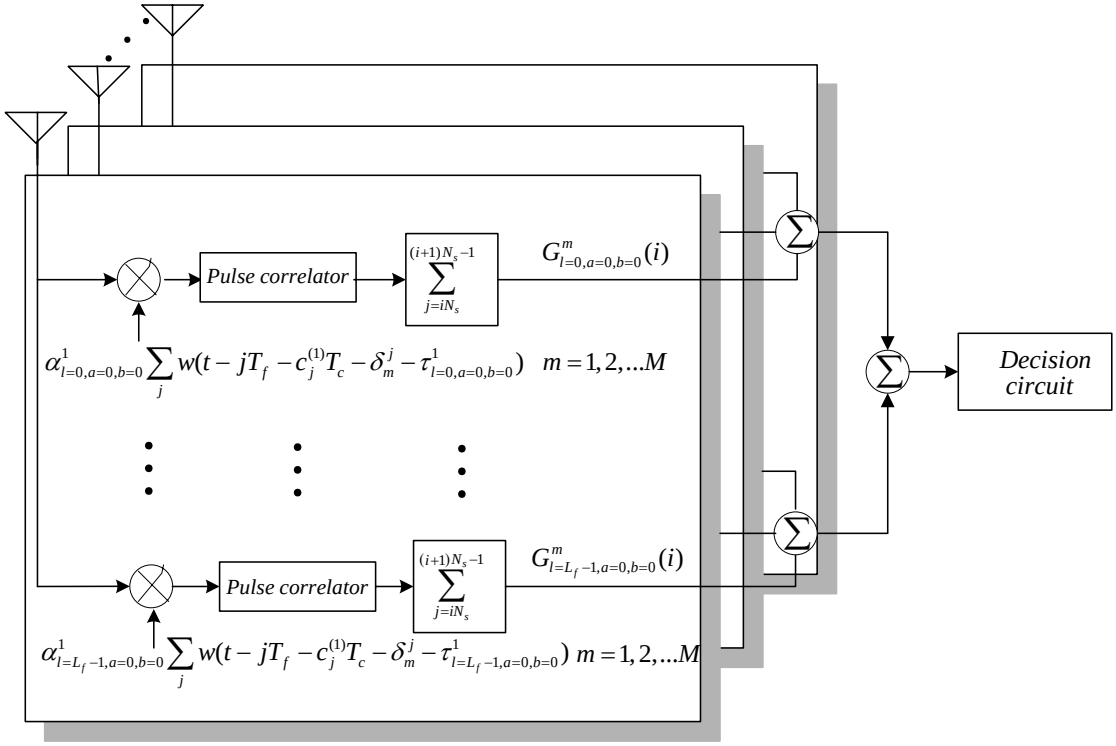

Figure 4-1: Structure of SRake receiver with $(A\times B)$ antenna array for M-ary signals

selects the first $L_f^{u=1}$ dominant paths of the user 1 and the received signal can be written as

$$r(t)=\sum_{a=0}^{A-1}\sum_{b=0}^{B-1}\sum_{l=0}^{L_f^1-1}\alpha^1_{l,a,b}y^{(1)}_{i,d_i^{(1)}}\left(t-\tau^1_{l,a,b}\right)+\underbrace{\sum_{a=0}^{A-1}\sum_{b=0}^{B-1}\sum_{l=L_f^1}^{L^1_{total}-1}\alpha^1_{l,a,b}y^{(1)}_{i,d_i^{(1)}}\left(t-\tau^1_{l,a,b}\right)}_{n_{NS}(t)}+\underbrace{\sum_{u=2}^{N_u}\sum_{a=0}^{A-1}\sum_{b=0}^{B-1}\sum_{l=0}^{L^u_{total}-1}\alpha^u_{l,a,b}Y^u\left(t-\tau^u_{l,a,b}\right)}_{n_{MA}(t)}+n_{a,b}(t) \tag{4.21}$$

In this expression, $n_{NS}(t)$ is the self interference from the non-selected paths of the user 1 (user of interest), $n_{MA}(t)$ is the multiple access interference from the undesired users and $n_{a,b}(t)$ is the AWGN noise for the $(a,b)^{th}$ element with double-sided power spectral density of $\frac{N_0}{2}$. The notation of $\tau^u_{l,a,b}$ is the time delay of the corresponding l^{th}

path of the $(a,b)^{th}$ element for the u^{th} user relative to the 1st path of the reference element (a_r, b_r) of the user 1, τ^1_{1,a_r,b_r}. We assume τ^1_{1,a_r,b_r} = 0.

The M-ary correlation receiver for user 1 consists of M-filters matched to the signals $\left\{ y^{(1)}_{i,m}\left(t-\tau^1_{l,a,b}\right)\right\}, m=1,2,...M$ at each finger of the receiver for each antenna element, followed by sampling and summation. The correlation receiver output at the selected l^{th} path of the $(a,b)^{th}$ element for the i^{th} data symbol is as follows

$$G^m_{l,a,b}(i)=\int_{t=iN_sT_f+\tau^1_{l,a,b}}^{(i+1)N_sT_f+\tau^1_{l,a,b}} r(t)\sum_{j=iN_s}^{(i+1)N_s-1}\alpha^1_{l,a,b}y^{(1)}_{i,m}\left(t-\tau^1_{l,a,b}\right)dt,\ m=1,2,...M \tag{4.22}$$

For each finger of the receiver, the associated path selected by that particular finger is treated as desired signal and the rest of the received paths are treated as noise. The test statistic of the i^{th} transmitted symbol depends on the sum of the correlation receiver outputs of each selected path of each antenna element and selects the maximum among the decision variables. The decision variables is

$$G^m(i)=\sum_{a=0}^{A-1}\sum_{b=0}^{B-1}\sum_{l=0}^{L^1_f-1}G^m_{l,a,b}(i),\quad m=1,2,...M \tag{4.23}$$

4.4 BER Analysis for M-ary Equally Correlated Signal

In decoding a symbol, the error probability is the probability for an incorrect decision variable exceeds the correct one. When i^{th} data symbol of $d^{(1)}_i=n$ is sent, the conditional symbol error probability can be written as [77]

$$P(e/d^{(1)}_i=n)=P(G^n\le G^m/d^{(1)}_i=n)\qquad m=1,2,...,M\quad n\neq m \tag{4.24}$$

We can use union bound to upper bound the above conditioned error probability. The union bound states that the probability of a particular G^n is less than the $M-1$ remaining decision variables is bounded by the sum of probabilities that G^n is less than G^m, $m=1,2,...,M$, $n \neq m$ individually. The union bound implies that

$$P(e/d_i^{(1)}=n) \leq \sum_{\substack{m=1 \\ m\neq n}}^{M} P(G^n \leq G^m / d_i^{(1)}=n) \tag{4.25}$$

The average probability of error is then satisfies the following

$$P(e) \leq \sum_{n=1}^{M} P\left(d_i^{(1)}=n\right) P\left(e/d_i^{(1)}=n\right) \tag{4.26}$$

$$\leq \frac{1}{M} \sum_{n=1}^{M} \sum_{\substack{m=1 \\ n\neq m}}^{M} P(G^n \leq G^m / d_i^{(1)}=n)$$

With properly pairing of the terms, the union bound of the average probability can be defined as

$$P(e) = \frac{1}{M} \sum_{m=1}^{M} \sum_{n=1}^{M} Pe_{m,n} \tag{4.27}$$

where

$$Pe_{m,n} = \frac{1}{2} P(G_n \leq G_m / d_i^{(1)}=n) + \frac{1}{2} P(G_m \leq G_n / d_i^{(1)}=m) \tag{4.28}$$

The $Pe_{m,n}$ is the probability of error in the binary test to decide between the signal pair of $y_{i,d_i^{(1)}=n}^{(1)}$ and $y_{i,d_i^{(1)}=m}^{(1)}$. The decision variable in this binary test is given as

$$G^{n,m}(i) = \sum_{a=0}^{A-1} \sum_{b=0}^{B-1} \sum_{l=0}^{L_f^1-1} G_{l,a,b}^{n,m}(i) \tag{4.29}$$

in which

$$G_{l,a,b}^{n,m} = \underbrace{\int_{t=iN_sT_f+\tau_{l,a,b}^1}^{(i+1)N_sT_f+\tau_{l,a,b}^1} \left(\alpha_{l,a,b}^1 y_{i,d_i^{(1)}}^1\left(t-\tau_{l,a,b}^1\right)\right)\alpha_{l,a,b}^1 v_{i,n,m}^1\left(t-\tau_{l,a,b}^1\right)dt}_{S_d} + \underbrace{N_{si}(t)+N_{mai}(t)+N_{awgn}(t)}_{n_{total}} \tag{4.30}$$

where

$$N_{si}(t) = \int_{t=iN_sT_f+\tau_{l,a,b}^1}^{(i+1)N_sT_f+\tau_{l,a,b}^1} \left(\sum_{l=0,l\neq l^{th}}^{L_{total}^1-1} \alpha_{l,a,b}^1 y_{i,d_i^{(1)}}^1\left(t-\tau_{l,a,b}^1\right)\right)\alpha_{l,a,b}^1 v_{i,n,m}^1\left(t-\tau_{l,a,b}^1\right)dt \tag{4.31}$$

$$N_{mai}(t) = \int_{t=iN_sT_f+\tau_{l,a,b}^1}^{(i+1)N_sT_f+\tau_{l,a,b}^1} \left(\sum_{u=2}^{N_u}\sum_{l=0}^{L_{total}^u-1} \alpha_{l,a,b}^u Y^u\left(t-\tau_{l,a,b}^u\right)\right)\alpha_{l,a,b}^1 v_{i,n,m}^1\left(t-\tau_{l,a,b}^1\right)dt \tag{4.32}$$

$$N_{awgn}(t) = \int_{t=iN_sT_f+\tau_{l,a,b}^1}^{(i+1)N_sT_f+\tau_{l,a,b}^1} n_{a,b}(t)\alpha_{l,a,b}^1 v_{i,n,m}^1\left(t-\tau_{l,a,b}^1\right)dt \tag{4.33}$$

with $d_i^{(1)} \in \{m,n\}$ and $v_{i,n,m}^1(t) = \left[y_{i,n}^{(1)}(t) - y_{i,m}^{(1)}(t)\right]$. The binary decision variable in (4.29) is a Gaussian random variable which consist of two components, one is the desired correlation signal output (s_d) and another one is due to noise (n_{total}). We assume that the channel coefficients remain unchanged for one bit duration. The conditional mean of the $G^{n,m}(i)$ when $d_i^{(1)} = n$, $\Theta_{n,m}$ can be written as

$$\Theta_{n,m} = E\left\{G^{n,m}(i)/d_i^{(1)} = n\right\} \tag{4.34}$$

$$= \left(\sum_{a=0}^{A-1}\sum_{b=0}^{B-1}\sum_{l=0}^{L_f^1-1} {\alpha_{l,a,b}^1}^2\right) E_s \frac{\int_{t=iN_sT_f+\tau_{l,a,b}^1}^{(i+1)N_sT_f+\tau_{l,a,b}^1} \left(y_{i,d_i^{(1)}=n}^1\left(t-\tau_{l,a,b}^1\right)\right)\left(y_{i,n}^{(1)}\left(t-\tau_{l,a,b}^1\right) - y_{i,m}^{(1)}\left(t-\tau_{l,a,b}^1\right)\right)dt}{\int_{t=iN_sT_f+\tau_{l,a,b}^1}^{(i+1)N_sT_f+\tau_{l,a,b}^1} \left(y_{i,d_i^{(1)}=n}^1\left(t-\tau_{l,a,b}^1\right)\right)^2 dt}$$

$$= \left(\sum_{a=0}^{A-1}\sum_{b=0}^{B-1}\sum_{l=0}^{L_f^1-1} {\alpha_{l,a,b}^1}^2\right) E_s\left(1-\rho_{n,m}\right)$$

$$= \left(\sum_{a=0}^{A-1}\sum_{b=0}^{B-1}\sum_{l=0}^{L_f^1-1} {\alpha_{l,a,b}^1}^2\right) E_s(1-\rho) \text{ as } \rho_{n,m} = \rho \text{ defined in (4.11)}$$

where $E\{\bullet\}$ is the expected value operator. The conditional mean of $G^{n,m}(i)$ when $d_i^{(1)} = n$ is defined as

$$\Theta_{n,m} = E\left\{G^{m,n}(i) / d_i^{(1)} = m\right\} \tag{4.35}$$

$$= \left(\sum_{a=0}^{A-1} \sum_{b=0}^{B-1} \sum_{l=0}^{L_f^1 - 1} {\alpha_{l,a,b}^1}^2 \right) E_s \left(\rho - 1\right)$$

which show that

$$\Theta_{n,m} = -\Theta_{m,n} \tag{4.36}$$

The conditional mean of $N_{ns}(t)$, $N_{mai}(t)$ and $N_{awgn}(t)$ terms are zero where

$$E\left\{N_{ns} / d_i^{(1)} = n\right\} = E\left\{N_{ns} / d_i^{(1)} = m\right\} = 0 \tag{4.37}$$

$$E\left\{N_{mai} / d_i^{(1)} = n\right\} = E\left\{N_{mai} / d_i^{(1)} = m\right\} = 0 \tag{4.38}$$

$$E\left\{N_{awgn} / d_i^{(1)} = n\right\} = E\left\{N_{awgn} / d_i^{(1)} = m\right\} = 0 \tag{4.39}$$

Hence,

$$E\left\{N_{total} / d_i^{(1)} = n\right\} = E\left\{N_{total} / d_i^{(1)} = m\right\} = 0 \tag{4.40}$$

The variance of the decision variable $G^{n,m}(i)$ in the present of N_u users can be defined as

$$\sigma_{total}^2 = E\left\{\left[G^{n,m}\right]^2\right\} \tag{4.41}$$

$$\sigma_{total}^2 = E\left\{\left[N_{ns}\right]^2\right\} + E\left\{\left[N_{mai}\right]^2\right\} + E\left\{\left[N_{wagn}\right]^2\right\}$$

$$\sigma_{total}^2 = \sigma_{si}^2 + \sigma_{mai}^2 + \sigma_{awgn}^2$$

where σ_{si}^2, σ_{mai}^2 and σ_{awgn}^2 are the variance of decision variable caused by self interference, multiple access interference and AWGN respectively.

The variance of decision variable caused by AWGN noise term, σ_{awgn}^2 is defined as

$$\sigma_{awgn}^2 = E\left\{\left[N_{wagn}\right]^2\right\} \tag{4.42}$$

$$= \frac{N_0}{2}\left(\sum_{a=0}^{A-1}\sum_{b=0}^{B-1}\sum_{l=0}^{L_f^1-1}{\alpha_{l,a,b}^1}^2\right)\int_{-\infty}^{\infty}(v_{i,n,m}^1)^2(t)\,dt$$

$$= N_0 E_s\left(\sum_{a=0}^{A-1}\sum_{b=0}^{B-1}\sum_{l=0}^{L_f^1-1}{\alpha_{l,a,b}^1}^2\right)(1-\rho)$$

For the analysis, asynchronous delays between different users and the arrival times of multipath components for each user are assumed to be uniformly distributed over a frame interval. Based on the assumptions above, by using central limit theorem, the variance of decision variable caused by interference from the non-selected paths can be written as

$$\sigma_{si}^2 = E\left\{\left[N_{si}\right]^2\right\} \tag{4.43}$$

$$\sigma_{si}^2 = \frac{N_s}{2T_f}\sum_{a=0}^{A-1}\sum_{b=0}^{B-1}\sum_{l=0}^{L_f-1}\sum_{k=0,(k\neq l)}^{L_{total}^1-1}\left(\alpha_{l,(a,b)}^1\alpha_{k,(a,b)}^1\right)^2\int_{-\infty}^{\infty}R^2(x)dx$$

where $R(x)$ is defined as

$$R(x) = \int_{-\infty}^{\infty}w(t-x)\left[w(t)-w(t-\tau_\delta)\right]dt \tag{4.44}$$

Similarly, by invoking the central limit theorem, the variance of decision variable caused by interference from the multiple users can be expressed as

$$\sigma_{mai}^2 = E\left\{\left[N_{mai}\right]^2\right\} \tag{4.45}$$

$$\sigma_{mai}^2 = \frac{N_s}{2T_f}\sum_{u=2}^{N_u}\sum_{a=0}^{A-1}\sum_{b=0}^{B-1}\sum_{l=0}^{L_f-1}\sum_{k=0}^{L_{total}^u-1}\left(\alpha_{l,(a,b)}^1\alpha_{k,(a,b)}^u\right)^2\int_{-\infty}^{\infty}R^2(x)dx$$

From (4.28), since $\Theta_{n,m} = -\Theta_{m,n}$ (defined in (4.36)), the average probability of error in binary test can be written as

$$Pe_{m,n} = Q\left(\sqrt{SNR^{(m,n)}\left(N_u\right)}\right) \tag{4.46}$$

where $Q(x)$ is the Gaussian-tail integral and has been defined in (3.47). Consequently, from (4.27), the union bound on the symbol error probability (SER) conditioned on particular SNR can be written as

$$P_{s/\gamma}\left(N_u\right) = \frac{1}{M}\sum_{m=1}^{M}\sum_{n=1}^{M} Q\left(\sqrt{SNR^{m,n}\left(N_u\right)}\right) \tag{4.47}$$

where $m \neq n$. For EC signals, as $SNR^{m,n}\left(N_u\right) = SNR\left(N_u\right)$, the upper bound of the SER is

$$P_{s/\gamma}\left(N_u\right) = \left(M-1\right)Q\left(\sqrt{SNR\left(N_u\right)}\right) \tag{4.48}$$

The upper bound of SER can be converted to upper bound of bit error probability as [77]

$$P_{b/\gamma}\left(N_u\right) = \left(\frac{M}{2}\right)Q\left(\sqrt{SNR\left(N_u\right)}\right) \tag{4.49}$$

whereby $SNR\left(N_u\right)$ is given as

$$SNR(N_u) = \frac{\Theta^2}{\sigma_{total}{}^2} \tag{4.50}$$

$$= \left[\left(\frac{\Theta^2}{\sigma_{awgn}^2 + \sigma_{si}^2}\right)^{-1} + \left(\frac{\Theta^2}{\sigma_{mai}^2}\right)^{-1}\right]^{-1}$$

$SNR\left(N_u\right)$ is user one's output symbol signal-to-noise ratio (SNR) observed in binary communications in the presence of N_u active users. $SNR\left(N_u\right)$ can be defined in terms of output bit SNR , $SNRb(N_u)$ as

$$SNR(N_u) = \log_2(M)\, SNRb(N_u) \tag{4.51}$$

The bit SNR $SNRb(N_u)$ is given as

$$SNRb(N_u) = \left[\left(SNRb(1)\right)^{-1} + \left(\frac{1}{R_b} \frac{\left(\sum_{a=0}^{A-1} \sum_{b=0}^{B-1} \sum_{l=0}^{L_f^1 - 1} \alpha_{l,a,b}^{1\ 2} \right)^2 \beta / T_f}{\sum_{u=2}^{N_u} \sum_{a=0}^{A-1} \sum_{b=0}^{B-1} \sum_{l=0}^{L_f - 1} \sum_{k=0}^{L_{total}^u - 1} \left(\alpha_{l,(a,b)}^1 \alpha_{k,(a,b)}^u \right)^2} \right)^{-1} \right]^{-1} \tag{4.52}$$

where

$$\beta = \frac{2\left[E_w\left(\frac{1 - \gamma_w(\tau_\delta)}{2} \right) \right]^2}{\frac{1}{T_f} \int_{-\infty}^{\infty} R^2(x)dx} \tag{4.53}$$

and

$$R_b = \frac{\log_2(M)}{N_s T_f} \tag{4.54}$$

R_b is the bit transmission rate. $SNRb(1)$ is the output bit SNR for transmissions over single user environments and can be written as

$$SNRb(1) = \log_2(M) \frac{\Theta^2}{\sigma_{awgn}^2 + \sigma_{si}^2} \tag{4.55}$$

If only the desired user is exist, the union bound of probability of bit error rate for single user environment with self interference conditioned on particular SNR is defined as

$$P_{b/\gamma}(1) = \left(\frac{M}{2} \right) Q\left(\sqrt{SNRb(1)} \right) \tag{4.56}$$

or

$$P_{b/\gamma}(1) = \left(\frac{M}{2} \right) Q\left(\sqrt{SNR(1)} \right) \tag{4.57}$$

where $SNR(1)$ is defined as

$$SNR(1) = \left[\left(\frac{\Theta^2}{\sigma_{awgn}^2} \right)^{-1} + \left(\frac{\Theta^2}{\sigma_{si}^2} \right)^{-1} \right]^{-1} \tag{4.58}$$

In this study, perfect power control is assumed. The average of SER over the fading is defined as

$$P_{E_s} = \int_0^\infty P_{s/\gamma}(x) pdf_\gamma(x)\, dx \tag{4.59}$$

and the average of BER over the fading is defined as

$$P_{E_b} = \int_0^\infty P_{b/\gamma}(x) pdf_\gamma(x)\, dx \tag{4.60}$$

where pdf_{γ_b} is the probability density function of the instantaneous output SNR. We compute the expectation of the SER/BER over the fading channel by using Monte Carlo method.

4.5 Multiple Access Capacity

4.5.1 Degradation Factor

Degradation factor is a measure of degradation in performance as the number of users with L_{total}^u paths increases. We can also think of it as a measure of additional amount of SNR required by desired user to combat the ill effect of MUI caused by the N_u users with L_{total}^u paths between u^{th} interference users and desired user.

As in [17], we define $SNRb_s$ is the specified bit SNR to achieve the desired probability of error. $SNRb_r$ is defined as the required value of $SNRb(1)$ to meet the requirement of

$$SNRb(N_u) = SNRb_s \tag{4.61}$$

$SNRb(1)$ is the bit SNR when only the desired user is active, and $SNRb(N_u) < SNRb(1)$ is the actual bit SNR value when N_u users are active in the system. $SNRb_r$ is defined as

$$SNRb_r(N_u) = \frac{SNRb_s}{1 - SNRb_s\left[(1/R_b)\,D\right]^{-1}} \tag{4.62}$$

and $SNRb_s$ is defined as

$$SNRb_s = \frac{SNRb_r\left(N_u\right)}{1 - SNRb_r\left(N_u\right)\left[(1/R_b)\,D\right]^{-1}} \tag{4.63}$$

where

$$D = \frac{\left(\sum_{a=0}^{A-1}\sum_{b=0}^{B-1}\sum_{l=0}^{L_f^1-1}\alpha_{l,a,b}^{1\ 2}\right)\beta/T_f}{\sum_{u=2}^{N_u}\sum_{a=0}^{A-1}\sum_{b=0}^{B-1}\sum_{l=0}^{L_f-1}\sum_{k=0}^{L_{total}^u-1}\left(\alpha_{l,(a,b)}^1\alpha_{k,(a,b)}^u\right)^2} \tag{4.64}$$

Degradation factor is defined as the ratio of required value of $SNRb(1)$ in multiuser environments to satisfy the condition of $SNRb(N_u) = SNRb_s$ to the value of specific bit SNR shown below

$$DF = \frac{SNRb_r(N_u)}{SNRb_s(1)} \tag{4.65}$$

$$= \frac{1}{1 - SNRb_s \left[\left(\frac{1}{R_b} \right) D \right]^{-1}}$$

where D is defined in (4.64).

From (4.65), we can get the bit transmission rate R_b as a function of DF. It can be written as follows

$$R_b(DF) = \frac{1}{SNRb_s} \left(1 - \frac{1}{DF} \right) D \tag{4.66}$$

The maximum value of R_b, $R_{\max}$ is defined as

$$R_{\max} \triangleq \lim_{DF \to \infty} R_b(DF) \tag{4.67}$$

$$= \frac{1}{SNRb_s} D$$

$R_{\max}$ is the largest value that R_b can accomplish when the performance with L_f paths selected is determined by the amount of multiple user interference caused by N_u users, each with L_{total}^u for a specific value of $SNRb_s$.

For a given number of N_u, $SNRb_s$ has a limit on the largest value that it could obtain. The limit of $SNRb_s$ can be derived by setting $SNRb_r(N_u) \to \infty$ for $SNRb_s$ in (4.63), hence

$$SNRb_{\lim}(N_u) \triangleq \lim_{SNRb_r(N_u) \to \infty} SNRb_s \tag{4.68}$$

$$= \left(\frac{1}{R_b} \right) D$$

4.5.2 Multiple Access Transmission Capacity

In this section, we perform an approximate analysis to estimate the multiple access capacity of IR system with equally correlated signals under ideal power control. By using Shannon capacity formula, we can derive the multiple-access capacity per users, $C_a\left(N_u\right)$ with antenna array at the receiver. Shannon capacity formula is defined as

$$C\left(B\right) = B\log_2\left(1+\left(\frac{1}{B}\right)R_b P\right) \tag{4.69}$$

where

$$B = \frac{1}{T_w} \tag{4.70}$$

and

$$P = R_b SNRb_s \tag{4.71}$$

B is the bandwidth of the signal and T_w is the duration of a monopulse. B is in the order of Gigahertz as T_w is in the order of nanosecond. P is the bit power to noise power density ratio. The maximum value of P can be obtain using the maximum value of $SNRb_s\left(SNRb_{\lim}\left(N_u\right)\right)$ by letting $SNRb_r\left(N_u\right)\to\infty$ and is defined in (4.68). Hence,

$$P_{\max}\left(N_u\right) \triangleq R_b SNRb_{\lim}\left(N_u\right) \tag{4.72}$$

$$= D = \frac{\left(\sum_{a=0}^{A-1}\sum_{b=0}^{B-1}\sum_{l=0}^{L_f^1-1}\alpha_{l,a,b}^{1\ 2}\right)^2 \beta/T_f}{\sum_{u=2}^{N_u}\sum_{a=0}^{A-1}\sum_{b=0}^{B-1}\sum_{l=0}^{L_f-1}\sum_{k=0}^{L_{total}^u-1}\left(\alpha_{l,(a,b)}^1\alpha_{k,(a,b)}^u\right)^2}$$

By substituting (4.72) into (4.69) and expanding (4.69) using power series [17], the maximum value of $C\left(B\right)$ can be written as

$$C(B) = \frac{B}{\log_e 2} \sum_{k=1}^{\infty} \frac{(-1)^{k+1}}{k} \left(\frac{1}{B} D \right)^k \tag{4.73}$$

Equally correlated signal that we utilize in this study are known to be optimal in the sense that they can achieve channel capacity as M approaches infinity. The signal set requires unbounded time and bandwidth resources when M approaches infinity. Consequently, by setting $B \to \infty$ (width of the pulse approach zero), the multiple-access capacity per user in bits per second can be written as

$$C_a(N_u) \triangleq \lim_{B \to \infty} C(B) \tag{4.74}$$

$$\simeq \frac{D}{\log_e 2}$$

4.6 Numerical Results

In this section, we evaluated the multiple access performance of an equally correlated M-ary IR system with antenna array receiver under multipath environments.

We consider uniform linear array (Rx= $A \times 1$) and rectangular planar array (Rx= $A \times B$) in this study. Rx is the total number of elements used for an antenna array at the receiver. We select the Gaussian monocycle pulse shape of

$$w(t) = \left(\left[1 - 4\pi \left(\frac{t - t_d}{\tau_m} \right)^2 \right] \exp \left[-2\pi \left(\frac{t - t_d}{\tau_m} \right)^2 \right] \right) \tag{4.75}$$

in which t_d corresponds to the location of the pulse center, and τ_m determines the width of the pulse. The parameters of generating the monopulse are set as $t_d = 0$ and $\tau_m = 0.7531\, ns$. Frame duration is taken as $T_f = 100\ ns$ and modulation index is chosen as

$\tau_\delta = 0.4073ns$. Parameters used for the channel model are cluster decay factor $\Gamma = 24$, ray decay factor $\gamma = 12$, $\sigma_1 = \sigma_2 = 3.3941dB$. The constant ray and cluster arrival rate are 0.5/ns and 0.1/ns respectively. The signals received at all antenna elements are assumed to be in phase, and have an azimuth angle (ϕ) of 15^0 with $\phi_0 = 45^0$ and $\theta_0 = 90^0$. The inter-element spacing of the array, $d_x = d_y = 6\,inch$. We assume the total number of multipath for each user is the same and is equal to 20 where $L_{total}^u = L_{total} = 20$. Note that the delay of each antenna element with reference to the reference antenna is small and is less than the time interval of two consecutive rays, $\tau_{a,b} < \tau_k$. Table 4-1shows the value of parameters of the system.

For different level of M, E_b and R_b are kept constant where $E_s = \log_2(M)E_b$ and $R_b = \log_2(M)/T_s$. Since $T_s = N_s T_f$ and T_f is constant, the value of N_s is to be increased when M increases in order to maintain the value of R_b. $N_s = \log_2(M)N_s^b$ where N_s^b is the number of pulses in an interval of T_s used in binary communications and is set to $N_s^b = 50$.

Parameter	Value
Location of monopulse, t_d	0
Width of monopulse, τ_m	0.7531ns
Duration of monopulse, τ_w	2ns
Frame duration, T_f	100ns
Modulation index, τ_δ	0.4073ns
Cluster decay factor, Γ	24
Ray decay factor, γ	12
Standard derivation of the cluster lognormal fading term, σ_1	3.3941dB
Standard derivation of the ray lognormal fading term, σ_2	3.3941dB

Table 4-1: Value of system parameters

Figure 4-2 depicts the number of simultaneous active users, N_u as a function of degradation factor with various number of elements for uniform linear array, Rx= (1×1), (3×1), (9×1), (25×1) at the receiver. For each set of antenna array, one path is selected ($L_f = 1$) at each antenna element. M is set to 4, R_b is set at 200*kbps* and $P_{E_b}(1)$ is taken as 10^{-5} in this figure. From this figure, the benefits of using antenna array at the receiver are evident. As observed in this figure, by increasing the number of employed antenna elements with a fixed value for bit transmission rate and probability of error, it is possible to increase the number of supported users for IR system. Higher spatial diversity gain can be obtained to combat the distortion caused by multipaths and interference from multiple users when higher number of antenna

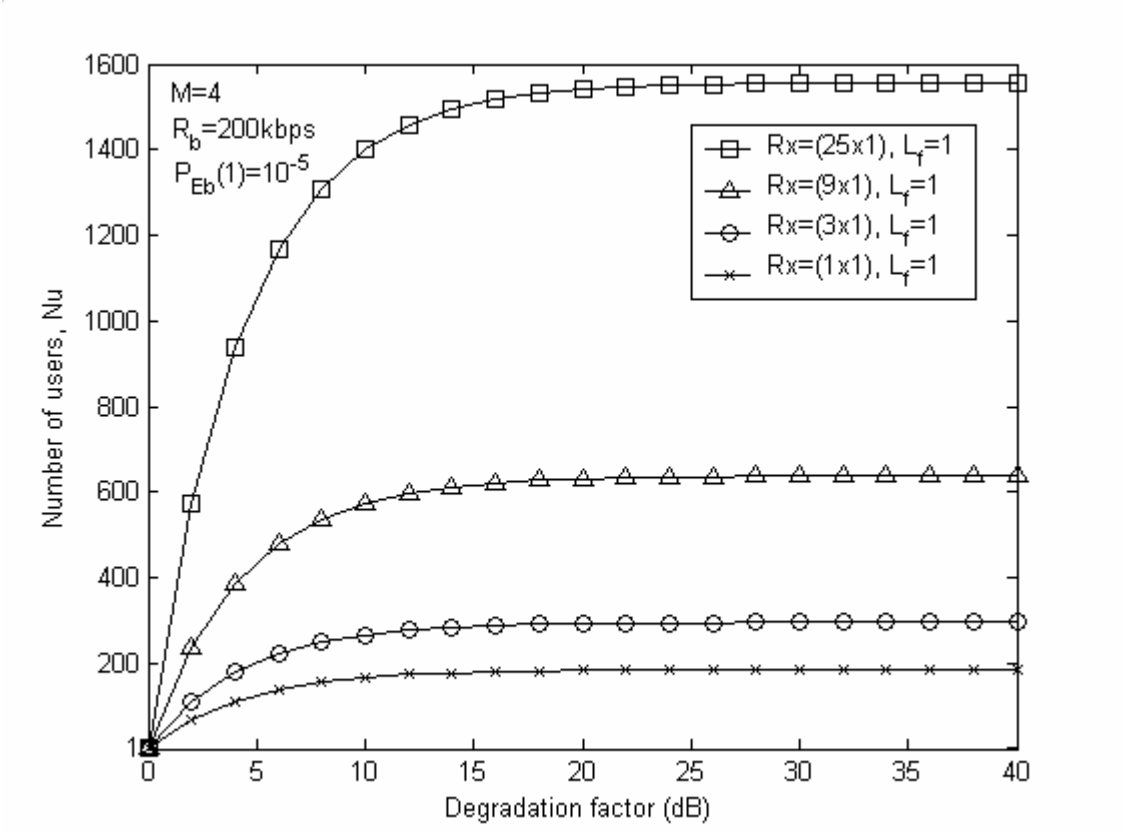

Figure 4-2: Number of active users, N_u as a function of degradation factor with various number of employed elements for uniform linear array

elements are being deployed at the receiver. By using antenna array, it allows coherent recombination of the multipath signal energy and thus effectively alleviating the impact of multiple access interference experiences from other users. This reduction in interference leads to an increase in multiple access capacity that can be supported by the system.

Figure 4-3 shows the effect of the number of selected paths on the multiple access performance for uniform linear array of the IR system. In this figure, M=4, $R_b = 200kbps$, $P_{E_b}(1) = 10^{-5}$ and 3 uniform linear antenna elements is used, Rx= (3×1) with $L_f = 1,2,5,10$ paths selected at each antenna element. For the same

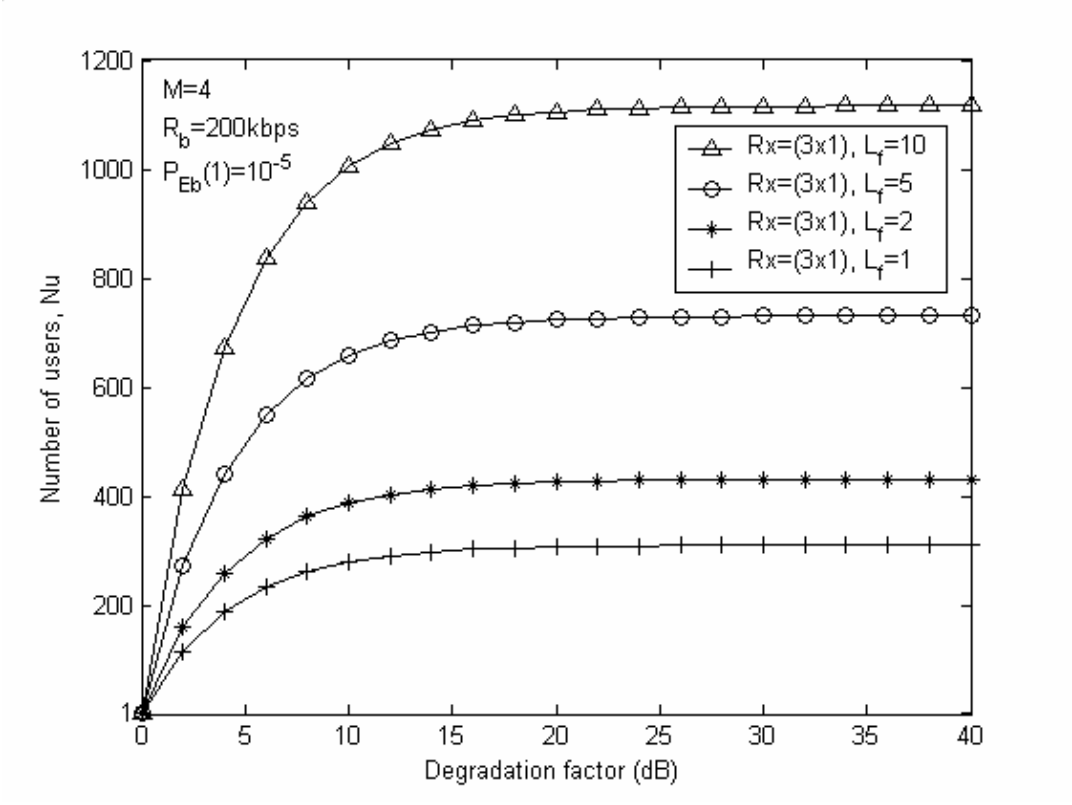

Figure 4-3: Number of active users, N_u as a function of degradation factor for uniform linear array of Rx= (3×1) with various numbers of selected paths at each element

value of degradation factor, the system is able to accommodate more users when more paths being selected and are added coherently at the receiver. In multipath fading environments, when L_f fingers are used in a Rake receiver, the receiver can achieve multipath diversity of order of L_f. With higher number of paths selected, the total amount of the energy captured by the receiver increases and thus the performance of the system improved.

Figure 4-4 and figure 4-5 show multiple access performance of the rectangular array. Fig. 4-4 depicts the numbers of users supported by the IR systems with rectangular array

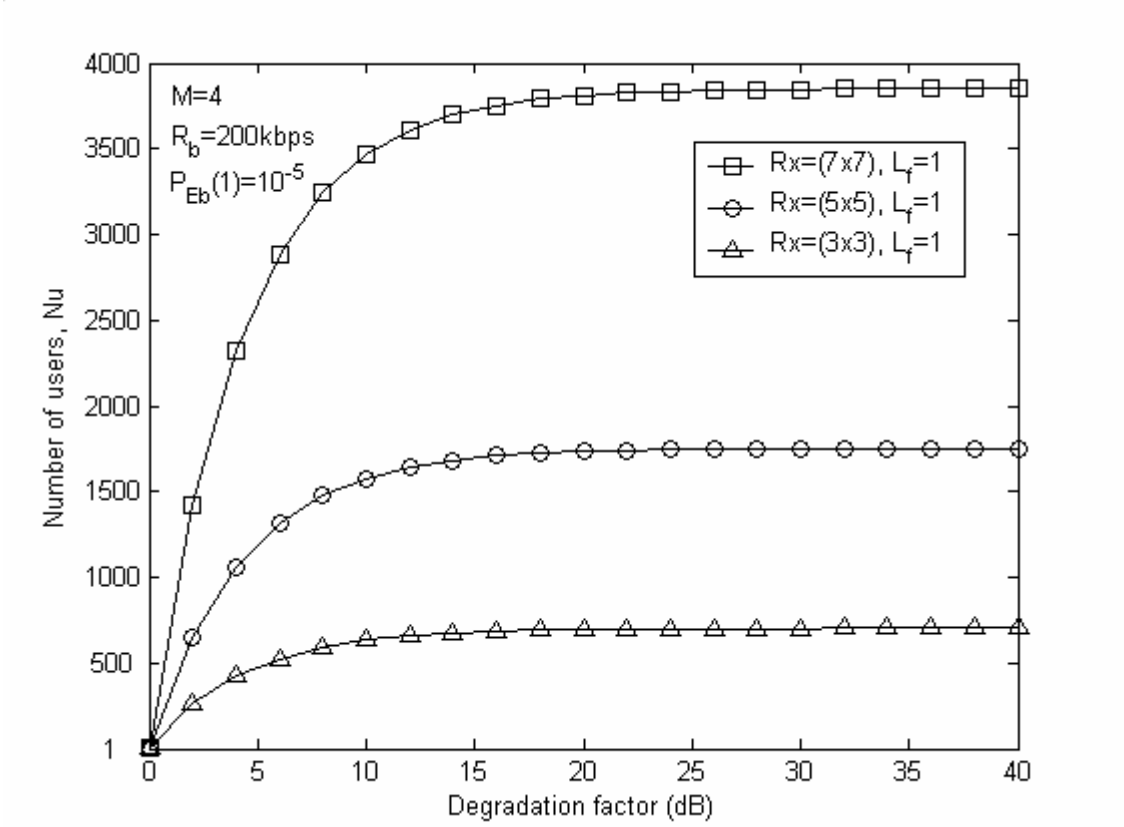

Figure 4-4: Number of active users, N_u as a function of degradation factor with various number of employed elements for rectangular planar array

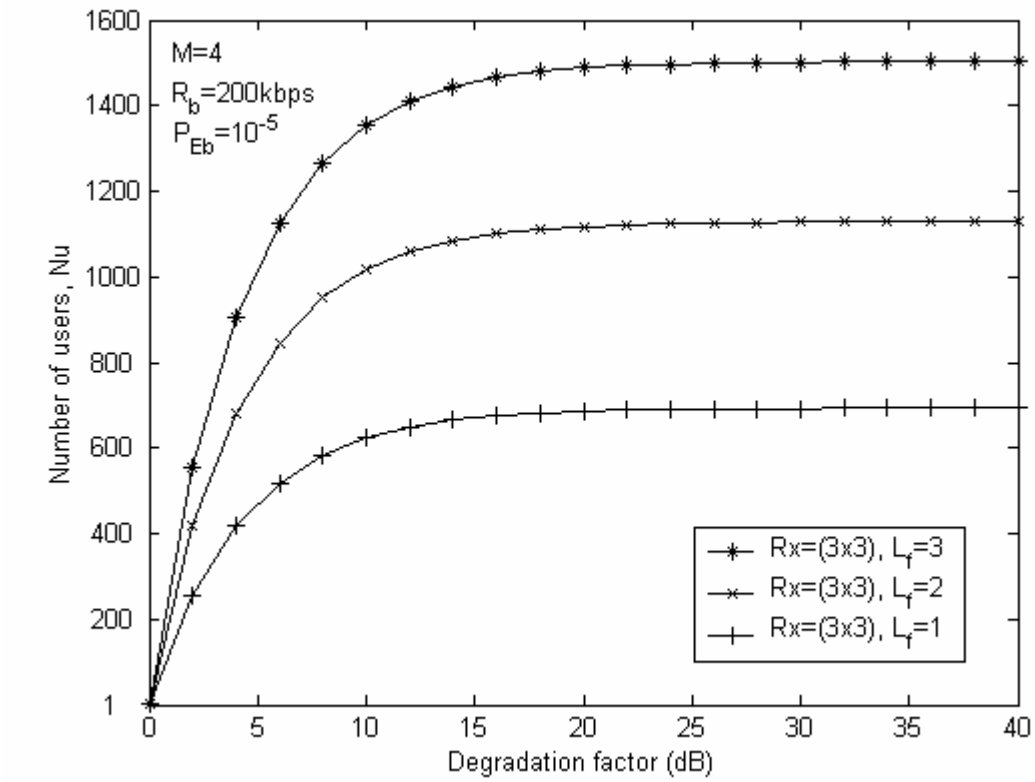

Figure 4-5: Number of active users, N_u as a function of degradation factor for rectangular linear array of Rx=(3×3) with various numbers of selected paths at each element

which consists of various number of deployed elements, Rx=(3×3), (5×5), (7×7) at the receiver. For each antenna element, the first dominant path ($L_f=1$) is selected. The rectangular array with higher number of deployed elements can support higher number of simultaneous users and attains higher immunity to MUI. Figure 4-5 demonstrates the effect of different number of selected paths for rectangular array on the multiple access performance of the IR system. For the same value of degradation factor, the system with the same configurations of array with higher number of selected paths can support higher number of simultaneous users. We can conclude that the performance of the UWB systems improves when the number of antenna elements, Rx and number of selected paths, L_f increase.

Figure 4-6 shows the multiple access performance of the uniform linear array with 5 antenna elements and 2 paths are selected at each antenna element for different value of M. In this figure, $R_b = 200kbps$ and $P_{E_b}(1) = 10^{-5}$. By using the higher value of M, it is possible to increase the number of supported users for a fixed probability of error and bit transmission rate without increasing each user's signal power. It can be seen that the benefit in going from one value of M to the next value actually decreases as M increases.

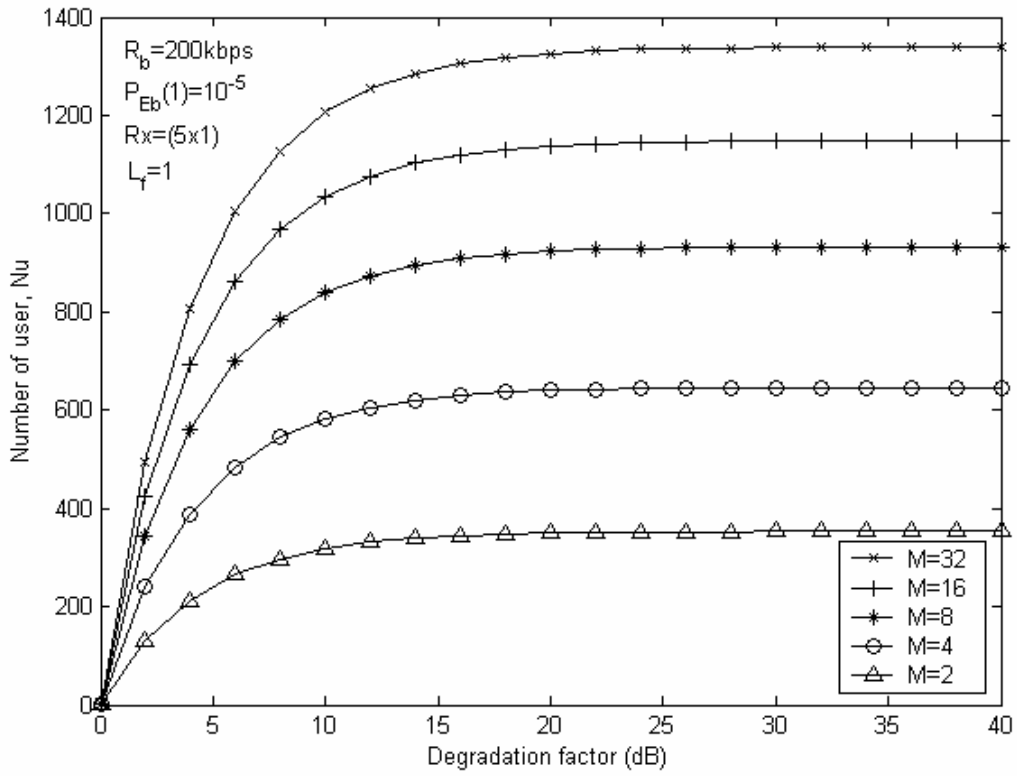

Figure 4-6: Number of active users, N_u as a function of degradation factor for uniform linear array of Rx= (5×1) with $L_f = 1$ for different value of M

From figure 4-2, 4-3, 4-4, 4-5 and 4-6, it can be observed that for a fixed bit error rate and bit transmission rate, the N_u curves have a threshold effect where the number of users grows significantly only in specific regions defined by DF. This threshold effect is also observed when value of M is varied in figure 8.

Figure 4-7 shows the bit transmission rate per user, R_b as a function of degradation factor for various numbers of uniform linear array antenna elements with 2 paths selected at each element in 100 active users' environment $(N_u = 100)$. $P_{E_b}(1)$ is taken as 10^{-5} and M is set to 4 in this figure. The result shows that for a fixed number of active users, the bit transmission rate per user increased when more antenna elements are deployed at the receiver without degrading the multiple access performance.

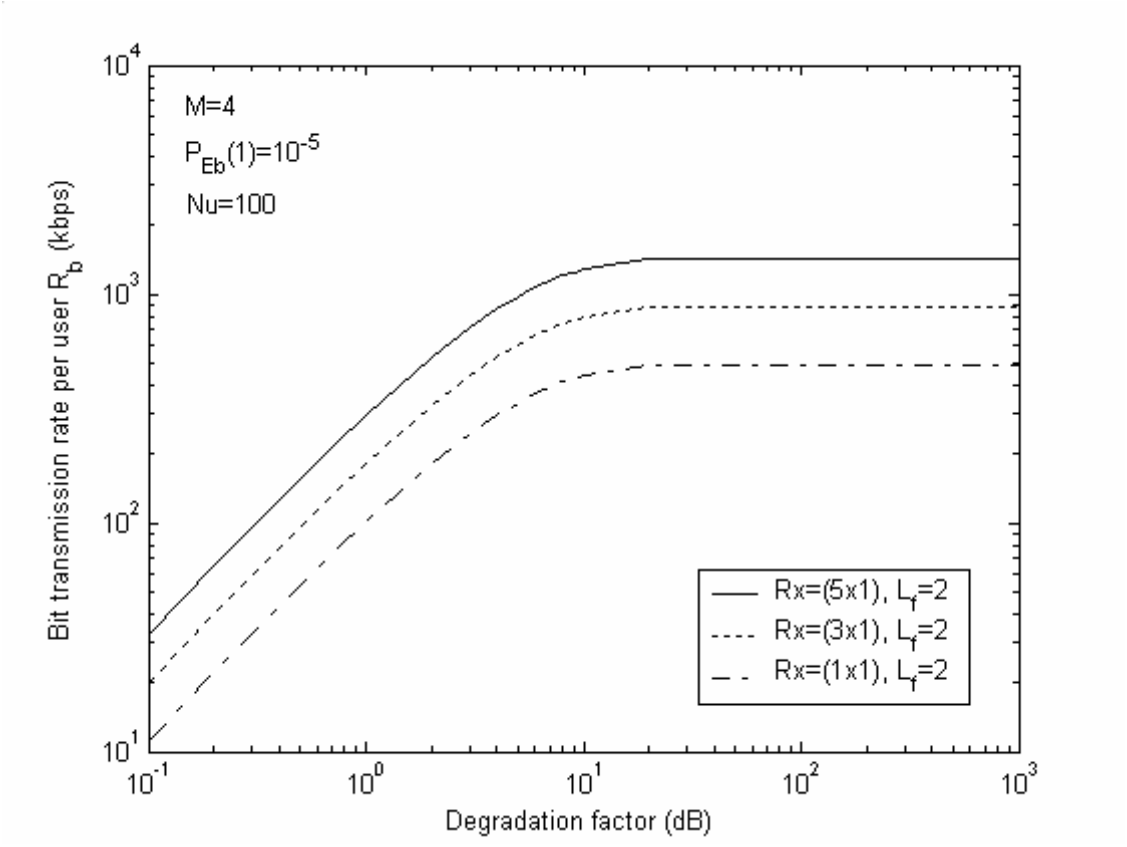

Figure 4-7: Data transmission rate per user R_b as a function of degradation factor for uniform linear array of Rx= (1×1), (3×1), (5×1) elements with

$L_f = 2$

We evaluate the multiple access capacity per user $C_a(N_u)$ in *kbps* as a function of number of active users in figure 4-8 when uniform linear array which consists of 9 or 25 elements being deployed at the receiver. For each antenna element, the first dominant path ($L_f = 1$) is selected. This figure suggests that the multiple access capacity per user $C_a(N_u)$ of the IR system can be improved by increasing the number of elements of the antenna array.

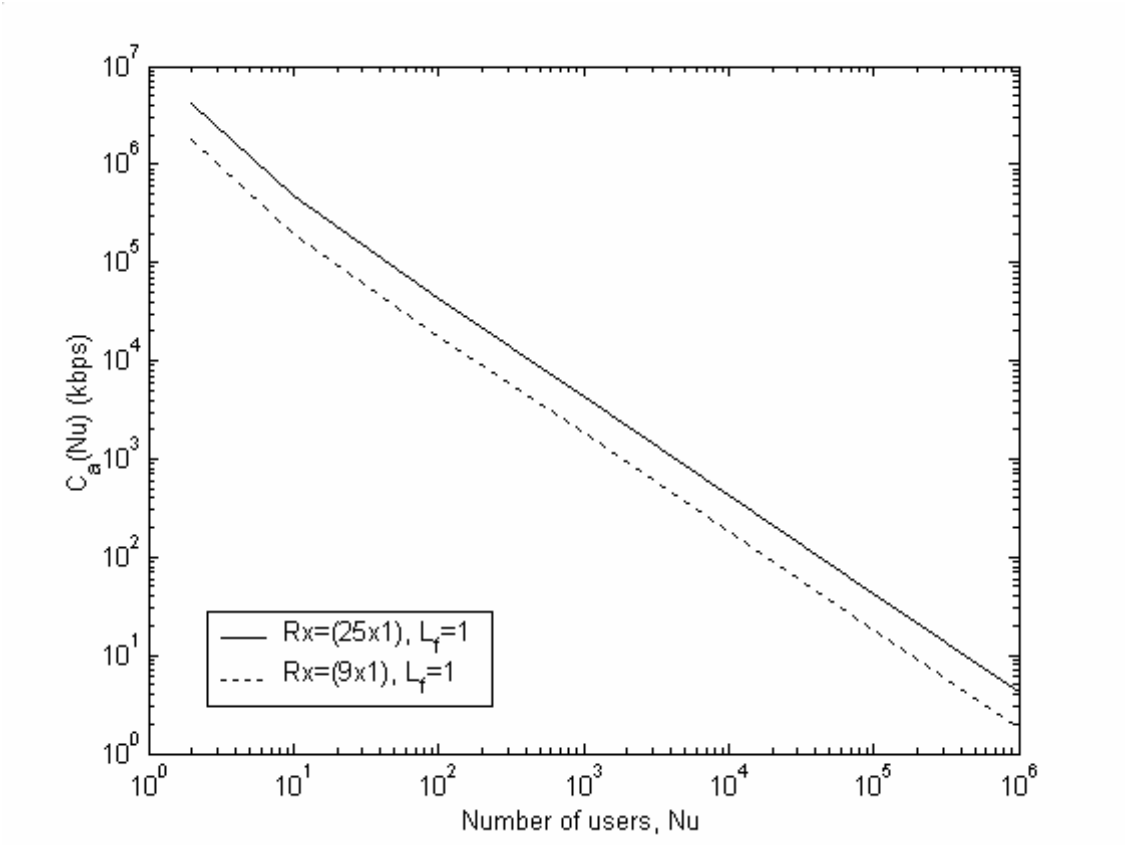

Figure 4-8: The multiple access capacity per user $C_a(N_u)$ as a function of number of active users N_u for Rx= (9×1), (25×1) elements of uniform linear array with $L_f = 1$

Figure 4-9 depicts the multiple access curves as a function of number of active users, N_u when uniform linear antenna array which consists of 9 and 25 elements are being deployed at the receiver. For each antenna element, one path $(L_f = 1)$ is selected. At a fixed E_b / N_0 of 10 dB, the performance degrades when the number of users increases as additional power is required to achieve an invariant BER performance. The system with 25 array elements performs substantially better than 9 elements in multipath fading environments. The result demonstrates that the system with higher number of array's element has greater tolerance to MUI over the MUI- contaminated environments. This is due to the diversity gain obtained across the array since more elements are coherently added at the receiver to cope with the effect of MUI. Higher

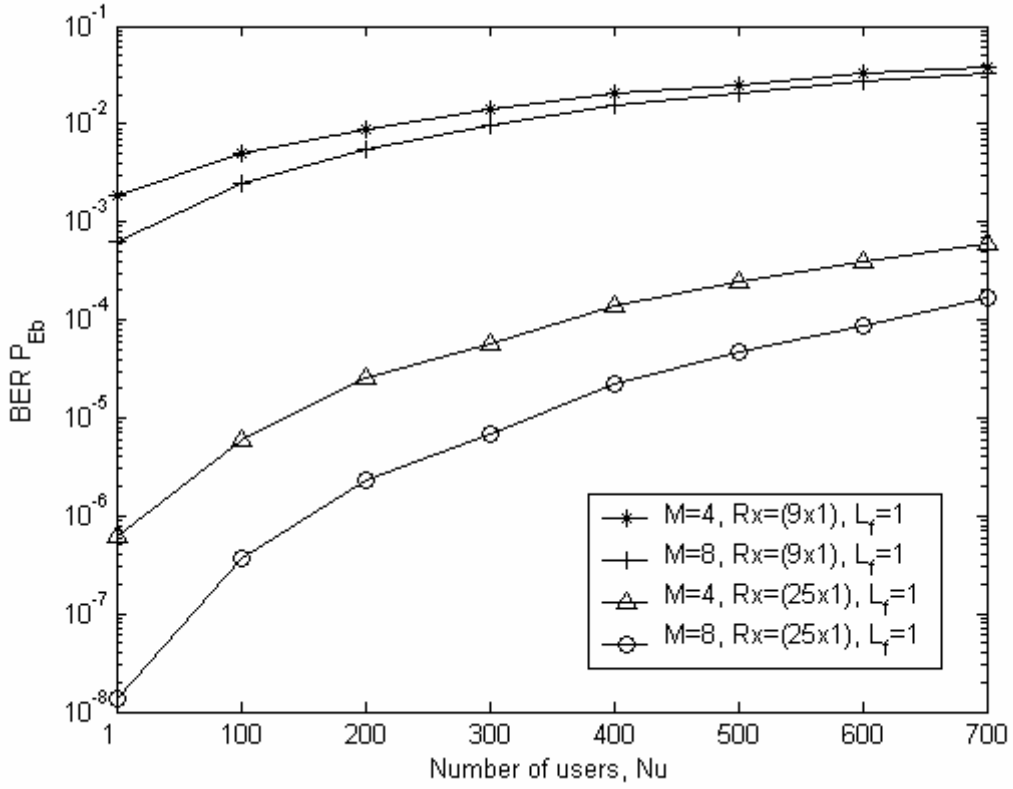

Figure 4-9: BER, P_{E_b} as a function of number of active users, N_u for Rx= (9×1), (25×1) elements of uniform linear array with $L_f = 1$ at a fixed E_b / N_0 of 10 dB

number of employed antenna elements is able to combine more energy of multipaths that separated in space and time. This figure shows that with larger number of employed elements and higher value of M , it is possible to increase the number of supported users for a fix E_b / N_0 .

We compare the multiple access performance of the rectangular array and uniform linear array in figure 4-10 where the BER performance of 25 antenna elements with uniform linear or rectangular array with each element select one path ($L_f = 1$) is shown with $M = 8$. At the fixed E_b / N_0 of 10dB, rectangular array outperforms the uniform linear array. The different geometry of the antenna array effects the performance of the

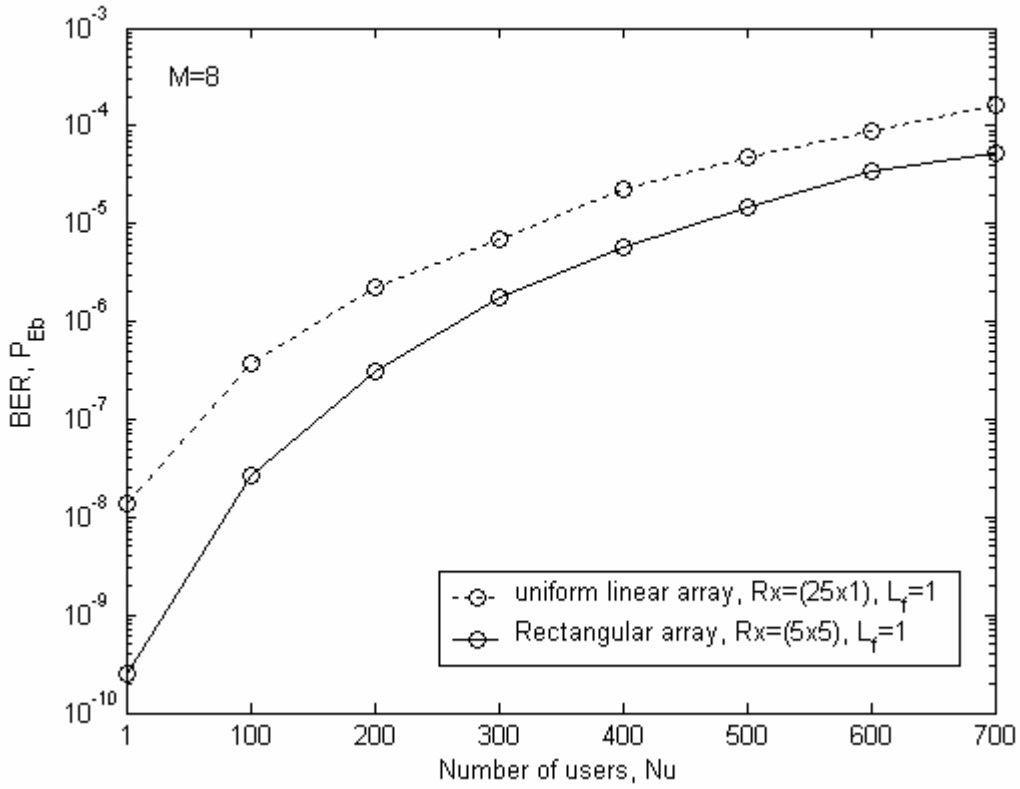

Figure 4-10: BER, P_{E_b} as a function of number of active users for 25 elements of rectangular and uniform linear array with $L_f = 1$ path being selected at each of the antenna element

IR system. The configuration of rectangular array is more concentrate and it enables the array to capture the multipath components with shorter propagation delay in average. Thus, the summed energy of the received multipath signal for rectangular array is higher.

4.7 Conclusions

In this thesis, the multiple access performance of an equally correlated M-ary UWB IR system employing uniform linear and rectangular planar array with SRake receiver in indoor multipath fading channel is presented.

In independent fading channel with multi-user environments, antenna array can be used in conjunction with the Rake receiver to exploit spatial and path diversity provided by the antenna array and the Rake receiver respectively to combine the different multipath components in a way that suppress the impact of multipaths and combat the degrading effect of interference from other undesired users. The diversity gain achieved enables the system to support a larger number of simultaneous active users for a given BER quality threshold.

The numerical results indicate that the BER performance and multiple access capacity of the UWB IR system improve when the number of the employed antenna elements and selected paths at the receiver increases. By using the higher value of M , it is possible to increase the number of supported users. The results also show that the data transmission rate supported by the system can be increased with higher spatial diversity without degrading the multiple access performance for a given number of

users. The results suggest that the antenna array can be used to enhance the multiple access performance of M-ary UWB IR systems.

CHAPTER 5

CONCLUSIONS AND FUTURE WORKS

5.1 Conclusions

Impulse radio is based on Ultra Wideband time hopping spread spectrum technique in which trains of short duration burst of impulses, typically in the duration of nanoseconds, are modulated to convey information by precisely shifting the position of the pulses in the time domain.

In this thesis, the performance of the UWB IR multiple access system with diversity reception in dense multipath environments is presented. Specifically, uniform linear array and rectangular planar array with Rake receiver are being employed at the receiver to realize the diversity. In multiuser environments with independent fading channels, antenna array can be used to exploit spatial diversity in conjunction with the path diversity provided by Rake receiver to combine the energy of different multipath components that is separated in space and time in a way that suppress the impact of multipaths and combat the degrading effect of interference from other undesired users. The diversity gain achieved enables the system to support a larger number of simultaneous active users for a given BER quality threshold.

In chapter 3, the diversity performance of binary IR systems is presented. Particular attention is given to the effect of the number of employed elements and the number of

selected paths at the receiver on the performance of the IR systems. The numerical results indicate the BER performance of the UWB system improves when the number of the employed antenna elements increases. The performance of the IR system will further improves when more multipaths are selected and added coherently at the receiver. Besides, IR system with rectangular array performs better than uniform linear array as the configuration of rectangular array enables it to capture the multipath component with shorter propagation delay in average and hence the summated power of the received multipath signal is higher.

In chapter 4, the multiple access performance of equally correlated M-ary block waveform PPM signal is evaluated. The numerical results indicate that the multiple access capacity of the UWB IR system improve when the number of the employed antenna elements and selected paths at the receiver increases. The results also show that the data transmission rate supported by the system can be increased with higher spatial diversity without degrading the multiple access performance for a given number of users. By using the higher value of M , it is possible to increase the number of supported users for a fixed probability of error and bit transmission rate without increasing each user's signal power.

These results suggest that the antenna diversity can be used to improve reliability and to enhance the performance of IR systems

5.2 Future Works

The recent UWB spectral allocation for unlicensed spectrum and the new definition of UWB adopted by the FCC have induced an alternative physical link design for UWB channels which is based on Orthogonal Frequency Division Multiplexing (OFDM) and Direct Sequence-Code Division Multiple Access (DS-CDMA). Application of antenna array can be extended for the multiband approach and DS-CDMA. Particular attention can be paid in performance comparison between multiband OFDM and DS-CDMA using diversity reception.

5.2.1 Multi-Band OFDM

A new method emerging today uses a multi-band approach, where information is encoded in multiple RF sub-bands at the same time. The MB-OFDM approach is a merged proposal by Intel, Texas Instruments, Femto Devices etc [78]. The fact that FCC specified UWB to be a minimum bandwidth of 500 Mhz allow the use of multiple bands to encode information in parallel. Information is independently encoded in the different bands. This process results in very high bit rate with relatively low signaling rates.

The basic concept of Multi-Band OFDM is to divide spectrum into 13 bands with each band occupying 528 MHz as shown in figure (5-1) [78]. The band plan can be grouped into 4 distinct groups, which is Group A, B, C and D. Group A is reserved for intended use of first generation devices using 3.1-4.9 GHz. Group B (4.9 – 6.0 GHz) and group D (8.1 – 10.6 GHz) are reserved for future use. Group C (8.1 – 10.6 GHz) is

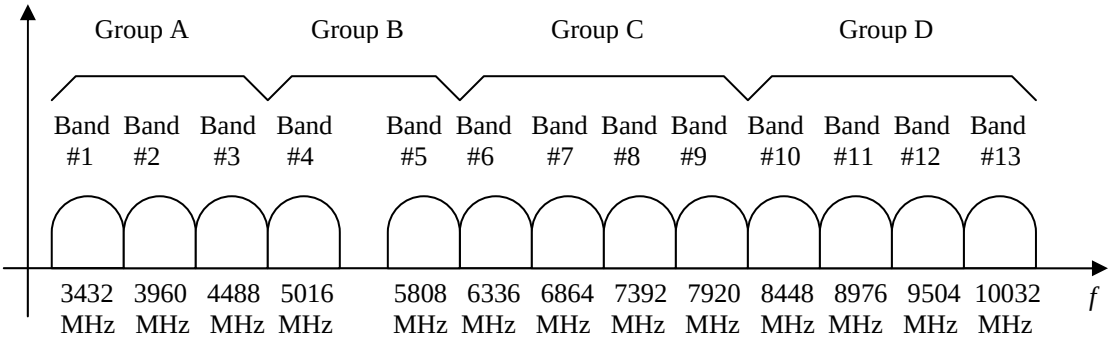

Figure 5-1: Spectrum band allocation in MB-OFDM

reserved for devices with improved simultaneously operating piconet (SOP) performance.

On each band, information is transmitted using OFDM modulation. Information is coded across all bands in use to exploit frequency diversity and provides robustness against multi-path and interference. QPSK modulation is employed by MB-OFDM to provide a simple modulation scheme. The multiple access method is such that the multiple piconet performance is governed by the bandwidth expansion factor which can be archived by spreading, time-frequency interleaving and coding.

A multi-band UWB system design yields many benefits such as more adaptivity than single band designs, better co-existence characteristic with systems such as 802.11a, provide good interference robustness, lower risk implementations, cost and power consumption. The multi-band approach can avoid the difficulties faced when using single band. A single band UWB system needs to employ notch filters where it can increase the receiver noise figure and is not adaptive.

5.2.2 DS-CDMA

The DS-CDMA approach is proposed by XtremeSpectrum, Communications Research Lab (CRL) and ParthusCeva and is supported by Motorola. Direct sequence CDMA spreads the data transmission throughout the 3.1 to 10.6 gigahertz UWB spectrum approved by the FCC. DS-CDMA utilized dual band approach where 7.5 GHZ spectrums is split into two band which is low band and high band as shown in figure 5-2 [79]. Low band is allocated for 3.1-5.15 GHz with 25 Mbps-450 Mbps whereas high band is allocated for 5.825-10.6 GHz with 25 Mbps-900 Mbps.

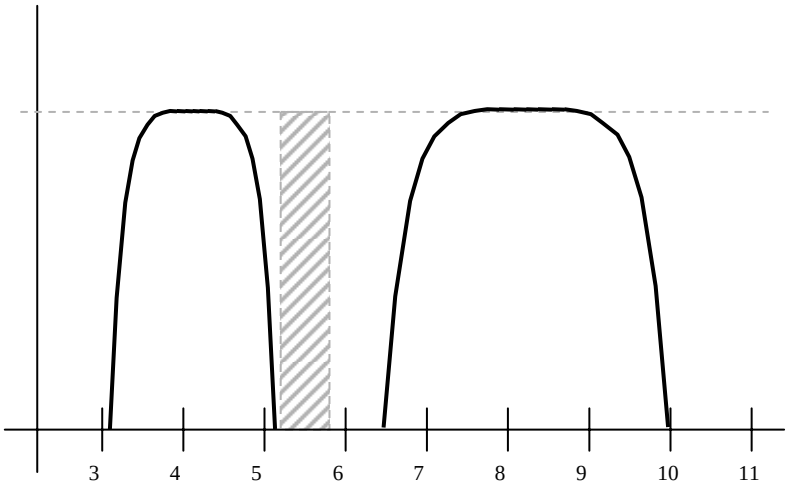

Figure 5-2: Dual band spectrum allocation of DS-CDMA

The DS-CDMA allows the usage of low, high or both bands. Multiple access of this approach can be feasible via ternary CDMA coding where orthogonal codes is used to create multi-user capability. The dual band approach employed short duration pulses to transmit over each band which are in access of 1 GHz. M-ary biorthogonal keying

(MBOK) is adopted for modulation scheme in DS-CDMA approach. A simple example of binary DS-CDMA signal with bit 1, -1, -1 is shown in figure 5-3.

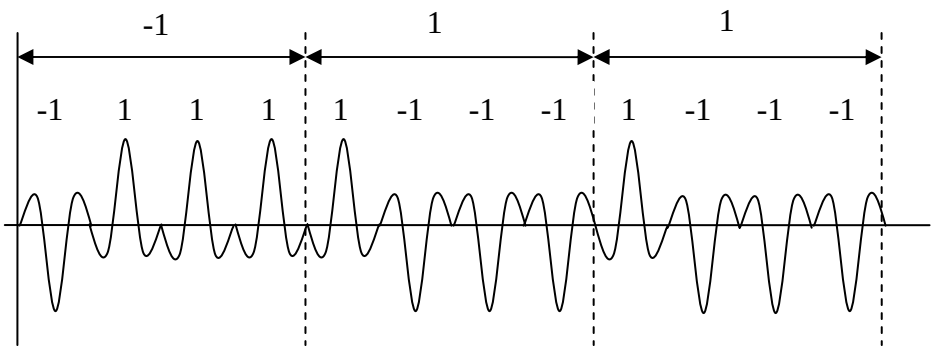

Figure 5-3: DS-CDMA example with bit -1, 1 ,1 transmitted

REFERENCE

[1] G. F. Ross, "The Transient Analysis of Certain TEM Mode Four Post Networks," *IEEE Trans. Microwave Theory Tech*, vol. MTT-14, p.528, Nov. 1966.

[2] J. D. Taylor, *"An Iintroduction to Ultra Wideband Radar Technology,"* Boca Raton: CRC press, 1995.

[3] C. L. Bennett and G. F. Ross, "Time-domain Electromagnetic and Its Applications," *Proc. IEEE*, Vol. 66, pp. 299-318, Mar. 1978

[4] FCC document 98-208, "Revision of the Rules Regarding Ultra-Wideband Transmission System," 47 CFR part 15, ET Docket 98-253, Sept. 1998.

[5] FCC document 00-163, "Revision of Part 15 Commission Rules ET Docket No. 98-153," adopted 5-10-2000

[6] FCC 02-48, "Revision of Part 15 of the Commission's Rules Regarding Ultra-Wideband Transmission Systems," First report and Order, ET Docket 98-153, released Apr. 22, 2002.

[7] http://grouper.ieee.org/groups/802/15/

[8] M. Z. Win and R. A. Scholtz, "Ultra-wide Bandwidth Time-Hopping Spread-Spectrum Impulse Radio for Wireless Multiple-Access Communications," *IEEE Trans. Comm.*, vol.48, pp. 679-691, Apr. 2000.

[9] R. A. Scholtz and M. Z. Min, "Impulse Radio," invited paper, *Proc. of PIMRC conference*, pp. 245-267, Sept. 1997.

[10] M. Z. Win and R. A. Scholtz, "Impulse Radio: How It Works" *IEEE Communications letters*, vol. 2, pp. 36-38, 1999.

[11] Fowler C., Entminger J. and Corum J., "Assessment of Ultra-Wideband (UWB) Technology," *IEEE AES Magazine*, vol. 5, pp. 45-49, Nov. 1990.

[12] D. R. McKinstry, "Ultra-Wideband Small Scale Channel Modeling and Its Application to the Receiver Design," Master of Science Thesis, Virginia Polytechnic Institute and state university, June, 2003.

[13] M. Welborn, K. Siwiak, IEEE P802.15 Working group for Wireless Personal Area Networks (WPANs), "Ultra-Wideband Tutorial," IEEE 802.15-02/133r1, March, 11, 2002.

[14] D. Porcino, W. Hirt, "Ultra-Wideband Radio Technology: Potential and Challenges Ahead," *IEEE Communications Magazine*, vol. 41, pp. 66-74, Jul. 2003.

[15] R. A. Scholtz, "Multiple Access with Time Hopping Modulation," *Proc. of IEEE MILCOM '93*, pp. 447-450, Oct. 1993.

[16] F. Ramirez-Mireles and R. A. Scholtz, "Multiple-Access with Time Hopping and Block Waveform PPM Modulation," *Proc. of IEEE ICC'98*, vol. 3, pp. 775-779, June 1998.

[17] F. Ramirez-Mireles, "Performance of Ultra Wideband SSMA Tsing Time Hopping and M-ary PPM," *IEEE Journal on Selected Areas in Communications*, vol.19, pp. 1186-1196, June 2001.

[18] F. Ramirez-Mireles, R. A. Scholtz, "Multiple-Access Performance Limits with Time Hopping and Pulse Position Modulation" *Prof. of IEEE MILCOM'98*, vol. 2, pp. 529-533, Oct. 1998.

[19] F. Ramirez-Mireles and R.A. Scholtz, "Wireless Multiple-Access using SS Time-Hopping and Block Waveform PPM, Part 1: Signal Design," *Proc. of IEEE ISITA '98*, Oct. 1998.

[20] D. Cassioli and M. Z. Win, "Performance of Low-Complexity Rake Reception in a Realistic UWB Channel," *Proc. ICC'2002*, pp. 763-767, 2002.

[21] J. D. Choi and W. E. Stark, "Performance Analysis of Rake Receivers for Ultra-Wideband Communications with PPM and OOK in Multipath Channels," *Proc. of ICC'2002*, vol.3, pp. 1969-1973, 2002.

[22] M. Z. Min and R. A. Scholtz, "On the Energy Capture of Ultrawide Bandwidth Signals in Dense Multipath Environments," *IEEE Communications Letter*, vol. 2, no.9, pp. 245 -247, Sept. 1998.

[23] M. Z. Win, G. Chrisikos and N. R. Sollenberger, "Performance of Rake Reception in Dense Multipath Channels: Implications of Spreading Bandwidth and Selection Diversity Order," *IEEE Journal on Selected Areas in Communications*, vol. 18, pp. 1516-1525, Aug. 2000.

[24] G. Durisi and G. Romano, "Simulation Analysis and Performance Evaluation of an UWB System in Indoor Multipath Cannel" *IEEE conference on UWB system and technology*, pp. 255-258, May 2002.

[25] A. Rajeswaran, V. S. Somayazulu and J. R. Foerster, "Rake Prformance for a Plse Bsed UWB System in a realistic UWB Indoor Channel," *Proc. of ICC'03*, vol. 4, pp. 2879-2883, 2003.

[26] A. Taha and K. M. Chugg, "Multipath Diversity Reception of Wireless Multiple Access Time-Hopping Digital Impulse Radio," *IEEE conference on UWB system and technology*, pp. 41-46, May 2002.

[27] H. Lee, B. Han, Y. Shin and S. Im, "Multipath Characteristics of Impulse Radio Channels," *Proc. of VTC'2000*, Tokyo, pp. 2487-2491,Spring 2000.

[28] R. J.-M. Cramer, M.Z. Win and R. A. Scholtz, "Evaluation of Multipath Characteristics of the Impulse Radio Channel," *Proc. of PIMRC'98*, Boston, USA, Sept. 1998

[29] J. R. Foester, "The Effects of Multipath Interference on the Performance of UWB Systems in an Indoor Wireless Channel," *Proc. of VTC'01*, pp. 1176-1180, 2001.

[30] F. Ramirez-Mireles, "On the Performance of Ultra-Wideband Signals in Gaussian Noise and Dense Multipath," *IEEE Trans. Vehicular Technology*, vol. 50, pp. 244-249, Jan. 2001.

[31] S. Ghassemzadeh and V. Tarokh, "UWB Path Loss Characterization in Residential Environments," *IEEE MTT-S International Microwave Symposium*, vol.1, pp. 365 -368, June 2003.

[32] M. Pendergrass, "Empirically Based Statistical Ultra-Wideband Channel Model," IEEE P802.15-02/240-SG3a.

[33] D. Cassioli, M. Z. Win, A. F. Molisch, "The Ultra-Wide Bandwidth Indoor Channel: From Statistical Model to Simulations" *IEEE Journal on Selected Areas in Communications*, vol 20, Issue: 6, pp. 1247 -1257, Aug. 2002.

[34] R. J.-M Cramer, R.A. Scholtz, M.Z. Win, "Evaluation of An Ultra-Wide-Band Propagation Channel," *IEEE Transactions on Antennas and Propagation*, vol. 50 Issue: 5, pp. 561 -570, May 2002.

[35] J. Foerster et al., report of IEEE P802.15 Wireless Personal Area Networks, "Channel Modeling Sub-committee Report Final," IEEE P802.15-02/368r5-SG3a, Dec. 2002.

[36] M. Hamalainen, V. Hoviven, "On the UWB System Coexistence with GSM900, UMTS/WCDMA, and GPS" *IEEE Journal on selected areas in Communications*, vol. 20, no.9, Dec. 2002.

[37] B. Parr, C. B. Lok, K. Wallace, Z. Ding, "A Novel Ultra-Wideband Pulse Design Algorithm," *IEEE Communications Letters*, vol. 7, Issue: 5, pp. 219 -221, May 2003.

[38] J. R. Foerster, "Interference Modeling of Pulse-based UWB Waveforms on Narrowband Systems," *Prof. of IEEE VTC'02 Spring*, vol. 4 , pp. 1931 -1935, May 2002.

[39] K. Eshima, Y. Hase and S. oomori, "M-ary UWB System using Walsh Codes," *IEEE conference on Ultra wideband systems and technology*, pp. 37-40, 2002.

[40] L. Zhao and A. M. Haimovich, "Performance of Ultra-Wideband Communications in the Presence of Interference," *IEEE Journal on Selected Areas in Communications*, vol. 20, Issue: 9, pp. 1684 -1691, Dec. 2002.

[41] E. Baccarelli, M. Biagi, L. Taglione, "A Novel Approach to In-band Interference Mitigation in Ultra Wideband Radio Systems," *IEEE Conference on Ultra Wideband Systems and Technologies*, pp. 297-301, May 2002.

[42] M. S. Iacobucci, M.-G. Benedetto, L. D Nardis, "Radio Frequency Interference Issues in Impulse Radio Multiple Access Communication System," *IEEE Conference on Ultra Wideband Systems and Technologies*, pp. 293 -296, May 2002

[43] I. Bergel, E. Fishler, H. Messer, "Narrowband Interference Suppression in Time-Hopping Impulse-Radio Systems" *IEEE Conference on Ultra Wideband Systems and Technologies*, pp. 303-307, May 2002.

[44] A. Taha, K.M. Chugg, "A Theoretical Study on the Effects of Interference on UWB Multiple Access Impulse Radio" *IEEE of Asilomar Conference on Signals, Systems and Computers*, vol. 1, pp. 728 -732, Nov. 2002.

[45] P. V. Rao, R. J. Barton, "Evaluation of Higher-Order Techniques for Blind Adaptive Channel Estimation on Impulse Radio Channels," *IEEE Asilomar Conference on Signals, Systems, and Computers*, vol. 2, pp. 1164 -1170, Oct. 1999.

[46] M. Z. Win and R. A. Scholtz, "Characterization of Ultra-Wide Bandwidth Wireless Indoor Channels: A Communication-Theoretic View" *IEEE Journal on Selected Areas in Communications, Invited tutorial*, vol. 20, pp. 1613-1627, Dec. 2002.

[47] V. Lottici, D. a'Andrea and U. Mengali, "Channel Estimation for Ultra-Wideband Communications," *IEEE Journal on Selected Areas in Communications*, vol. 20, pp. 1638-1645, Dec. 2002.

[48] E. A. Homier, R. A.Scholtz, "Rapid Acquisition of Ultra-Wideband Signals in the Dense Multipath Channel," *IEEE Conference on Ultra Wideband Systems and Technologies*, pp. 105-109, May 2002.

[49] M. Yao, F. Chin, B. Kannan, S. Pasupathy, "Acquisition Performance of an Ultra Wide-Band Communications System over a Multiple-Access Fading Channel," *IEEE Conference on Ultra Wideband Systems and Technologies*, pp. 99-103, May 2002.

[50] F. Ramirez-Mireles, M. Z. Win, R. A. Scholtz, "Signal Selection for the Indoor Wireless Impulse Radio Channel," *Proc. of IEEE VTC'1997*, vol.3, pp.2243 -2247, May 1997.

[51] L. Zhao, A. M. Haimovich, "Capacity of M-ary PPM Ultra-Wideband Communications over AWGN Channels," *Proc. of IEEE VTC'2001 Fall*, vol. 2, pp. 1191-1195, Oct. 2001.

[52] L. Zhao, A.M. Haimovich, “The Capacity of an UWB Multiple-Access Communications System,” *Proc. of IEEE ICC’02*, vol. 3, pp. 1964-1968, April 2002

[53] M. Z. Win, R. A. Scholtz, “Energy Capture vs. Correlator Resources in Ultra-Wide Bandwidth Indoor Wireless Communications Channels,” *Proc. of IEEE MILCOM’97*, vol. 3, pp. 1277-1281, Nov. 1997.

[54] W. Namgoong, “A channelized DSSS Ultra-Wideband Receiver,” *Proc. of IEEERAWCON’01*, pp. 105-108, Aug. 2001.

[55] J. D. Choi, W. E. Stark, “Performance of Ultra-Wideband Communications with Suboptimal Receivers in Multipath Channels,” *IEEE Journal on Selected Areas in Communications*, vol. 20, Issue: 9, pp. 1754-1766, Dec. 2002.

[56] E. Saberinia, A. H. Tewfik, “Receiver Structures for Multi-Carrier UWB Systems,” *International Symposium on Signal Processing and Its Applications*, vol. 1, pp. 313 -316, July 2003.

[57] D. Gerakoulis, P. salmi, “Link Performance of an Ultra Wide Bandwidth Wireless In-home Network,” *International Symposium on Computers and Communications*, pp. 699-704, July 2002.

[58] L. D. Nardis, P. Baldi, M.-G. Benedetto, “UWB Ad-hoc Networks,” *IEEE Conference on Ultra Wideband Systems and Technologies*, pp. 219-223, May 2002.

[59] F. Cuomo, C. Martello, “MAC Principles for an Ultra Wide Band Wireless Access” *Proc. of IEEE GLOBECOM '01*, vol. 6, pp. 3548-3552 Nov. 2001.

[60] S. S. Kolenchery, J. K. Townsend, J. A. Freebersyser, G. Bilbro, “Performance of Local Power Control in Peer-to-Peer Impulse Radio Networks with Bursty Traffic,” *Proc. of IEEE GLOBECOM '97*, vol. 2, pp. 910-916, Nov. 1997.

[61] D. H. Johnson and D. E. Dudgeon, “*Array Signal processing: Concepts and Techniques*”, Englewood Cliffs, NJ: Prentice Hall, 1993.

[62] S. S. Tan, B. Kannan and A. Nallanathan, " Performance of Ultra-Wideband Time-Hopping Spread Spectrum Impulse Radio Systems with Antenna Array," *Proc. of IEEE ICCS'02*, pp. 398-402, Singapore, Nov. 2002.

[63] S. S. Tan, B. Kannan and A. Nallanathan, “Ultra-Wideband Impulse Radio Systems with Temporal and Spatial Diversities," *Proc. of IEEE VTC'03*, vol. 1, pp.607-611, Florida, U.S.A, Oct. 2003.

[64] S. S. Tan, B. Kannan and A. Nallanathan, " Performance of UWB Multiple Access Impulse Radio Systems in Dense Multipath Environments with Antenna Array," *Proc. of IEEE GLOBECOM'03*, vol. 4, pp.2182-2186, San Francisco, U.S.A, Dec. 2003.

[65] S. S. Tan, B. Kannan and A. Nallanathan, “Performance of UWB Multiple Access Impulse Radio Systems with Antenna Array in Dense Multipath Environments,” submitted to IEEE Transaction on Communications.

[66] S. S. Tan, B. Kannan and A. Nallanathan, “Multiple Access Performance of UWB M-ary Impulse Radio Systems with Diversity Reception,” *IEEE Joint UWBST&IWUWBS2004*, pp. 346-350, Japan, May 2004.

[67] S. S. Tan, B. Kannan and A. Nallanathan, “Multiple Access Performance of UWB M-ary Impulse Radio Systems with Spatial and Temporal Diversities,” submitted to IEEE Transaction on Wireless Communications.

[68] A. Taha, “Performance Considerations of Wireless Multiple-Access Digital Impulse Radio under Realistic Multipath Channels,” PHD Dissertation, University of Southern California, Mar. 2003.

[69] S. W. Chen, “Ultra Wide-Band Baseband Design and Implementation,” Master of Science Thesis, University of California at Berkeley.

[70] C. Xiaomin and S. Kiaei, “Monocycle Shapes for Ultra Wideband System,” *IEEE International Symposium on Circuits and Systems*, vol. 1, pp. I-597-I-600, May 2002.

[71] T. S. Rappaport, *Wireless Communications*, Prentice Hall, second ed., 2002.

[72] R. Price and P. E. Green, “A Communication Technique for Multipath Channel,” *Proceedings of the IRE*, pp. 555-570, March, 1958.

[73] R. J.-M Cramer, “An Evaluation of Ultra-Wideband Propagation Channels,” PHD Dissertation, University of Southern California, Dec. 2000.

[74] R. J.-M. Cramer, M. Z. Win and R. A. Scholtz, “Impulse Radio Multipath Characteristics and Diversity Reception,” *Prof. of IEEE ICC’98*, vol. 3, pp. 1650-1654, 1998

[75] A. Saleh and R. Valenzuela, “A Statistical Model for Indoor Multipath Propagation,” *IEEE Journal on Selected Areas in Communications*, vol. SAV-5, no.2, pp. 128-137, Feb. 1997

[76] J. G. Proakis, *Digital Communications*, McGraw-Hill, Inc., fourth ed., 2001.

[77] F. Ramirez-Mireles, “Multiple-Access with Ultra-Wideband Impulse Radio Modulation using Spread Spectrum Time-Hopping and Block Waveform Pulse-Position-Modulated Signals,” PHD dissertation, University of Southern California, 1998.

[78] V. Brethour et al. “Multi-band OFDM Physical Layer Proposal Response to No Voters,” IEEE 802.14-03/34r1, Sept. 2003.

[79] M. Welborn, M. M. Laughlin and R. Kohno, “Merger #2 Proposal DS-CDMA,” IEEE P802.15-03/343r3, Sept. 2003.

LIST OF PUBLICATIONS AND SUBMISSIONS

[1] S. S. Tan, B. Kannan and A. Nallanathan, " Performance of Ultra-Wideband Time-Hopping Spread Spectrum Impulse Radio Systems with Antenna Array," *Proc. of IEEE ICCS'02*, pp. 398-402, Singapore, Nov. 2002.

[2] S. S. Tan, B. Kannan and A. Nallanathan, "Ultra-Wideband Impulse Radio Systems with Temporal and Spatial Diversities," *Proc. of IEEE VTC'03*, vol. 1, pp.607-611, Florida, U.S.A, Oct. 2003.

[3] S. S. Tan, B. Kannan and A. Nallanathan, " Performance of UWB Multiple Access Impulse Radio Systems in Dense Multipath Environment with Antenna Array," *Proc. of IEEE GLOBECOM'03*, vol. 4, pp.2182-2186, San Francisco, U.S.A, Dec. 2003.

[4] S. S. Tan, B. Kannan and A. Nallanathan, "Performance of UWB Multiple Access Impulse Radio Systems with Antenna Array in Dense Multipath Environments," submitted to IEEE Transaction on Communications.

[5] S. S. Tan, B. Kannan and A. Nallanathan, "Multiple Access Performance of UWB M-ary Impulse Radio Systems with Diversity Reception," *IEEE Joint UWBST&IWUWBS2004*, pp. 346-350, Japan, May 2004.

[6] S. S. Tan, B. Kannan and A. Nallanathan, "Multiple Access Performance of UWB M-ary Impulse Radio Systems with Spatial and Temporal Diversities," submitted to IEEE Transaction on Wireless Communications.